UNIVERSITÁ DEGLI STUDI DI MILANO
FACOLTÁ DI MEDICINA E CHIRURGIA

DOTTORATO DI RICERCA IN FISIOLOGIA
SETTORE SCIENTIFICO DISCIPLINARE BIO-09
CICLO XXVIII

Tesi di Dottorato di Ricerca

SLEEP-LIKE CORTICAL BISTABILITY IN VEGETATIVE STATE PATIENTS

Dottorando: Dott. Matteo Fecchio
Matricola: R10146

Tutor: Dott. Mario Carmine Emiliano Rosanova

Coordinatore: Prof. Michele Mazzanti

Anno Accademico 2014-2015

SUMMARY

ABSTRACT

The human brain is able to generate a wide repertoire of behavioral and psychological phenomena spanning from simple motor acts to cognition, from unimodal sensory perceptions to conscious experience. All these abilities are based on two key parameters of cortico-thalamic circuits functioning: the reactivity to a direct, local stimulation (cortical excitability) and the ability to causally interact (cortical effective connectivity). Indeed, alterations of these parameters have been suggested to underlie neurologic and psychiatric conditions. Over the last ten years, high-density electroencephalography combined with transcranial magnetic stimulation (TMS/hd-EEG) has been used to non-invasively probe cortical excitability and connectivity and to track over time pathological alterations, plastic changes and therapy-induced modifications in cortical circuits.

A recently proposed theory suggests that consciousness depends on the brain's ability to engage in complex activity patterns that are, at once, distributed among interacting cortical areas (integrated) and differentiated in space and time (information-rich). In a recent series of experiments the electroencephalographic TMS-evoked brain response was recorded in healthy subjects during wakefulness, non-rapid eyes movement sleep (NREM), under pharmacological conditions (anesthesia), and pathological conditions (severely brain-injured, vegetative state patients). Indeed, TMS/hd-EEG measurements showed that during wakefulness the brain is able to sustain long-range specific patterns of activation, while when consciousness fades in NREM sleep, anesthesia and vegetative state, the thalamo-cortical system produces either a local or a global slow wave which underlies respectively a loss of differentiation or integration.

We hypothesize that, like spontaneous sleep slow waves, the slow waves triggered by TMS are due to bistability between periods of neuronal activity (up-state) and silence (down-state) in cortical networks. Thalamo-cortical bistability could impair the ability of thalamo-cortical circuits to sustain long-range, differentiated patterns of activation, a key theoretical requisite for consciousness. Animal studies show that the extracellular signature of the down-state is a transient suppression of high frequency (>20Hz) power in the local field potential (LFP). More recently, intracranial recordings during NREM sleep in humans have shown that a intracranial stimulations induce a

widespread suppression of high frequencies (i.e. cortical down-states) that impair the ability of thalamo-cortical circuits to engage in causal interactions.

In the present thesis we use a TMS/hd-EEG approach in patients affected by disorders of consciousness such as vegetative state (VS) and minimally conscious state (MCS) to investigate whether bistability could underlie also pathological loss of consciousness. To verify this hypothesis, we recorded TMS-evoked potentials (TEPs) in awake VS and MCS patients as well as in healthy controls (HC) during wakefulness and NREM sleep. TEPs were analyzed by means of time-frequency analyses (power and phase-locking factor - PLF). We observed that TEPs recorded in VS patients were characterized by a large positive-negative deflection, closely resembling the one recorded in HC during NREM sleep. This sleep-like slow-wave was associated with a significant suppression of power in the high frequency band (>20 Hz) together with an early drop of PLF. Interestingly, in VS patients the power suppression slowly recovered to the baseline whereas in the NREM sleep of HC it was replaced by a late increase of power. Finally, the recovery of consciousness assessed in two patients evaluated longitudinally was paralleled by the resurgence of TEPs high frequency oscillations and by an increase of PLF duration.

These results suggest that the slow waves evoked by TMS in VS patients possibly reflect a condition of cortical bistability that prevents the entrainment of thalamocortical modules in effective interactions and, hence, the emergence of consciousness. Intriguingly, the resumption of TEPs high frequency oscillations and a longer duration of phase-locked components (PLF) seem to be associated with the recovery of consciousness. Since bistability is, in principle, reversible and its mechanisms are well understood at the cellular and network level, it may represent a suitable target for novel therapeutic approaches in patients in whom consciousness is impaired, in spite of preserved cortical activity.

OUTLINE and MY CONTRIBUTION

CHAPTER 1: in this chapter I briefly introduce the scientific problem of consciousness. According to theorethical and experimental neuroscience the human thalamo-cortical network is able to generate and sustain consciousness due to an optimal balance between functional integration and functional differentiation, otherwise defined as brain complexity. Here, cortical networks bistability is also introduced as a possible neurophysiological mechanism responsible for loss of consciousness (LOC) in physiological, pharmacological and pathological conditions.

CHAPTER 2: in this section I present a well established perturb-and-measure approach aimed at non-invasively assess human cortical excitability and effective connectivity. The approach is based on a combination of transcranial magnetic stimulation and electroencephalography (TMS/EEG) and eventually lead to measure brain complexity in the human brain through the calculation of the Perturbational Complexity Index (PCI).

Indeed, alterations of excitability and effective connectivity have been suggested to underlie neurologic and psychiatric conditions as shown in three studies that I have co-authored and that are presented in this chapter:

- Casarotto S., Canali P., Rosanova M., Pigorini A., **Fecchio M.**, Mariotti M., Lucca A., Colombo C., Benedetti F., Massimini M., "Assessing the effects of electroconvulsive therapy on cortical excitability by means of transcranial magnetic stimulation and electroencephalography." Brain Topography (2013) 26:326–337.

- Canali P., Sferrazza Papa G., Casali A.G., Schiena G., **Fecchio M.**, Pigorini A., Smeraldi E., Colombo C., Benedetti F., "Changes of cortical excitability as markers of antidepressant response in bipolar depression: preliminary data obtained by combining transcranial magnetic stimulation (TMS) and electroencephalography (EEG)." Bipolar Disorders (2014) 16: 809–819.

- Canali P., Sarasso S., Rosanova M., Casarotto S., Sferrazza Papa G., Gosseries O., **Fecchio M.**, Massimini M., Mariotti M., Cavallaro R., Smeraldi E., Colombo C., Benedetti

F., "Shared reduction of oscillatory natural frequencies in bipolar disorder, major depressive disorder and schizophrenia." Journal of Affective Disorders 184 (2015) 111–115.

Then, a review of a series of recent studies published by our group in which TMS/EEG has been employed to systematically measure excitability, connectivity and complexity of human cortical circuits in physiological (non-REM sleep), pharmacological (anesthesia) and pathological (vegetative state) LOC is presented.

- Sarasso S., Rosanova M., Casali A.G., Casarotto S., **Fecchio M.**, Boly M., Gosseries O., Tononi G., Laureys S., Massimini M., "Quantifying cortical EEG responses to TMS in (un)consciousness." Clinical EEG and Neuroscience (2014) Vol. 45(1) 40–49.

CHAPTER 3: in this section I propose a possible neurophysiological mechanism responsible for the collapse of brain complexity during LOC, firstly from an intracerebral perspective, then using TMS/EEG.

Specifically, I first report a recent study where intracranial stimulation and recordings have been employed to measure cortical excitability in humans in wakefulness and NREM sleep. This study shows that when directly perturbed in wakefulness cortical circuits engage in sustained and deterministic electrical oscillations. On the contrary, during non-REM sleep cortical circuits respond to a direct perturbation with a neuronal silence (OFF-period or downstate) which impairs the ability of thalamo-cortical modules to engage in causal interactions. This bistability possibly disrupts the ability of the thalamocortical system to integrate information and to sustain consciousness.

- Pigorini, A.**,** Sarasso, S., Proserpio, P., Szymansky, C., Arnulfo, G., Casarotto, S., **Fecchio, M.**, Rosanova, M., Mariotti, M., Lo Russo G., Palva, J.M., Nobili, L., Massimini, M., "Bistability breaks-off deterministic responses to intracortical stimulation during non-REM sleep", NeuroImage 112 (2015) 105–113.

In the second paragraph, I move from intracranial stimulations and recordings towards non-invasive methodologies based on TMS/EEG. Thus, I present the main project of this thesis that stems from the results of the TMS/EEG approach applied in vegetative state patients. These results show that, similarly to non-REM sleep, vegetative state is characterized by cortical

bistability that, hence, could be an important common neurophysiological mechanism underlying both physiological and pathological LOC.

This paragraph is focused on a recently submitted study:

- **Fecchio M.**, Rosanova M., Pigorini A., Sarasso S., Casarotto S., Seregni F., Gosseries O., Landi C., Casali A.G., Mariotti M., Trimarchi D., De Valle G., Laureys S., Massimini M., "Sleep-like cortical bistability in vegetative state patients", *submitted*

LIST OF PUBLICATIONS

- Casarotto S., Canali P., Rosanova M., Pigorini A., **Fecchio M.**, Mariotti M., Lucca A., Colombo C., Benedetti F., Massimini M., "Assessing the effects of electroconvulsive therapy on cortical excitability by means of transcranial magnetic stimulation and electroencephalography." Brain Topography (2013) 26:326–337.

- Canali P., Sferrazza Papa G., Casali A.G., Schiena G., **Fecchio M.**, Pigorini A., Smeraldi E., Colombo C., Benedetti F., "Changes of cortical excitability as markers of antidepressant response in bipolar depression: preliminary data obtained by combining transcranial magnetic stimulation (TMS) and electroencephalography (EEG)." Bipolar Disorders (2014) 16: 809–819.

- Canali P., Sarasso S., Rosanova M., Casarotto S., Sferrazza Papa G., Gosseries O., **Fecchio M.**, Massimini M., Mariotti M., Cavallaro R., Smeraldi E., Colombo C., Benedetti F., "Shared reduction of oscillatory natural frequencies in bipolar disorder, major depressive disorder and schizophrenia." Journal of Affective Disorders 184 (2015) 111–115.

- Sarasso S., Rosanova M., Casali A.G., Casarotto S., **Fecchio M.**, Boly M., Gosseries O., Tononi G., Laureys S., Massimini M., "Quantifying cortical EEG responses to TMS in (un)consciousness." Clinical EEG and Neuroscience (2014) Vol. 45(1) 40–49.

- Pigorini, A.**,** Sarasso, S., Proserpio, P., Szymansky, C., Arnulfo, G., Casarotto, S., **Fecchio, M.**, Rosanova, M., Mariotti, M., Lo Russo G., Palva, J.M., Nobili, L., Massimini, M., "Bistability breaks-off deterministic responses to intracortical stimulation during non-REM sleep", NeuroImage 112 (2015) 105–113.

LIST OF ABBREVIATIONS

AMPA: α-amino-3-hydroxy-5-methyl-4-isoxazolepropionic acid

BA: Brodmann area

BDNF: brain-derived neurotrophic factor

BPD: bipolar disorder

CamKII: enzymes Ca2+/calmodulin-dependent protein kinase II

CCEPs: cortico-cortical evoked potentials

CREB: cyclic adenosine monophosphate response element-binding protein

CRS-R: coma recovery scale–revised

ECS: electroconvulsive seizures

ECT: electroconvulsive therapy

EF: electric field

EI: effective information

EMCS: emergence from minimally conscious state

EMG: electromyogram

EOG: electrooculogram

ERSP: event-related spectral perturbation

GABA: Y-aminobutyric acid

GluR1: glutamate receptor 1

GMFP: global mean field power

GSK3B: glycogen synthase kinase 3 beta

HC: healthy controls

hd-EEG: high-density electroencephalography

HDRS: Hamilton depression rating scale

ICA: independent component analysis

IITC: information integration theory of consciousness

IRA: immediate response area

IRS: immediate response slope

LFP: local field potential

LMFP: local mean field power

LOC: loss of consciousness

LTP: long-term potentiation

max PLFt: latency at which PLF dropped below significance level

max SHFp: maximum level of suppression of high-frequency power

max SHFt: timing of the maximum high frequency suppression

max SWa: maximum amplitude of the evoked slow wave

MCS: minimally conscious state

MDD: major depressive disorder

MR: magnetic resonance

MRI: magnetic resonance imaging

NBS: navigated brain stimulation system

NMDA: N-methyl-D-aspartate

NREM: non-rapid eye movement

PCI: perturbational complexity index

PET: positron emission tomography

PLF: phase locking factor

REM: rapid eye movement

ROI: region-of-interest

RRM: random regression model

rTMS: repetitive TMS

SCZ: schizophrenia

SD: standard deviation

SEEG: stereotactic EEG

SPES: single-pulse electrical stimulation

TEPs: TMS-evoked potentials

TMS: transcranial magnetic stimulation

TrkB: receptor tyrosine kinase B

UWS: unresponsive wakefulness syndrome

VS: vegetative state

CHAPTER 1 – INTRODUCTION

It's really hard define what consciousness is. It seems something obvious, something we take for granted, but we can be in trouble if someone ask us to define it, and we can try to say only when it disappears, when we don't have experience of that.

Consciousness is "*what you lose on entering a dreamless deep sleep… deep anesthesia or coma… what you regain after emerging from these states*" (Edelman, 2007) and we know that "*every night, when we fall into dreamless sleep, consciousness fades, and reappears when we wake up or when we dream*"(Tononi, 2008).

During everyday life we assume that people around us are conscious, and, if in doubt, as when someone is resting with eyes closed, we can ask: if she/he answers that she/he was thinking or daydreaming, we infer she/he was conscious. But at times matters is not so clear: someone fast asleep shows no purposeful activity and will not respond to questions, yet she/he may be dreaming. Similarly, assess consciousness in some patients with severe brain injuries, with eyes open but unresponsive, may be not so straightforward and thus they can be judged clinically unconscious, even if they may be able to generate brain signals indicating they understood a question or a command (Cruse et al., 2011; Owen et al., 2006). In general, the problem is that while we assess the level of consciousness based on an individual's ability to connect and respond to the external environment, these features are not necessary for consciousness. Yet, to this day, we do not have a scientifically well-grounded measure of the level of consciousness that is independent of processing sensory inputs and producing appropriate motor outputs. Nevertheless, neuroscience is making progress in identifying the neural correlates of consciousness. While many of the proposed neural substrates of consciousness undoubtedly have heuristic value, empirical evidence still does not provide criteria for necessity and sufficiency. For example, measurements performed during seizures (Blumenfeld and Taylor, 2003) where subjects are unconscious and unresponsive despite increased brain metabolism suggested that the overall levels of brain activity may not be a reliable marker of the presence of consciousness. Along the same lines, positron emission tomography (PET) measurements showed that brain-injured patients can recover

consciousness from vegetative state, without necessarily increasing their brain metabolic rates (Laureys et al., 2004). On the other hand, recent measurements have still focused attention on the hypothesis that the level of consciousness could be critically determined by the power/synchronization of spontaneous, fast frequency oscillations in the thalamocortical system. Indeed, this hypothesis fails to explain the loss of consciousness (LOC) observed during non-rapid eye movement (NREM) sleep, propofol anesthesia and generalized tonic-clonic seizures, where hyper-synchronous broad-band oscillations can be observed (Arthuis et al., 2009). As a consequence, even apparently simple questions like "why does consciousness fades during early NREM sleep?" and "why does it restores during dreaming?" have been (and still are) unanswered, thus pointing to the need of robust empirical studies complemented by a self-consistent, general and parsimonious theoretical approach (Sarasso et al., 2014).

With the accumulation of empirical data, over the last decade theories of consciousness aimed at coherently account for experimental and clinical observations have been formulated. In particular, the Information Integration Theory of Consciousness (IITC), a recently proposed theory by Giulio Tononi (Tononi, 2008, 2004), suggests that consciousness depends not so much on the overall level of neuronal activation, on the occurrence of specific patterns of synchronous activity, or on the ability of cortical neurons to respond to sensory inputs, but rather on the joint presence of functional integration and functional differentiation in thalamo-cortical networks, otherwise defined as brain complexity (Massimini et al., 2012). Although integrated information can be measured exactly only in small simulated systems, the theory makes clear-cut predictions: integrated information should be high when consciousness is present and low whenever consciousness is lost. Practically, a straightforward way to gauge the conjoint presence of integration and information in real brains involves directly probing the cerebral cortex (to avoid possible subcortical filtering and gating) by employing a perturbational approach (thus testing causal interactions rather than temporal correlations) and examining to what extent cortical regions can interact as a whole (integration) to produce differentiated responses (information) (Sarasso et al., 2014).

In the next chapter a noninvasive perturbation approach based on a combination of transcranial magnetic stimulation and electroencephalography (TMS/EEG) is presented to gauge the brain

capacity to integrate information. This technique allows stimulating directly different subsets of cortical neurons and recording the immediate reaction of the rest of the brain. As shown in paragraphs 2.2.1, 2.2.2 and 2.2.3, TMS/EEG is also used to estimate time-domain markers of biological cortical excitability and cortical effective connectivity, key parameters of cortico-thalamic circuits functioning. In paragraph 2.3, based on measurements performed in sleeping subjects (Massimini et al., 2007, 2005a), anaesthesia (Ferrarelli et al., 2010) and patients affected by disorder of consciousness (Rosanova et al., 2012) we argue that TMS/EEG represents an effective way to appreciate to what extent different regions of the thalamocortical system can interact globally (integration) to produce specific responses (information) and how it was possible developing a short index to measure the balance between information and integration and, possibly, the brain's capacity for conscious experience.

Finally, in the third chapter, after "understanding" how to distinguish a conscious brain from another one that is not and after trying to quantify the brain's capacity for conscious experience, the question that arises is "which is the mechanism underlying the loss of consciousness?". Here we propose a possible neurophysiological mechanism responsible for reducing interactions between different thalamocortical regions, firstly from an intracerebral perspective during deep sleep, and then using a noninvasive TMS/EEG approach in a pathological condition of loss of consciousness, the vegetative state patients. Indeed, during NREM sleep, bistability may be mainly caused by increased activity of leak K+ channels, brought about by decreased brainstem cholinergic activity (McCormick et al., 1993), however increased inhibition within thalamocortical networks may play a crucial role in inducing bistability (Mann et al., 2009). We suggest that bistability in thalamocortical networks, the key mechanism responsible for the occurrence of sleep slow waves, may also be what prevents the brain from effectively integrating information during physiological LOC. Due to bistability, cortical neurons are unable to sustain balanced patterns of activation and tend to fall into a silent, hyperpolarized down-state after an initial activation (Massimini et al., 2012). We hypothesize that also during pathological LOC bistability may prevent the emergence of consciousness making portions of the thalamocortical system, otherwise healthy, unable to sustain balanced pattern of activations.

As an example, a direct lesion of brainstem activating systems may cause bistability through the very same mechanisms governing NREM sleep. Specifically, brainstem lesions that reduce the cholinergic, noradrenergic, histaminergic and glutamatergic ascending drive may result in enhanced leak and depolarization dependent K+ currents in cortical neurons (McCormick et al., 1993). Localized alterations, such as undetected cortical epileptic foci, can also exert a strong inhibitory drive on brainstem activating systems, thus producing diffuse cortical bistability (Englot et al., 2010). Alternatively, a form of bistability similar to the one observed during midazolam-induced LOC may result from cortical and subcortical lesions that alter the cortical balance between excitation and inhibition in favor of inhibition. For instance, recovery of language and motor function after stroke can be blocked by excessive inhibitory activity in the perilesional area; (Classen et al., 1997) this excessive inhibition may be generated locally or may be projected by healthy areas that become hyperactive (Murase et al., 2004). Thus, cortical lesions that, by themselves, would not necessarily impair consciousness may induce LOC by causing a general unbalance between excitation and inhibition in healthy portions of the thalamocortical system. An excess of thalamocortical inhibition from a hyperactive, subcortical inhibitory area could also explain the paradoxical effects of the sedative zolpidem, a nonbenzodiazepine hypnotic that potentiates $GABA_A$ receptors, on behavioral improvement of alertness and interactive behavior in severely brain-injured patients (Brefel-Courbon et al., 2007; Schiff, 2010; Whyte and Myers, 2009) .Another crucial event that may induce bistability following brain injury is cortical deafferentation. Severing the white matter with a cortical undercut results in slow waves and in a continuous alternation between up- and down-states in the partially deafferented gyrus, even when the animal and the rest of the brain are awake (Nita et al., 2007).

In all cases, evaluating the presence of bistability in the cerebral cortex of brain-injured patients is critically important. Indeed, while anatomical lesions and disconnections cannot be reversed, it may still be possible to reduce bistability and functional disconnections by acting pharmacologically on intrinsic neuronal properties (Sarasso et al., 2014).

CHAPTER 2 – EMPLOYING TMS/EEG TO MEASURE CORTICAL REACTIVITY IN HEALTHY SUBJECTS, PSYCHIATRIC AND NEUROLOGICAL PATIENTS

Different methods have been proposed in order to infer on a subject's level of consciousness solely based on brain activity. Some of these methods, such as spectral analysis (Berthomier et al., 2007) and the proprietary 'bispectral index' (Myles et al., 2004) seem to correlate empirically with consciousness but have no clear theoretical foundation. Other measures, such as neural complexity (Tononi, 2004) and causal density (Seth, 2005), are theoretically motivated (Seth et al., 2008) but have not yet been tested empirically. More or less explicitly, all these measures attempt to capture the coexistence of functional integration and functional differentiation in spontaneous (mainly EEG) brain signals. Yet, to dependably appreciate the brain's capacity for consciousness (defined as integrated information) one should go beyond spontaneous activity levels or patterns of temporal correlation among distant neuronal groups (functional connectivity). First, this is because the repertoire of available states is, by definition, potential and, thus, not necessarily observable. Second, because it is difficult to say whether a system is actually integrated or not by just observing the spontaneous activity it generates (Massimini et al., 2009). Indeed, the ability to integrate information can only be demonstrated from a causal perspective; one must employ a perturbational approach (effective connectivity) and examine to what extent subsets of neurons can interact causally as a whole (integration) to produce responses that are specific for that particular perturbation (information) (Massimini et al., 2009). Moreover, one should probe causal interactions by directly stimulating the cerebral cortex in order to avoid possible subcortical filtering or gating. Finally, since causal interactions among thalamocortical neurons develop on a sub-second time scale (just as phenomenal consciousness does), it is very important to record the neural effects of the perturbation with the appropriate temporal resolution.

Thus, in practice, one should find a way to stimulate different subsets of cortical neurons and measure, with good spatial-temporal resolution, the effects produced by these perturbations in the rest of the thalamocortical system. Today, this measurement can be performed non-invasively in

humans thanks to the development of a novel electrophysiological technique, based on the combination of TMS and hd-EEG (Ilmoniemi et al., 1997) (Figure 2.1).
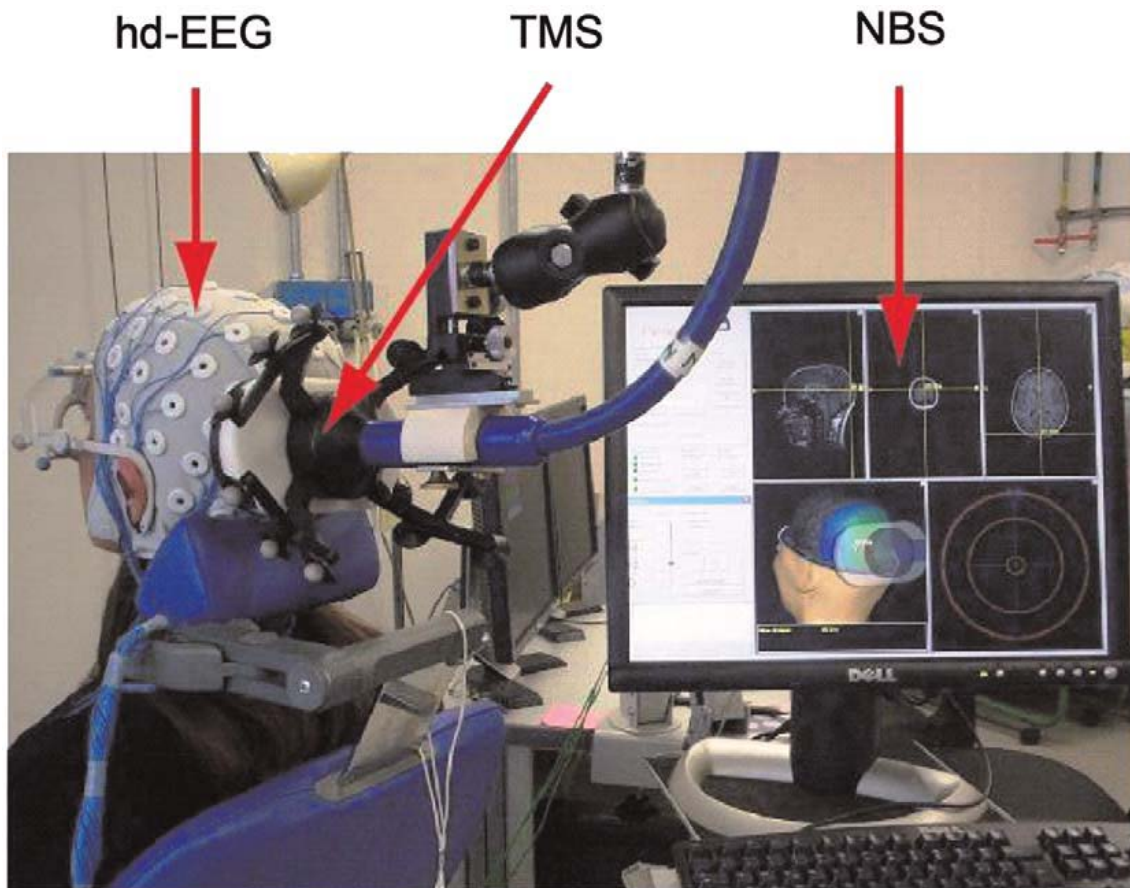
Figure 2.1 - TMS/EEG setup. In this example, a subject is sitting on an ergonomic chair while TMS is targeted to the occipital cortex. The red arrows indicate, from left to right, the three fundamental elements that compose the set-up: (1) a cap for high-density (60 channels) EEG recordings (hd-EEG) that is connected to a TMS-compatible amplifier; (2) a focal figure-of-eight stimulating coil (TMS), held in place by a mechanical arm; (3) the display of the navigated brain stimulation system (NBS). This system employs an infrared camera (not visible in this picture) to navigate TMS on a 3D reconstruction of the subject's MRI. The location and the intensity of the electric field induced by TMS are estimated and displayed in real time. To prevent the subject from perceiving the click associated with the coil's discharge, noise masking is played through inserted earplugs.

With TMS, the cerebral cortex is stimulated directly by generating a brief but strong magnetic pulse (<1 ms, 2 Tesla) through a coil applied to the surface of the scalp. The rapid change in magnetic field strength induces a current flow in the tissue, which results in the activation of underlying neuronal populations. The synchronous volley of action potentials thus initiated propagates along the available connection pathways and can produce activations in target cortical regions. By integrating TMS with MR-guided infrared navigation systems, it is also possible to render the perturbation controllable and reproducible, in most cortical regions. Finally, using multi-channel

EEG amplifiers that are compatible with TMS (Virtanen et al., 1999) one can record, starting just a few milliseconds after the pulse, the impact of the perturbation on the stimulated target and in distant cortical areas. Indeed, the integrated use of neuro-navigation systems, TMS and multichannel TMS-compatible EEG amplifiers together constitute a new brain scanning method in which stimulation is navigated into any desired brain target and the concurrently recorded scalp potentials are processed into source images of the TMS-evoked neuronal activation (Komssi and Kähkönen, 2006).

It is worth highlighting some of the specific advantages that TMS/EEG may offer as a tool to probe the brain:

1) TMS-evoked activations are intrinsically causal (Paus, 2005). Thus, unlike methods based on temporal correlations, TMS/EEG immediately captures the fundamental mechanism that underlies integration, that is the ability of different elements of a system to affect each other.

2) TMS/EEG by-passes sensory pathways and subcortical structures to probe directly the thalamocortical system. Therefore, unlike peripherally evoked potentials and evoked motor activations, TMS/EEG does not depend on the integrity of sensory and motor systems and can access any patient (deafferentated or paralyzed). Moreover, with TMS one can stimulate most cortical areas (including associative cortices) employing several different parameters (intensity, angle, current direction), thus probing a vast repertoire of possible responses, above and beyond observable ongoing brain states.

3) TMS-evoked potentials can be recorded with millisecond resolution, a time scale that is adequate to capture effective synaptic interactions among neurons.

4) TMS/EEG does not require the subject to be involved in a task and the observed activations are not affected by the willingness of the subject to participate nor by his effort and performance. Hence, this approach is well suited to assess the objective capacity of thalamo-cortical circuits independently on behavior.

5) TMS/hd-EEG can be made portable in order to overcome the logistical and economic hurdles that may separate severely brain-injured patients from advanced imaging facilities.

Thus, at least in principle, TMS/EEG may represent an appropriate tool to approximate a theoretical measure of consciousness not only in healthy subjects, but above all at the patient's bedside. However, the question whether this technique may actually detect changes in the brain's capacity to integrate information can only be answered experimentally. For example, one should demonstrate that TMS-evoked activations are widespread (integration) and specific (information) in a conscious brain but that they become either local (revealing a loss of integration) or stereotypical (revealing a loss of information) when the same brain becomes unconscious. In this chapter we first describe methodological aspects of TMS/EEG data analysis and then we describe the results of experiments where TMS/EEG was used to understand what changes in human thalamo-cortical circuits when consciousness fades upon falling asleep, during anesthesia and in pathological conditions (disorder of consciousness).

2.1 – TMS/hd-EEG Recording

2.1.1 – TMS Targeting

A Focal Bipulse 8-Coil (mean/outer winding diameter ca. 50/70 mm, biphasic pulse shape, pulse length ca. 280 μs, focal area of the stimulation hot spot 0.68 cm^2) driven by a Mobile Stimulator Unit (Eximia TMS Stimulator, Nexstim Ltd., Helsinki, Finland) was targeted to specific cortical locations using a Navigated Brain Stimulation (NBS system (Nexstim Ltd., Helsinki, Finland). Structural MRI images at 1 mm^3 spatial resolution were acquired with a 1T Philips scanner from all subjects enrolled in the studies. The NBS system employs a 3D infrared Tracking Position Sensor Unit to map the positions of TMS coil and subject's head within the reference space of individual structural MRI in order to precisely identify the TMS stimulation target. Optimal alignment between MRI fiducials and digitized scalp landmarks (nasion, left and right tragus) was verified prior to all experiments. NBS also calculates on-line the distribution and intensity of the intracranial electric

field induced by TMS, using a best-fitting spherical model of subjects' head and brain and taking into account the exact shape, 3D position and orientation of the coil. TMS hot spot (i.e. 98% of the maximum stimulating electric field calculated at individually-determined depth) was kept fixed to the stimulation target with the current perpendicular to its main axis. The reproducibility of the stimulation coordinates across sessions was guaranteed by an aiming device that indicated in real-time any deviation from the desired target greater than 3 mm.

2.1.2 – hd-EEG Recording

TMS-evoked potentials were recorded by a TMS-compatible 60-channel EEG amplifier (Nexstim Ltd., Helsinki, Finland). Impedance at all electrodes was kept below 5 kΩ. The EEG signals, referenced to an additional electrode on the forehead, were filtered (0.1-500 Hz) and sampled at 1,450 Hz with 16 bit resolution. At the end of each experiment, a pen visible to the infrared camera was used to digitise the EEG electrode positions on the subject's head. Two extra electrodes were used to record the vertical electrooculogram (EOG).

During EEG recording, subject's perception of the clicks produced by TMS coil's discharge was eliminated by means of inserted earplugs continuously playing a masking noise (always below 90 dB). A thin layer of foam was placed between coil and scalp (resulting in less than 1 mm thickness when coil was pressed against the head) in order to attenuate bone conduction. As previously demonstrated, this procedure effectively prevented any contamination of EEG signals by auditory potentials elicited by TMS-associated clicks (Massimini et al., 2007, 2005a).

2.1.3 – EEG Pre-processing

Trials containing activity from other sources than neural were automatically rejected if EOG exceeded 70 μV (ocular activity) and/ or absolute power of EEG channel F8 in the fast beta range (N25 Hz) exceeded 0.9 μV^2/Hz (van de Velde et al., 1998)(indicating activity of fronto-temporal muscles). After averaging, channels with bad signal quality or large residual artifacts were excluded from further analysis. In all TMS sessions we retained at least 50 good channels, with an inter-session variation of at most 4 channels in each subject, thus ensuring an estimation of cortical

generators that was reliable and comparable across sessions (Laarne et al., 2000). Signals were low pass filtered (45 Hz), down-sampled to 725 Hz and re-referenced to the common average reference. Independent component analysis (ICA) was performed in order to remove the remaining artefacts. Figure 2.1.1A exhibits an example of pre-processed single-subject TMS-evoked potentials after stimulation of BA19.
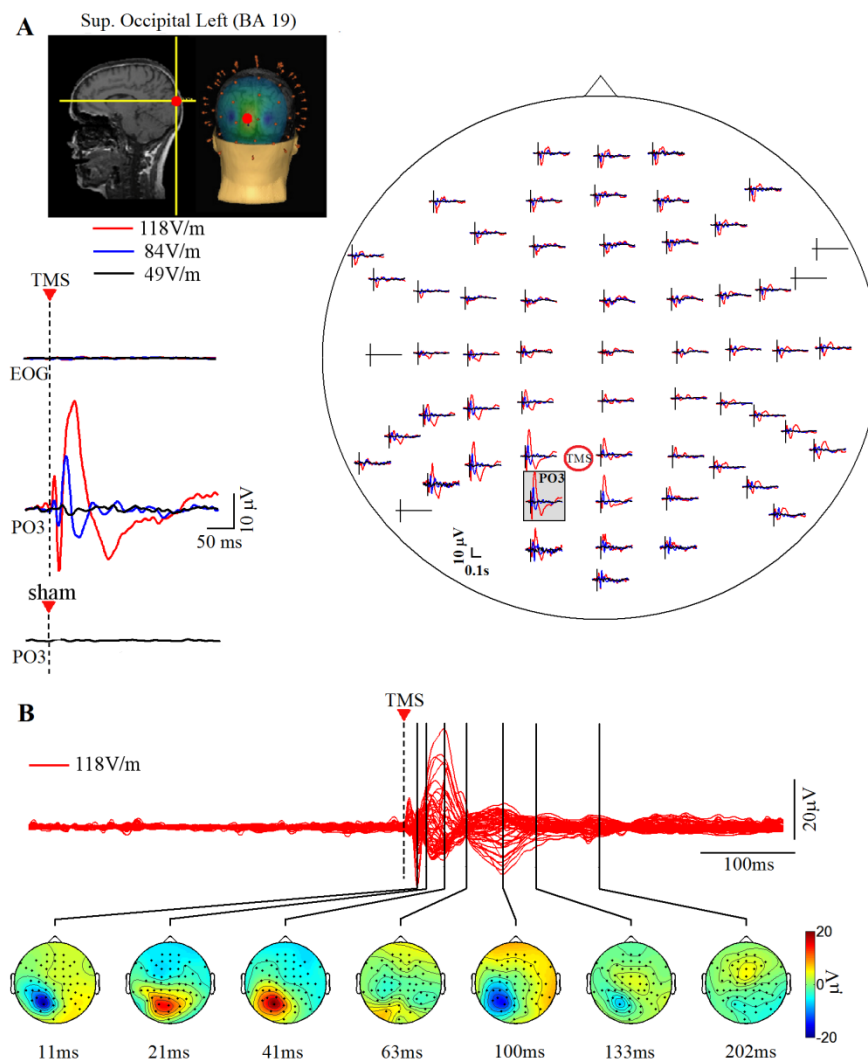
Figure 2.1.1 - Single-subject TMS-evoked potentials. A) Top Left: Location of the TMS stimulation target (left superior occipital lobule, BA 19) is shown on individual MRI, together with the approximate distribution of the electric field induced by TMS pulses in the cortex. The orange spots represent the digitized positions of EEG electrodes on the scalp. Right: Averaged TMS-evoked potentials recorded from 60 electrodes on the scalp at three different intensities of stimulation (red 118V/m, blue 84V/m, black 49V/m). Approximate location of the TMS target is reported with a red circle. Bottom left: zoom on averaged EOG activity, TMS-evoked potentials recorded on PO3 lead, and also during a sham TMS session, when the TMS coil was discharged while separated from the scalp by a 4 cm Plexiglas cube. B) Superimposition of the averaged TMS-evoked potentials recorded from all channels (Butterfly plot) at a stimulation intensity of 118V/m. Color-coded instantaneous topographic distribution of the potential on the scalp is displayed for 7 relevant time samples after TMS pulse delivery.

2.2 – TMS/EEG to assess key parameters of human cortical circuits functioning

Despite a highly static structure, the human brain generates a large repertoire of behavioral and psychological phenomena spanning from simple motor acts to cognition and consciousness. This ability relies on the activation of highly specialized thalamic and cortical structures that interact on a subsecond timescale by means of long-range bundles of fibers (Park and Friston, 2013; Sporns, 2013). Hence, the electrical reactivity of the cerebral cortex to a direct, local stimulation (cortical excitability) and the ability of distant cortical regions to causally interact (cortical effective connectivity) are key parameters of cortico-thalamic circuits functioning. Since recently, by combining navigated TMS with EEG (TMS/EEG), it is possible to record the immediate response of the human brain to a cortical perturbation. In this way, TMS/EEG allows to measure directly and non-invasively changes of cortical excitability and effective connectivity occurring in physiological, pharmacological and pathological conditions (Ziemann et al., 2015).

In the following paragraphs, three different studies are reported, showing the application of TMS/EEG to estimate time-domain markers of biological excitability and connectivity.

Specifically:

- paragraph 2.2.1 is referred to the paper titled "Assessing the Effects of Electroconvulsive Therapy on Cortical Excitability by Means of Transcranial Magnetic Stimulation and Electroencephalography" by Casarotto et al., 2013 published on Brain Topograpghy.

- paragraph 2.2.2 is referred to the paper titled "Changes of cortical excitability as markers of antidepressant response in bipolar depression: preliminary data obtained by combining transcranial magnetic stimulation (TMS) and electroencephalography (EEG)" by Canali et al., 2014 published on Bipolar Disorders.

- paragraph 2.2.3 is referred to the paper titled "Shared reduction of oscillatory natural frequencies in bipolar disorder, major depressive disorder and schizophrenia" by Canali et al., 2015 published on Journal of AffectiveDisorders.

2.2.1 – Assessing the Effects of Electroconvulsive Therapy on Cortical Excitability by Means of Transcranial Magnetic Stimulation and Electroencephalography

Electroconvulsive therapy (ECT) is generally recommended to drug-resistant patients suffering from severe major depression, because of its significant short-term antidepressant effects (UK ECT Review Group, 2003). The mechanism of action of ECT still needs to be fully characterized, although several hypotheses have been conceived, involving neurotransmitter systems (Yatham et al., 2010), endocrinological pathways (Kunugi et al., 2006), and neurogenesis (Madsen et al., 2000; Nibuya et al., 1995).

In animals, electroconvulsive seizures (ECS) have several effects on synaptic plasticity, gene transcription, and cell proliferation. ECS induces potentiation-like long-lasting synaptic changes (Stewart et al., 1994), increases the expression of neurotrophins, especially brain-derived neurotrophic factor (BDNF), and thus the activation of their receptor tyrosine kinase B (TrkB) (Altar et al., 2004; Nibuya et al., 1995) and stimulates the proliferation of neuronal and glial cells in the frontal cortex and hippocampus (Madsen et al., 2004; Malberg et al., 2000; Perera et al., 2007) of rats and nonhuman primates. BDNF/TrkB receptors promote neuronal function, growth and regeneration (Mamounas et al., 1995) and are mainly located at glutamatergic synapses, where they trigger synaptic potentiation and serve as activity-dependent modulators of synaptic plasticity (Mattson, 2008; Minichiello, 2009). Glial cells are also involved in the glutamatergic neurotransmitter system, by providing energy to neurons and releasing neurotrophic factors (Ben Achour and Pascual, 2010).

On the other hand, clinical studies have associated stress and depression with atrophy and loss of neurons and glia, especially in the prefrontal cortex and hippocampus (Duman and Voleti, 2012; Salvadore et al., 2011). An abnormally reduced expression of BDNF/TrkB has been observed in the frontal cortex and hippocampus of suicide patients (Dwivedi Y et al., 2003). Moreover, depressive symptoms have been correlated with dysfunction of the prefrontal cortex (George et al., 1994), particularly concerning its relationship with limbic structures implicated in the regulation of mood and anxiety (Drevets, 2000; G E Alexander et al., 1986; Suwa et al., 2012).

The existence of a causal relationship among depression, plasticity and neurotrophins proposed by previous literature (Manji et al., 2001; Zarate et al., 2003) has encouraged to explore the modulation of motor cortex excitability induced by ECT in humans (Bajbouj et al., 2006, 2005; Chistyakov et al., 2005; Sommer et al., 2002). The results of these studies are not conclusive, since cortical excitability was found to be either decreased (Bajbouj et al., 2006, 2005; Sommer et al., 2002) or increased (Chistyakov et al., 2005) after treatment as compared to baseline. However, two of these studies (Bajbouj et al., 2005; Sommer et al., 2002) referred to single cases and all of them used the peripheral muscular responses to transcranial magnetic stimulation (TMS) of the primary motor cortex to estimate cortical excitability.

Today, a complementary, direct measure of cortical excitability in humans can be obtained non-invasively by means of transcranial magnetic stimulation combined with electroencephalography (TMS/EEG) (Ilmoniemi et al., 1997; Komssi and Kähkönen, 2006; Ziemann, 2011). This approach allows to directly perturb cortical regions and to record the immediate electrophysiological responses of the stimulated neurons. Most important, TMS-evoked potentials (TEPs) are characterized by high test–retest reproducibility, provided that stimulation parameters (site, intensity and angle) are accurately controlled across subsequent sessions by means of a magnetic resonance (MR)-guided navigation system (Casarotto et al., 2010). Hence, TMS/EEG has been successfully applied to detect, at the group level, cortical excitability changes induced by repetitive TMS (rTMS) in healthy individuals (Esser et al., 2006; Veniero et al., 2010). In these cases, the local synaptic potentiation deliberately induced in the motor cortex by high-frequency rTMS was measured as an increase of the amplitude of early TMS-evoked EEG responses between 0 and 80 ms (Esser et al., 2006; Veniero et al., 2010). Similarly, a recent TMS/EEG study (Huber et al., 2013) has allowed to detect a physiological increase of cortical excitability with time awake, that became significant at the single-subject level after one night of sleep deprivation.

In this work, we employ TMS/EEG to study the electrophysiological changes induced by ECT in human cortical circuits. Thus, we measured the changes in the immediate EEG response to TMS of the frontal cortex before and after a course of ECT. The aim of this study was to contribute to the

understanding of the electrophysiological mechanisms of ECT in the human brain and to evaluate novel tools for monitoring and guiding neuromodulation protocols for the treatment of depression.

2.2.1.1 Materials and Methods

The experimental protocol involved two TMS/EEG recording sessions for each patient, that were performed, respectively, the day before the first administration of ECT (pre-ECT) and the day after the last administration of ECT (post-ECT), early in the afternoon at about 3:00 pm. The same stimulation parameters were applied to each patient in both sessions.

Participants

Eight inpatients suffering from Major Depressive Disorder, as diagnosed according to the DSM-IV criteria, participated in this study (Table 2.1). Physical examination, laboratory tests and electrocardiograms were performed at admission. All patients were referred to ECT because they were drug-resistant, i.e. showed a lack of improvement to at least two different treatments with antidepressants, at adequate dosage and duration (>6 weeks) (Fava, 2003). No patient had received ECT within 6 months prior to study enrolment. Additional diagnosis on axis I besides major depression, mental retardation on axis II, history of drug/alcohol abuse or dependency, and major medical/neurological disorders were regarded as exclusion criteria. In addition, patients with medical history of seizures, convulsions, loss of consciousness and traumatic brain injury, carriers of intracranial metallic objects and/or of cardiac pace-makers were excluded to prevent potential adverse effects of TMS. Severity of the current major depression episode was rated on the 21-item Hamilton Depression Rating Scale (HDRS) (Hamilton, 1960), administered by a qualified psychiatrist. HDRS was assessed at baseline, after each ECT session, and at the end of the whole treatment. All patients were properly acquainted with the experimental procedures (Mini-Mental State Examination was always above 26) before signing a written informed consent to participation. Moreover, we explicitly reassured them about the possibility of interrupting the experiment upon any unpleasant feeling. The study was approved by the Local Ethical Committee.

Table 2.1 - Demographic characteristics

Patient	Gender	Age (years)	Age of onset of depression	Family history	*n°* previous episodes	Duration current episode (months)	Concurrent drug treatment
1	F	54	50	No	2	16	TCA,NL
2	M	42	28	No	2	24	TCA
3	F	60	57	No	1	24	TCA
4	M	53	31	Yes	2	36	TCA
5	F	44	15	Yes	3	6	SNRI
6	F	51	35	Yes	2	24	TCA
7	F	61	41	Yes	7	7	SNRI
8	F	51	39	Yes	3	12	SNRI

F female, M male, SNRI serotonin norepinephrine reuptake inhibitors, TCA tricyclics, NL neuroleptics, SSRI selective serotonin reuptake inhibitors

ECT Delivery

ECT was administered twice a week with bilateral electrode placement (spECTrum 5000Q®, MECTA, Tualatin, OR, USA). Two circular flat electrodes (diameter: 5.08 cm) were positioned on both sides of the head with midpoints approximately 2.54 cm above the center of a line connecting the tragus and the external canthus. Current was delivered through trains (duration: 1.39 ± 0.13 s) of rectangular, constant-current pulses (amplitude: 800 mA) with alternating polarity (pulse width: 1.41 ± 0.12 ms; pulse pairs per second: 57.36 ± 7.36 Hz). The dose titration method for eliciting adequate seizures and other technical parameters were established according to (American Psychiatric Association. Task Force on Electroconvulsive Therapy.2001). Brief general anesthesia was induced with thiopental (i.v. 5 mg/kg) and succinylcholine (i.v. 1 mg/kg) for relaxation. In addition, pre-medication with atropine (i.m. 0.5 mg/kg) was used to reduce the risk of vagal immediate bradyarrhythmia or asystole. Each patient was administered a variable number of ECT sessions, according to the individual clinical needs evaluated by experienced clinicians (Table 2.2). Each patient was carefully evaluated by qualified psychiatrists throughout the whole ECT protocol, in order to monitor the therapeutic and cognitive effects of treatment. In particular, ECT was

administered until remission of depressive symptoms (at least 50 % reduction of HDRS score as compared to pre-ECT assessment) or onset of unwanted side effects pertaining cognitive functions.

Table 2.2 - Clinical and neurophysiological effects of ECT

Patient	n° ECT sessions	HDRS			IRA (μV^2)			IRS ($\mu V/ms$)		
		Pre-ECT	Post-ECT	p	Pre-ECT	Post-ECT	p	Pre-ECT	Post-ECT	p
1	8	38	18		47	58	.034	0.57	0.80	.006
2	7	27	13		74	82	.014	0.76	1.07	.000
3	3	22	3		57	75	.020	0.64	0.67	.771
4	8	20	12		9	18	.026	0.04	0.46	.004
5	7	25	16		132	196	.002	0.21	0.52	.000
6	9	19	12		14	23	.010	0.09	0.14	.268
7	5	25	2		9	21	.002	0.15	0.31	.000
8	3	19	3		24	33	.024	0.36	0.37	.717
Mean ± SE	6.3 ± 0.82	24.4 ± 2.22	9.9 ± 2.23	.025	45.7 ± 14.94	63.2 ± 20.90	.025	0.35 ± 0.1	0.54 ± 0.11	.025

SE standard error, ECT electroconvulsive therapy, HDRS Hamilton Depression Rating Scale, IRA immediate response area, IRS immediate response slope

TMS/EEG Recording

TMS was delivered with a Focal Bipulse 8-Coil (mean/outer winding diameter ca. 50/70 mm, biphasic pulse shape, pulse length ca. 280 µs, focal area of the stimulation hot spot 0.68 cm2; Eximia TMS Stimulator, Nexstim Ltd., Helsinki, Finland). Stimulation parameters were controlled by means of a Navigated Brain Stimulation (NBS) system (Nexstim Ltd., Helsinki, Finland), that employs a 3D infrared Tracking Position Sensor Unit (Polaris, Northern Digital Inc., Waterloo, Canada) and integrates T1-weighted structural MR images recorded from all patients (3.0 tesla scanner, Intera, Philips Medical Systems, Best, The Netherlands; 0.9 × 0.9 × 0.8 mm spatial resolution). This equipment maps in real time the positions of TMS coil and subject's head within the reference space of individual MR images by aligning the fiducials selected on structural images

with the corresponding digitized scalp landmarks (nasion, left and right tragus). The NBS system (Ruohonen and Ilmoniemi, 1999; Ruohonen and Karhu, 2010) allowed (i) to precisely stimulate a cortical target selected a priori on individual MR images, (ii) to estimate the electric field (EF) induced on the cortical surface by TMS pulses, and (iii) to accurately repeat the same stimulation parameters between sessions. The induced EF clearly depends on stimulation intensity, expressed as percentage of the maximal stimulator output, on the relative position between subject's head and TMS coil, and on the geometrical and physical properties of head tissues between the stimulator and the cortical surface. The distribution and intensity (expressed in V/m) of the intracranial induced EF was estimated on-line using a locally best-fitting spherical model of the subjects' head and brain and taking into account the exact shape, 3D position and orientation of the TMS coil. Precise control over stimulation coordinates across sessions was obtained by means of a virtual aiming device, that displayed in real time on a screen any deviation from the desired target greater than 3 mm and therefore allowed manual adjustments of the stimulator position.

The middle-caudal portion of the superior frontal gyrus close to the midline (near the boundary between Brodmann areas 6 and 8) was selected as target area. Indeed, the prefrontal cortex is maximally involved by current flow during bilateral ECT (Boylan et al., 2001; Lee et al., 2012) and its metabolic activity is significantly modulated by treatment (Nobler et al., 2000; Suwa et al., 2012). Moreover, this targeting ensured maximal distance from cranial muscles, which are mainly distributed over the lateral surface of the scalp and whose unwanted activation by TMS would affect EEG recordings. TMS pulses were delivered to the target area nearby the mid-sagittal plane: however, since TMS is not suited to properly stimulate along the longitudinal fissure (Thielscher et al., 2011), the coil was slightly moved either towards the left or the right side of the head in order to better deliver TMS pulses on the convexity of the middle-caudal portion of the superior frontal gyrus, with the current perpendicular to its main axis. Patients were randomly divided into two groups of equal size for being predominantly stimulated either on the left (four patients) or right (four patients) hemisphere. This protocol was applied to obtain a comparable amount of data from stimulation of both hemispheres in a small group of patients, in the lack of a priori assumptions about laterality of the effects of bilateral ECT. Moreover, this approach allowed to shorten the

duration of TMS/EEG sessions, thus limiting any additional stress to patients. Two patients were particularly collaborative and therefore agreed to being stimulated on both hemispheres. Excitation threshold has been reported to change with cortical location (Boroojerdi et al., 2002; Gerwig et al., 2003; Stewart et al., 2001); moreover, we specifically delivered TMS pulses over the prefrontal cortex. Therefore, we set stimulation intensity relying on the actual intracranial induced EF estimated by the NBS system rather than referring to the minimum stimulator output needed to produce a reliable electromyographic response (motor threshold; Rossi et al., 2009). In all patients, the maximum EF induced by TMS on the cortical surface was kept in the range 90–130 V/m by means of the NBS system (corresponding to 56–75 % of the maximal stimulator output). Previous works have shown that this stimulation intensity elicits EEG responses with good signal-to-noise ratio (Casali et al., 2010; Komssi et al., 2007; Rosanova et al., 2009). The location of the maximum EF induced by TMS on the cortical surface was labeled TMS hotspot and was always located within the target area. Inter-stimulus interval was randomly jittered between 1500 and 1800 ms (equivalent to ca. 0.56–0.67 Hz). This stimulation rate does not induce significant reorganization/plasticity processes that might possibly either affect EEG responses to TMS or interfere with the longitudinal measurements (Casarotto et al., 2010). During TMS stimulation, patients wore inserted earplugs continuously playing a masking noise that abolished the auditory potentials elicited by TMS-associated clicks (Massimini et al., 2005a).

A 60-channel TMS-compatible EEG amplifier (Nexstim Ltd., Helsinki, Finland) was used to record artifact-free electrical brain responses to single TMS pulses (Virtanen et al., 1999). On average, 247 ± 11 (mean ± standard error) pulses were delivered in each session (range 199–332 pulses). Impedance at all electrodes was kept below 5 kΩ. EEG signals were band-pass filtered between 0.1 and 500 Hz and sampled at 1,450 Hz with 16 bit resolution. In order to monitor ocular movements and blinks, vertical electrooculogram was recorded with two extra sensors. The position of EEG electrodes on the scalp was digitized and provided to the NBS system for integration with individual MR images and for allowing a precise replacement of the EEG cap between sessions.

Data Analysis

Data analysis was carried out using MATLAB® (2006a, The MathWorks, Natick, MA, USA). Principal Component Analysis was applied to automatically reduce ocular artifacts (Casarotto et al., 2004). Single TEPs residually contaminated by muscular activity (absolute power of EEG channel F8 above 25 Hz > 0.9 µV2/Hz)(van de Velde et al., 1998) were automatically rejected. After averaging a minimum of 90 artifact-free trials (mean ± standard error across sessions: 127 ± 10 trials; range 90–189 trials), channels containing high-frequency muscular activity or large residual artifacts were excluded from further analysis. Bad channels (always fewer than ten) were usually contaminated by high-frequency muscular activity and were mostly located peripherally over fronto-temporal muscles. Signal quality of channels nearby the stimulated site was always acceptable. In order to apply data analysis to the same number of channels across sessions and patients, we have interpolated bad channels using "Matlab 4 griddata method" (Sandwell, 1987). Artifact-free signals were band-pass filtered between 2 and 80 Hz, down-sampled to 725 Hz, and re-referenced to the common average reference.

We measured cortical excitability from the immediate EEG response to TMS. In all patients, TMS triggered a large, early TEP component, consisting in a positive wave (Figure 2.2.1a, white reversed U-shaped trace) followed by a negative wave (Figure 2.2.1a, white U-shaped trace) and with maximum amplitude in the electrode overlying the TMS target. We selected for each patient the six neighboring EEG channels (region-of-interest (ROI)) where this component had the largest amplitude (Figure 2.2.1a, black traces) and we quantified two morphological features of this component, the immediate response area (IRA) and slope (IRS). IRA was obtained from the local mean field power (LMFP) of the TEPs across the ROI channels (computed as the square root of squared TEPs averaged across the ROI channels; Figure 2.2.1b) (Lehmann and Skrandies, 1980): in particular, we detected the two local minima encompassing the early consecutive positive and negative evoked waves (light gray shadow, Figure 2.2.1), and then we calculated the integral of the LMFP within this interval (dark gray shadow, Figure 2.2.1b). Since TEPs were highly reproducible across sessions, we used the same time interval in both pre- and post-ECT sessions. IRS was

computed on single-trial TEPs averaged in space across the ROI channels: specifically, it was defined as the mean first derivative of the rising side of the positive wave (Vyazovskiy et al., 2008) of the early TMS-evoked component (Figure 2.2.1c). Identification of the ROI channels, of the early TMS-evoked component, and of the local minima of the LMFP was performed for each patient separately with a computerized procedure and was then verified manually.

In order to study the effects of ECT at the group level, we applied a non-parametric paired sign test to compare the HDRS score, IRA, and IRS values between pre- and post-ECT sessions across patients. In addition, IRA and IRS values were statistically compared between sessions at the single-subject level. In the case of IRA, we applied the following non-parametric permutation-based statistical analysis: (i) under the null hypothesis of equivalence between pre- and post-ECT recordings, 1000 "mixed" TEPs were constructed by averaging single trials randomly selected from the two sessions; (ii) LMFP was computed from these surrogate TEPs and was used to estimate the empirical null distribution of IRA; (iii) cortical excitability in each patient was considered significantly affected by ECT with probability of false positives α when the actual IRA values laid beyond the α-th percentile tails of the null distribution. IRS was compared between sessions by non-parametric Wilcoxon rank sum test applied to single-trial slope values in each patient.
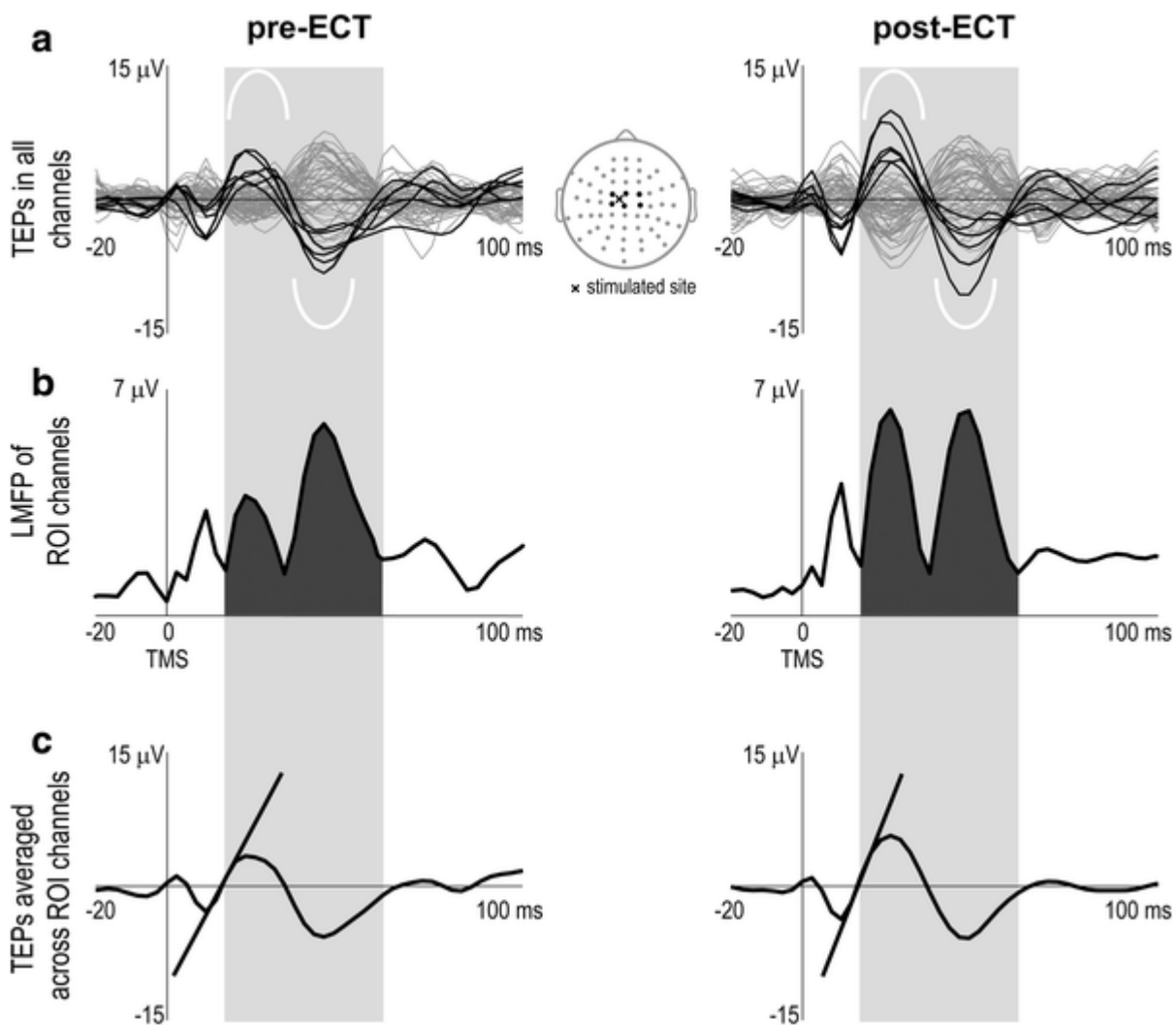
Figure.2.2.1 - Computation of cortical excitability in patient 1. a Lateral plots represent the average TEPs superimposed in all EEG channels before (pre-) and after (post-) ECT. Central map depicts the electrodes arrangement (black and gray dots) on the scalp. Black traces correspond to ROI channels, located nearby the stimulated site (black cross) and containing a large, early TEP component, consisting in a positive wave (white reversed U-shaped trace) followed by a negative wave (white U-shaped trace). **b** LMFP of the ROI channels. Cortical excitability was measured by the subtended area (dark gray shadow) between the two local minima (light gray shadow) encompassing the early consecutive positive and negative waves triggered by TMS (IRA). **c** TEPs averaged across the ROI channels in the two conditions. Slanting lines highlight the slope of the rising

2.2.1.2 Results

At the group level, the clinical effect of ECT was a significant reduction of the HDRS score (p < .025) as compared to baseline values (Table 2.2, Figure 2.2.2a left panel). TEPs displayed similar morphology across patients and were characterized by an early evoked component consisting of a positive wave between 13 ± 2 and 27 ± 5 ms followed by a negative wave peaking at about 47 ± 5 ms; the grand average TEP across patients (Figure 2.2.2a right panel) shows that the amplitude of this component was clearly increased after ECT. IRA and IRS values were significantly increased

at the group level after ECT (Table 2.2). Moreover, the increase of IRA after ECT as compared to baseline was significantly correlated with the corresponding increase of IRS (Pearson's correlation = .86, R^2 = .70, p < .006).

Statistical analysis further confirmed that the modulation of cortical excitability brought about by ECT was significant at the single-subject level. Figure 2.2.2b displays the time course of individual TEPs and LMFP within the ROI channels. The morphology of the immediate EEG response to TMS was generally comparable among individuals and was highly reproducible between pre- and post-ECT sessions in the same patient. Most important, in all patients we observed an increase of the consecutive positive and negative waves early evoked by TMS and a corresponding increase of the LMFP after ECT. Non-parametric statistical comparison between pre- and post-ECT sessions showed that IRA was significantly increased in each and every patient (Table 2.2; Figure 2.2.2c), while IRS increase was significant in all but 3 patients (Table 2.2; Figure 2.2.2d; patients 3, 6, 8).

At the group level, the percentage reduction of HDRS by treatment was inversely correlated with the number of ECT sessions (Pearson's correlation = −.89, R^2 = .75, p < .004), indicating that mood improved more in patients with a faster response to ECT. A positive trend was observed between the percentage reduction of HDRS in post-ECT compared to pre-ECT session and the corresponding percentage increase of IRA, although correlation was not statistically significant (Pearson's correlation = .53, R^2 = .28, p < .18).
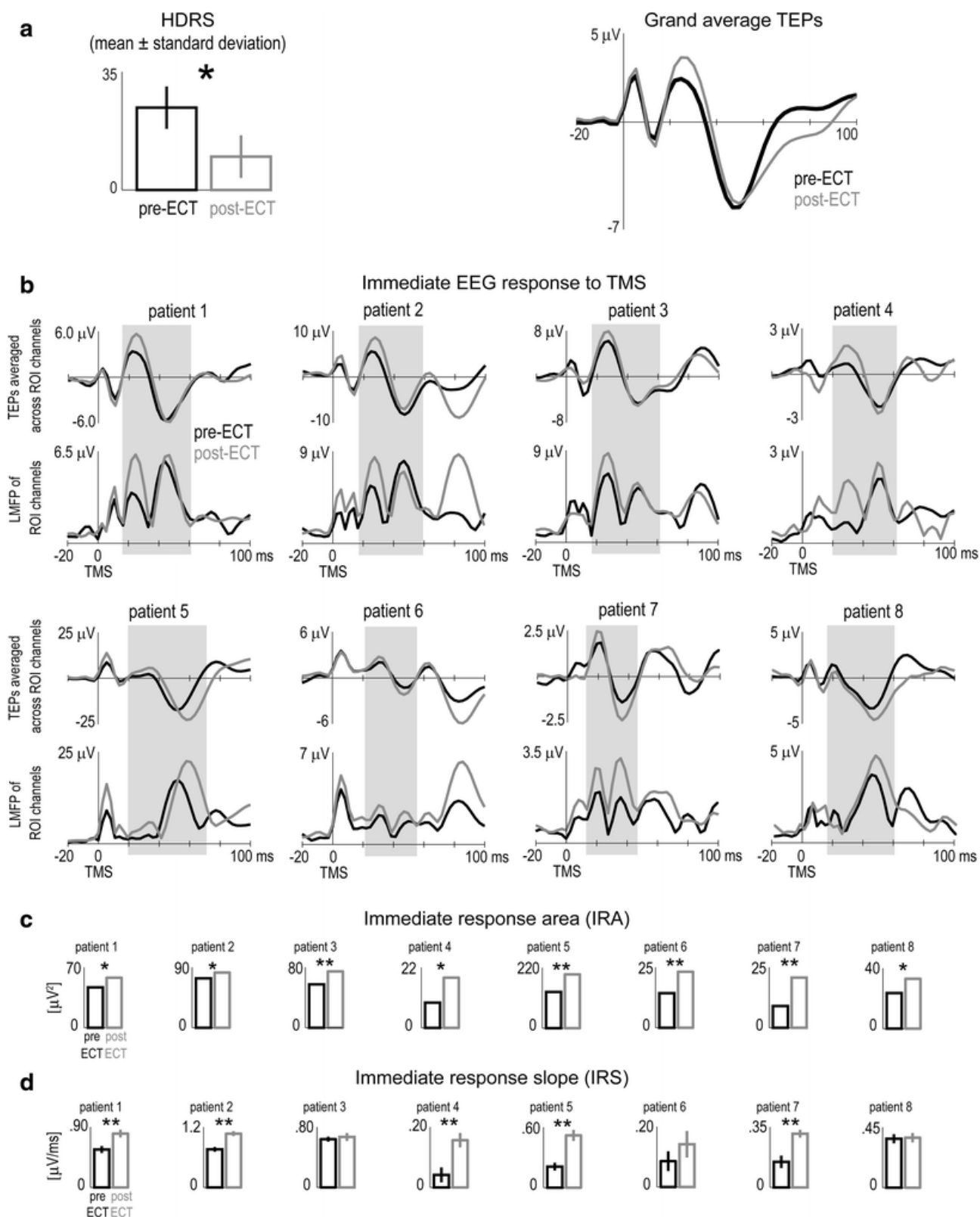
Figure 2.2.2 - a (Left) At the group level, the HDRS assessed after (gray bar) ECT was significantly smaller (p < .025) than before treatment (black bar). (Right) Superimposition of grand average TEPs collected before (black trace) and after (gray trace) ECT. b Individual time courses of the TEPs averaged across ROI channels and of the LMFP of ROI channels before (black traces) and after (gray traces) ECT. c Single-subject comparisons (using permutation-based statistics) between cortical excitability, as measured by the IRA, before (black bars) and after (gray bars) ECT. d Single-subject comparisons (Wilcoxon rank sum test) between the IRS before (black bars) and after (gray bars) ECT. *p < .05; **p < .005

23

2.2.1.3 Discussion

This study provides the first experimental evidence that ECT increases frontal cortex excitability in patients affected by severe major depression. This result was obtained by measuring the immediate (early and local) EEG response to a direct perturbation with navigated TMS.

Previous attempts to measure cortical excitability during a course of ECT were performed on the peripheral motor evoked potentials (electromyogram (EMG)) induced by TMS of the primary motor cortex (Bajbouj et al., 2006, 2005; Chistyakov et al., 2005; Sommer et al., 2002). While single-case studies (Bajbouj et al., 2005; Sommer et al., 2002) showed a reduction of cortical excitability after ECT (increase of intracortical inhibition, cortical silent period duration, and resting motor threshold), group results (Chistyakov et al., 2005) indicated an increase of cortical excitability as reflected by reduced motor threshold and intracortical inhibition. In the present study, we stimulated the frontal cortex, which is mostly involved by ECT effects (Boylan et al., 2001; Lee et al., 2012), and we analyzed the local EEG responses immediately triggered in this area by TMS. Notably, the TMS/EEG approach proposed here provides a direct measure of cortical excitability that is complementary to the TMS/EMG approach, because it by-passes spinal motorneurons and because it is applicable outside the motor cortex.

Developing TMS/EEG as a clinical tool for monitoring plastic/excitability changes in cortical circuits requires an adequate protocol for recording and analyzing data. The TMS/EEG apparatus used in this work was equipped with a neuronavigation system and took into account individual anatomical variability (Ruohonen and Karhu, 2010). Previous works have shown that TMS-evoked responses recorded several days/weeks apart under the same experimental conditions are statistically identical (Casali et al., 2010; Lioumis et al., 2009): therefore, the significant TEP changes we observed in the same patient between pre- and post-ECT sessions cannot be ascribable to unknown experimental variables or measurement uncertainty, but are actually due to significant changes in neural responsiveness. The reliability of TEPs is strictly contingent on the use of neuronavigation, which ensures a reproducible targeting across sessions. Hence, MR-guided

navigated stimulation may be an important requirement for the application of TMS/EEG as a clinical monitoring tool.

We found that the early response of frontal cortical neurons to a direct stimulation was significantly larger after a course of ECT treatment as compared to baseline. This result was observed in a rather limited population of patients; however, the effect was strong and consistent, since IRA increase was statistically significant in each and every patient. Whether this increase in cortical excitability reflects synaptic potentiation as suggested by animal models of ECT (Altar et al., 2004; Nibuya et al., 1995; Stewart et al., 1994) remains an open question. Indeed, the complex relationship between depression and neuroplasticity clearly involves multiple signaling cascades that regulate neuronal activity, including inhibitory neurotransmitters (Sackeim, 2004), besides the glutamatergic system (Biedermann et al., 2012; Sanacora et al., 2008). Nonetheless, the possible involvement of neuroplasticity processes might be supported by the observation that also the slope of early TEPs was increased. Indeed, in the animal model, changes in slope of the first local field potential component elicited by electrical stimulation of cortical axons reflect changes in excitability related to the strengthening or weakening of cortical synapses. Accordingly, in vivo long-term potentiation-inducing procedures increase the local field potential slope (Bliss and Lømo, 1973; Stewart et al., 1994), whereas long-term depression-inducing procedures reduce it (Kirkwood et al., 1993). Actually, IRS increase was significant in most, but not all, of the patients: however, it is challenging to properly record the local and immediate neuronal response to TMS, due to unwanted activation of cranial muscles nearby the stimulated site. Therefore, although we succeeded in recording good-quality early TEPs from most patients, IRA might be an alternative, more reliable measure of cortical excitability with respect to IRS in a clinical context. Nonetheless, finding a significant increase of IRS at the single-subject level in most patients further supports the possible interpretation of increased cortical excitability in terms of neuroplasticity processes.

Previous studies have related the neurobiological substrates of depression to an inter-hemispheric imbalance (Davidson and Irwin, 1999; Hecht, 2010; Maeda et al., 2000): indeed, emotions seem to be differently processed in the left and right hemisphere (Grimm et al., 2006) and cerebral blood flow and metabolism at rest have been observed to be abnormally reduced in the left prefrontal

cortex and abnormally increased in the right prefrontal cortex in major depressed patients as compared to healthy subjects (Mayberg, 2003). Moreover, therapeutic repetitive TMS is clinically delivered at a high-frequency rate over the left hemisphere (to increase cortical activity) and at a low-frequency rate over the right hemisphere (to suppress cortical activity) (Fitzgerald et al., 2003; Gershon et al., 2003). As a consequence, it is possible that the mechanism of action of any antidepressant treatment could be in principle affected by this asymmetry. The present study was not intended to specifically investigate the electrophysiological effects of ECT in the left and right hemisphere separately: rather, TMS pulses were delivered on the scalp nearby the mid-sagittal plane, slightly on the left side of the head in half of the patients and slightly on the right side in the other half. Basically, we stimulated mainly one hemisphere in a region close to the midline and we involved, to a lesser extent, also the contralateral hemisphere. The possibility that we actually obtained a direct stimulation of both hemispheres is supported by observing that the induced EF peaking at 90–130 V/m in the TMS target area actually activated above threshold a cortical area of several cm2, as estimated by the navigation system, and that the ROI channels with the largest early TMS-evoked EEG response were usually located bilaterally. In two patients we were able to record EEG responses to stimulation of both hemispheres: results revealed a significant increase of both IRA and IRS in each patient bilaterally. These observations confirm that ECT induces a comparable increase of cortical excitability on both sides of the brain, as could be expected by the bilateral electrode placement used in this therapeutic protocol. Clearly, most of the patients were prevalently stimulated on one hemisphere and therefore we could have missed the observation of a possible cortical excitability imbalance at baseline. This issue should be considered in future studies on larger sample size by comparing the immediate EEG response to TMS of the left and right hemisphere in the same patients.

The present results, showing increased frontal cortical excitability after ECT, fit with the observation that while stress reduces the expression of BDNF in the hippocampus and frontal cortex, antidepressants produce the opposite effect and promote neurons/glia survival and growth (Duman and Voleti, 2012; Dwivedi Y et al., 2003; Manji et al., 2001; Salvadore et al., 2011). Accordingly, ECT increases neurotrophins, e.g. BDNF (Altar et al., 2004; Nibuya et al., 1995) and

26

synaptic efficacy (Stewart et al., 1994), and BDNF/TrkB potentiate cortical excitability through interaction with glutamate and its receptors (Mamounas et al., 1995; Mattson, 2008; Minichiello, 2009). In humans, the glutamate/glutamine levels as measured by proton MR spectroscopy have been reported to be significantly smaller at baseline in depressed patients as compared to healthy subjects and to increase after successful ECT (Michael et al., 2003).

We observed a positive, yet not significant, trend between IRA increase and mood improvement as measured by HDRS. Although we do not aim to convey any prognostic information due to our limited sample size, we propose to further investigate the relationship between clinical and electrophysiological measurements of neuromodulatory treatments on larger populations, possibly accounting for confounding factors, e.g. gender, disease severity, or social influences.

A limitation of the present study consists in the lack of a control group, i.e. a comparable group of depressed patients treated with "sham" ECT, due to ethical reasons and to the limited number of available patients. Previous studies have necessarily applied a classical randomized placebo-controlled design to demonstrate the therapeutic efficacy of ECT (Freeman et al., 1978; West, 1981). However, we took for granted the general antidepressant effects of ECT and we specifically focused on the electrophysiological modifications induced by this neuromodulatory treatment in frontal cortical circuits. Therefore, for our purposes it was unethical to preclude severely depressed patients at high risk from receiving a generally effective treatment and, at the same time, to submit them to a dose of anesthetic. Since we observed a significant increase of cortical excitability after ECT in each and every patient, despite the reduced sample size, we believe it is very unlikely that an unknown and uncontrollable variable other than ECT would have been able to significantly modulate TEPs consistently across patients. This study showed a clear-cut neurophysiological effect of ECT on cortical excitability, that could be detected statistically at the single-subject level: therefore, it suggests that a new tool based on TMS/EEG could be available to guide and monitor different antidepressant treatments. Clearly, ECT engenders a coarse effect on brain circuits. Thus, it would be interesting to employ TMS/EEG study the effects of more refined neuromodulatory treatments, e.g. repetitive TMS (O'Reardon et al., 2007; Padberg and George, 2009; Slotema et al., 2010). rTMS is a non-convulsive mean to induce neuromodulation that does

not require anesthesia, and has negligible side effects compared to ECT. In addition, the local activation of prefrontal cortical circuits by rTMS has been shown to indirectly affect subcortical regions involved in mood regulation (Li et al., 2004). Still, the antidepressant effects of rTMS are weaker as compared to ECT (Knapp et al., 2008) and can be unpredictable at the single-patient level (Eranti et al., 2007; Hasey, 2001), possibly because of inadequate optimization of stimulation parameters, e.g. frequency, intensity, targeting (Hasey, 2001; Lam et al., 2008). To the extent that an increase of frontal cortex excitability is the desired electrophysiological effect of antidepressant treatment, TMS/EEG measures may represent a reliable tool to quantify objectively and optimize therapeutic neuromodulation and may be used to identify effective stimulation parameters on an individual basis. For example, IRA can be calculated automatically from a small subset of electrodes nearby the TMS target and is able to detect significant effects at the single-subject level. Therefore, simpler experimental set-ups could be developed to study the effects of different treatments in larger cohorts of depressed patients. In future studies TMS/EEG set-ups may be used to evaluate the effects of other treatments, such as sleep deprivation, rTMS, and transcranial direct current stimulation.

2.2.2 Changes of cortical excitability as markers of antidepressant response in bipolar depression: preliminary data obtained by combining transcranial magnetic stimulation and electroencephalography

Despite the specific effects of some antidepressants, there is still a high level of uncertainty about which biological changes are needed to recover from a major depressive episode (Millan, 2006). In the last decade, new approaches have focused on intracellular signalling pathways involved in the regulation of synaptic plasticity, cellular survival, and growth (Chen et al., 2010). Neuroimaging and postmortem studies revealed cellular and morphological changes in depression, associated with reduced grey matter volumes and abnormal decreases in neuron size and glial density (Drevets, 2000; Manji et al., 2001). These changes remain key targets of antidepressant treatments which may reverse depressive symptoms by restoring neuronal growth and activity (Palazidou, 2012).

A recent hypothesis, the synaptic homeostatic hypothesis, suggests that learning and plasticity processes during wakefulness lead to a net increase of synaptic strength in several cortical circuits, and that, after falling asleep, the synaptic potentiation is followed by a homogeneous reduction in the strength of all cortical synapses (Huber et al., 2013; Tononi and Cirelli, 2006). In vitro and in vivo studies demonstrated a net prevalence of synaptic potentiation processes during wakefulness, which results in a gradual build-up of cortical excitability (Bushey et al., 2011; Liu et al., 2010; Vyazovskiy et al., 2009, 2008; Yan et al., 2011). In animal models, the increase of the slope of the electrical evoked local field potential (LFP), which is a classic marker of synaptic strength in vivo, was paralleled by an increase in the level of the glutamate receptor 1 (GluR1)-containing α-amino-3-hydroxy-5-methyl-4-isoxazolepropionic acid (AMPA) receptor in synaptoneurosomes, and by changes in phosphorylation of AMPA receptors and of the enzymes Ca2+/calmodulin-dependent protein kinase II (CamKII) and glycogen synthase kinase 3 beta (GSK3B) after prolonged wakefulness (Vyazovskiy et al., 2008).

The observed correlation between cortical evoked potentials, synaptic strength, and neurobiology observed with direct intra-cortical stimulation in rodents (Vyazovskiy et al., 2008) prompted direct and non-invasive investigations in humans of the homeostatic changes of cortical excitability by means of combined transcranial magnetic stimulation (TMS) and electroencephalography (EEG) (Canali, 2014; Ilmoniemi et al., 1997; Komssi and Kähkönen, 2006). Recent studies in humans confirmed that the slope and amplitude of the early EEG response to TMS steadily increased during prolonged wakefulness, thus paralleling homeostatic sleep pressure (Hanlon et al., 2011), and decreased after sleep (Huber et al., 2013). These changes may be used to assess the responsiveness of cortical neurons in a way that is more similar to the method classically employed in animals, where the slope and amplitude of early LFP induced by electrical cortical stimulation are correlates of synaptic building (Bliss and Lømo, 1973; Vyazovskiy et al., 2008).

Chronobiological research in psychiatry hypothesized that the disruption of the homeostatic mechanism of synaptic building could be a key biological correlate and a therapeutic target of depressive illness and bipolar disorder (Bhattacharjee, 2007; Wirz-Justice et al., 2004). In agreement with this hypothesis, we observed an increase of TMS/EEG measures of cortical

excitability after successful antidepressant response to electroconvulsive therapy in a pilot trial in nine depressed patients (Casarotto et al., 2013).

The circadian homeostatic mechanisms are directly targeted by chronotherapeutics, which combines interventions in the sleep–wake cycle, such as sleep deprivation, and interventions in the molecular machinery of the circadian pacemaker, such as light therapy (Wirz-Justice et al., 2005). Sleep deprivation can acutely reverse depressive symptoms in approximately 60% of patients (Benedetti and Colombo, 2011), including the most severely affected patients with bipolar depression (Benedetti et al., 2014), by acting on many neurotransmitters (Benedetti et al., 2010, 2007a, 2003; Hefti et al., 2013), and multiple neurobiological factors implicated in plasticity processes (Benedetti and Smeraldi, 2009). Sleep deprivation has long been proposed as a model experimental treatment to study the neurobiological correlates of rapid antidepressant response (Gillin et al., 2001; Schloesser et al., 2012), and recent advances confirmed its pivotal role in studying biomarkers of antidepressant response (Benedetti and Terman, 2013; Zarate et al., 2013). Due to high response rate and rapidity of action, in the last decade clinical chronotherapeutics of mood disorders has been developed into a practicable everyday method for the treatment of bipolar depression (Benedetti et al., 2014; Wirz-Justice et al., 2013, 2005).

If an increased cortical excitability, with enhanced synaptic building and activity, is a necessary correlate of antidepressant response, and if sleep deprivation promotes neuroplasticity, it can be hypothesized that changes in cortical excitability would parallel clinical changes in patients treated with antidepressant sleep deprivation. In the present study, we tested this hypothesis by using a TMS/EEG technique in a homogeneous sample of depressed patients with bipolar disorder treated with chronotherapeutics (combined sleep deprivation and light therapy).

2.2.2.1 Materials and methods

Patients

We included in the study 21 consecutively admitted inpatients (female = 16; male = five) affected by a major depressive episode, without psychotic features, in the course of bipolar disorder type I

(Structured Clinical Interview for DSM-IV disorders). Inclusion criteria were (i) a baseline Hamilton Depression Rating Scale (HDRS) score ≥18; (ii) absence of other diagnoses on Axis I and of mental retardation on Axis II; (iii) absence of pregnancy, history of epilepsy, or major medical and neurologic disorders; (iv) no treatment with long-acting neuroleptic drugs in the last three months before admission; and (v) absence of a history of drug or alcohol dependence or abuse within the last six months.

After a complete description of the study had been provided to the patients, written informed consent was obtained. The local ethical committee approved the experimental protocol.

Treatment and data collection

All patients were treated for one week with a combined repeated total sleep deprivation and light therapy chronotherapeutic treatment (Benedetti et al., 2005). According to established protocols (Benedetti, 2012; Wirz-Justice et al., 2013, 2005), each patient was totally sleep deprived on Days 1, 3, and 5 and each sleep deprivation night lasted for about 36 hours, from 7:00 a.m. to 7:00 p.m. of the subsequent day. Under the constant supervision of a nurse, sleep deprivation was carried out in a room with 80-lux ambient light. On Days 2, 4, and 6, all patients were allowed to recover their sleep (Benedetti et al., 1996). All patients were administered 10,000-lux white light for 30 min, given at 3:00 a.m. during the sleep deprivation night and in the morning after recovery sleep, half an hour after awakening. Patients were either taking lithium at admission and continued treatment (n = 6), or started taking lithium together with the chronotherapeutic procedure to enhance its effect and prevent relapse (n = 15) (Baxter, 1985; Benedetti et al., 2014, 1999).

Electrophysiological measures were recorded during the sleep deprivation treatment. TMS/EEG sessions were performed at baseline evening (Day −1: 6:30 p.m.), in the morning and in the evening before and after the first night of sleep deprivation (Day 0 and Day 1: 8:30 a.m. and 6:30 p.m.), in the morning after the first recovery night (Day 2: 8:30 a.m.), and in the morning after the third and last sleep deprivation (Day 5: 8:30 a.m.) (Figure 2.2.3). Spontaneous EEG was continuously recorded for about three min before each TMS/EEG session.

Severity of depression was rated in the mornings of Days 0, 1, 2, and 6 with a modified 21-item HDRS from which items that could not be meaningfully rated due to the sleep deprivation procedure and to the time frame were excluded (i.e., weight changes and insomnia: items #4, 5, 6, and 16) (HDRS-Now) (Leibenluft et al., 1993). A decrease of 50% in HDRS scores after treatment was considered the response criterion.

EEG recording and TMS/EEG targeting

The experimental set-up included TMS with a focal bipulse 8-coil (Eximia TMS Stimulator; Nexstim Ltd, Helsinki, Finland) equipped with a Navigated Brain Stimulation (NBS) system (Nexstim Ltd) and a 3D infrared Tracking Position Sensor Unit (Polaris, Northem Digital Inc., Waterloo, Canada). EEG was recorded with a 60-channel TMS-compatible EEG amplifier (Nexstim) equipped with sample-and-hold circuits that prevents the recording from the powerful TMS-related artefact (Virtanen et al., 1999). This equipment provides in real time the TMS coil position and subject's head, within the reference space of individual magnetic resonance imaging (MRI), by co-registration between the fiducial points (nasion, left tragus, and right tragus), selected on the individual MRI, and the corresponding digitized scalp landmarks. The exact location of the stimulation site was previously adjusted on the individual MRI in order to prevent accidental muscle twitches that often affect EEG recordings, and to estimate the electrical field induced by TMS pulses, which clearly depends on the stimulation intensity (expressed in V/m). The TMS intensity can thus be adjusted according to the maximum electric field intensity (expressed in V/m) estimated on the cortical surface, rather than relying on individual motor threshold or on the percentage of maximum stimulator output. While bypassing sensory and motor pathways, this method allows measurement of cortical excitability and connectivity by directly stimulating any given cortical region and simultaneously recording the immediate electrical response (Esser et al., 2006; Kähkönen et al., 2001).

Patients were randomly divided into two groups depending on the TMS target location, which was slightly adjusted across subjects either to the left (n = 11) or to the right (n = 10) Brodmann area

(BA) 6. These prefrontal brain areas showed the greatest changes of metabolic rate and its EEG correlates between wake and sleep (Horne, 1993).

EEG data analysis

Data analysis was carried out using Matlab (2007b; The Mathworks Inc., Natick, MA, USA). Each TMS-evoked response was obtained by averaging 100–200 (mean ± standard deviation across sessions: 152 ± 44 pulses) artefact-free trials (Casali et al., 2010; Casarotto et al., 2010). In order to quantify the EEG response, we obtained three different cortical excitability measures (Figure 2.2.3): (i) slope of the first evoked component, defined as the first positive deflection; (ii) local mean field power (LMFP), which measures the local amount of electrical activity induced by TMS; and (iii) global mean field power (GMFP), which quantifies the overall impact of TMS at all 60 electrodes.

In order to reduce point-by-point variability and the number of time-points to allow statistical analyses with repeated ANOVAs, we aligned the first EEG component across all patients. We then analysed the pattern of changes of cortical potentials, sampled every 2.5 ms, during the first 70 ms (where TEP components occurred for all patients), beginning 10 ms after the TMS pulse, due to the presence of early and small artefacts. The procedure yielded 21 consecutive time-points for each patient.

The spontaneous EEG was then analysed in order to quantify the spectral power in the theta frequency band (4–7 Hz).
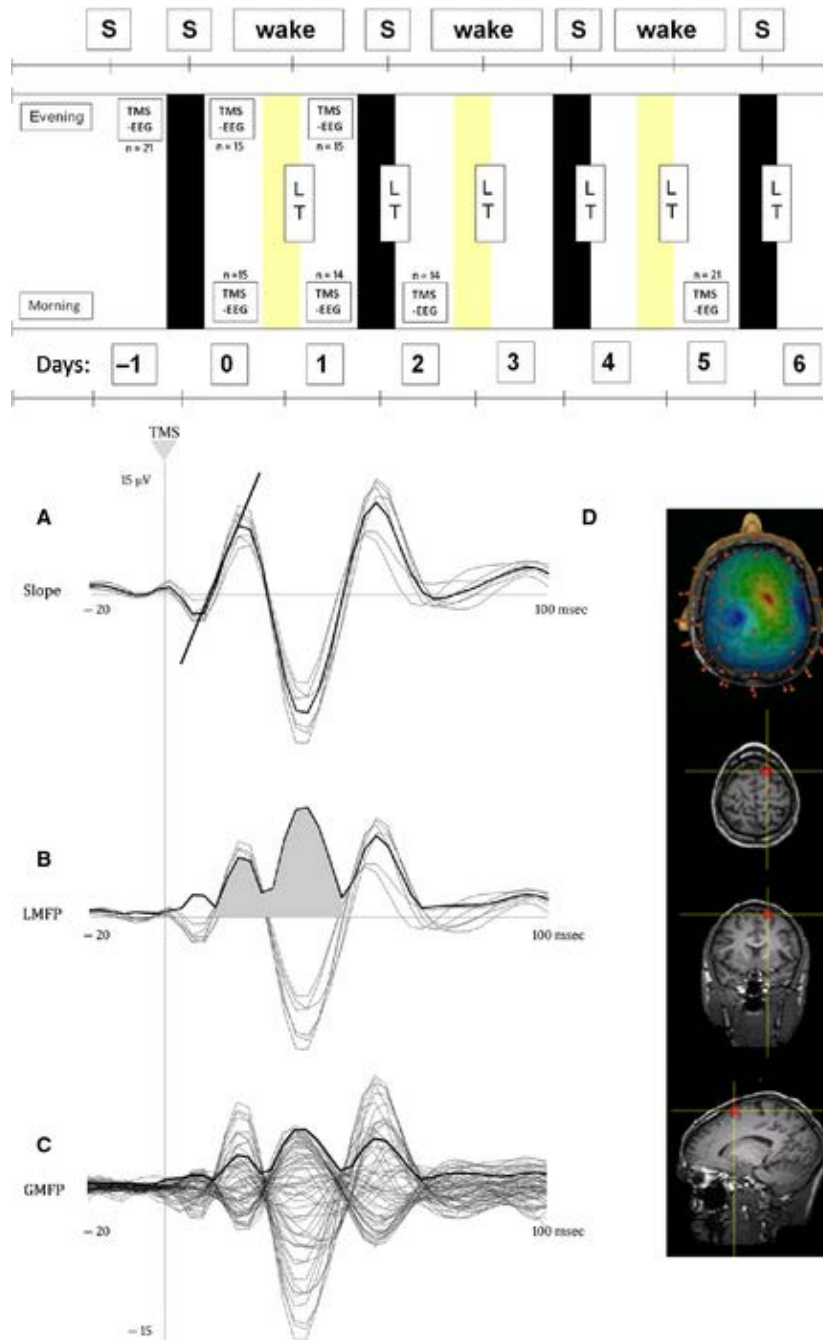
Figure 2.2.3. - Top panel: Schedule of treatment and data collection, and number of patients participating in each transcranial magnetic stimulation (TMS)–electroencephalography (EEG) session. LT = light therapy; S = sleep; TMS–EEG = experimental session; W = wake. Bottom panels: (A) Average EEG response to TMS in a subset of six selected channels (grey traces). Slope of the first component was computed on TMS-evoked potentials from single trials averaged in space across the selected subset of six electrodes (black traces). (B) The electrical response under the site of stimulation was quantified by the local mean field power (LMFP) (black trace) and the strength of the first two EEG components was calculated as the integral of the LMFP (grey area). (C) Global mean field power (GMFP) was measured as the overall impact of TMS at all 60 electrodes. (D) TMS targeting over the prefrontal area by means of a neuro-navigation system that ensure stimulation reproducibility across sessions.

Statistical analyses

We analyzed the pattern of change over time of the estimated measures of cortical excitability and synaptic weights as a function of response to treatment. Of the 21 participants, 12 completed all recording sessions and nine missed a mean of mean ± standard deviation (SD) 3 ± 1 sessions. Therefore, we followed two separate analytic approaches in the two groups.

In the subgroup with a complete dataset, a conservative repeated-measures analysis of variance was performed in the context of the general linear model. Two repeated measures factors were considered in order to investigate (i) circadian changes, morning to evening, during days 0 and 1; and (ii) days on treatment. Staying awake at night (sleep deprivation) or asleep (recovery) were also modeled as factors. The statistical significance of the effect of the single independent factors on the dependent variable at each level was then calculated (least square method) by using parametric estimates of the predictor variable. Analyses were performed using commercial available software and following standard computational procedures. This analysis was performed on the slope of the first evoked component, which was the main outcome measure. With a similar approach, we analyzed the patterns of change of GMFP and LMFP values after the TMS pulses, using time after stimulus and recording sessions as within-subject factors, and response to treatment as a between-subject factor. We also modeled clinical and demographic characteristics (age, age at onset, and number of previous episodes) as nuisance covariates.

In the whole group and using all the available data, we assessed the effects of response to treatment on cortical excitability over time using a random regression model (RRM) (Hedeker and Gibbons, 1996). The random-effects approach accounts for correlations among repeated measurements on the same subjects and has the unique advantage of being unaffected by unequal numbers of assessment among individuals, allowing us to use all available data for each patient (Gibbons et al., 1993). In the RRM, we included slope values as the dependent variables, time (seven recording sessions) and intercept as random effects, and response to treatment plus its interaction with time as fixed effects (Gibbons et al., 1993).

2.2.2.2 Results

Clinical and demographic characteristics of the sample divided according to the response to treatment are shown in Table 2.3. Confirming previous results (Benedetti et al., 2005), 60% of the patients responded to the treatment and did not significantly differ from non-responders on any baseline variable. Patients on ongoing lithium treatment and newly started on lithium treatment responded equally well.

Table 2.3 - Clinical and demographic characteristics of the patients according to response to treatment

	Responders (n = 12)	Non-responders (n = 9)	R or χ^2	*p* value
Sex, male/female, n	3/9	2/7	0.14	0.71
Age, years, mean ± SD	44.08 ± 9.42	41.22 ± 12.02	−0.61	0.54
Age at onset, years, mean ± SD	27.33 ± 6.63	30.44 ± 11.25	0.79	0.43
Duration of illness, years, mean ± SD	16.75 ± 8.85	10.77 ± 8.82	−1.53	0.14
Previous depressive episodes, mean ± SD	7.16 ± 6.14	3.75 ± 2.37	−1.48	0.15
Previous manic episodes, mean ± SD	2.91 ± 2.19	2.44 ± 2.29	−0.47	0.63
Duration of current episode, weeks, mean ± SD	33.16 ± 42.33	23.33 ± 19.33	0.64	0.52
Education, years, mean ± SD	12.36 ± 4.15	14.00 ± 6.00	0.70	0.49
Ongoing lithium treatment, yes/no, n	4/8	2/7	0.01	0.94
HDRS score (17 items), mean ± SD				
Baseline	19.58 ± 5.66	20.66 ± 4.15	−0.48	0.63
Day 1	10.91 ± 6.96	15.22 ± 6.07	−1.47	0.15
Day 2	9.50 ± 5.12	14.66 ± 3.60	−2.57	0.01
Day 6	4.33 ± 3.42	16.00 ± 5.31	−6.12	0.00

HDRS = Hamilton Depression Rating Scale; SD = standard deviation.
aHDRS 50% reduction from Day 1 to Day 5.

Synaptic strength (slope of the first-evoked component)

The pattern of change of the slope of the first component over time was influenced by circadian phase (morning versus evening), sleep, and sleep deprivation treatment (Figure 2.2.4). The overall change over time during treatment was highly significant because of a sawtooth pattern of increase after wake and decrease after sleep, with a significant trend of progressive increase during the whole treatment (GLM repeated measures ANOVA, Day −1 to 5: F = 4.35; df = 6,66; p = 0.00092). Slope significantly increased during the day, from morning to evening, starting before the first sleep deprivation (Day 0: F = 7.90; df = 1,11; p = 0.01691 and continuing to the day after sleep deprivation (Day 1: F = 19.02; df = 1,11; p = 0.00113). The size of the circadian change did not significantly differ before and after sleep deprivation (F = 0.44; df = 1,11; p = 0.51944).

Sleep deprivation significantly increased the slope (F = 13.23; df = 1,11; p = 0.00389), while recovery sleep decreased it (F = 18.99; df = 1,11; p = 0.00113), with a significant interaction between the two effects (F = 41.96; df = 1,11; p = 0.00004). This effect of sleep was not observed at baseline (F = 3.13; df = 1,11; p = 0.10), thus leading to significant differences in the effects of sleep before and after the first sleep deprivation: baseline sleep did not influenced the slope, while recovery sleep after sleep deprivation decreased it (F = 4.90; df = 1,11; p = 0.04875).

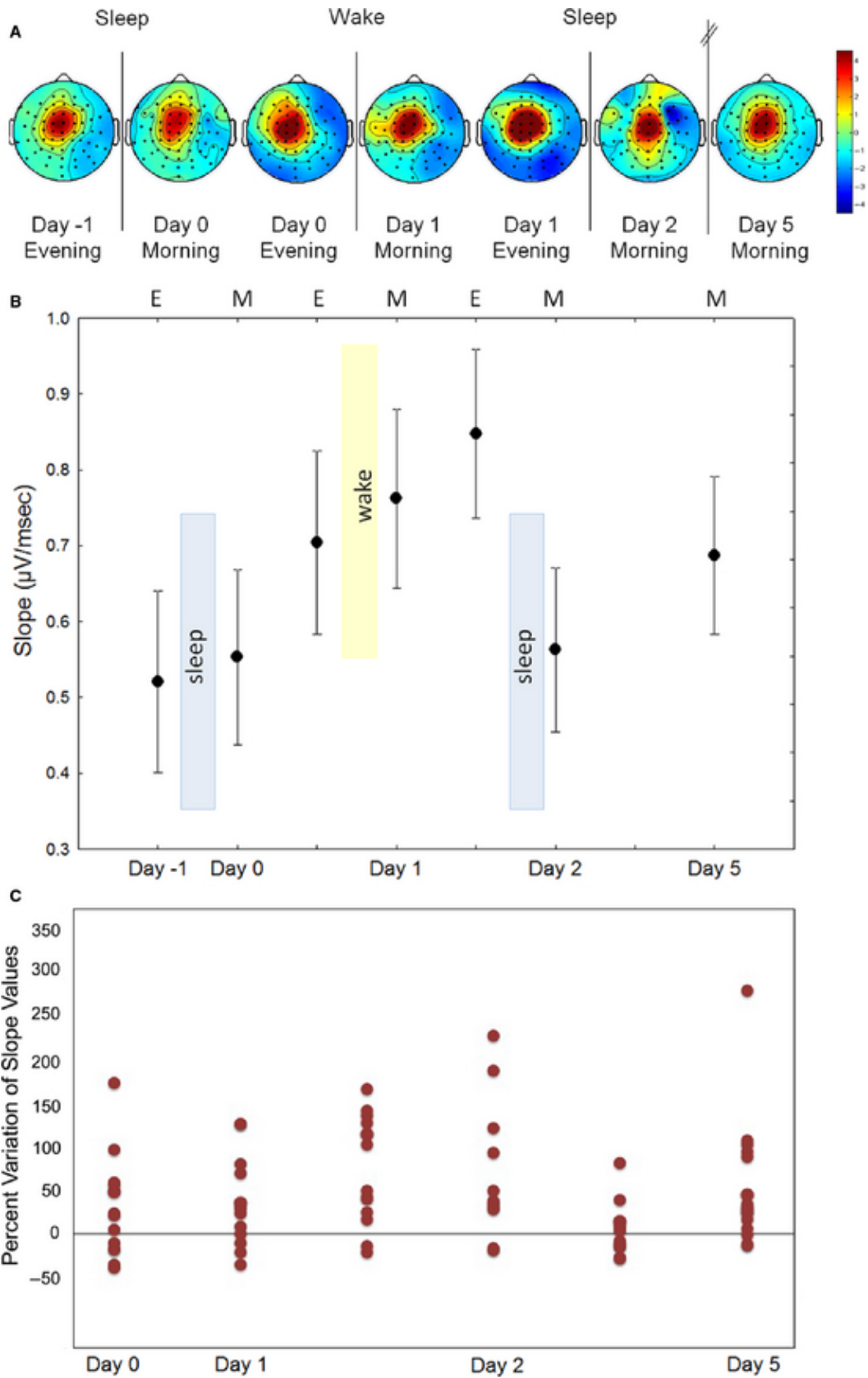**Figure 2.2.4. - (A)** Topographical maps of scalp voltages in a representative subject of the responder group throughout the experimental week. **(B)** Pattern of change of slope values (µV/ms) over time (M = morning, E = evening) in the whole sample. Points = means; whiskers = standard errors. **(C)** Percent variation of slope values from baseline for each participant.

Effect of treatment

The patterns of mood change during treatment markedly differed between responders and non-responders (Figure 2.2.5A). RRM analyses in the whole dataset confirmed the significance of the progressive increase of slope values over time ($p = 0.00565$) and showed a significant effect of response ($p = 0.043$); i.e., patients who responded to treatment had higher slope values than non-responders throughout the study period (Figure 2.2.5B).
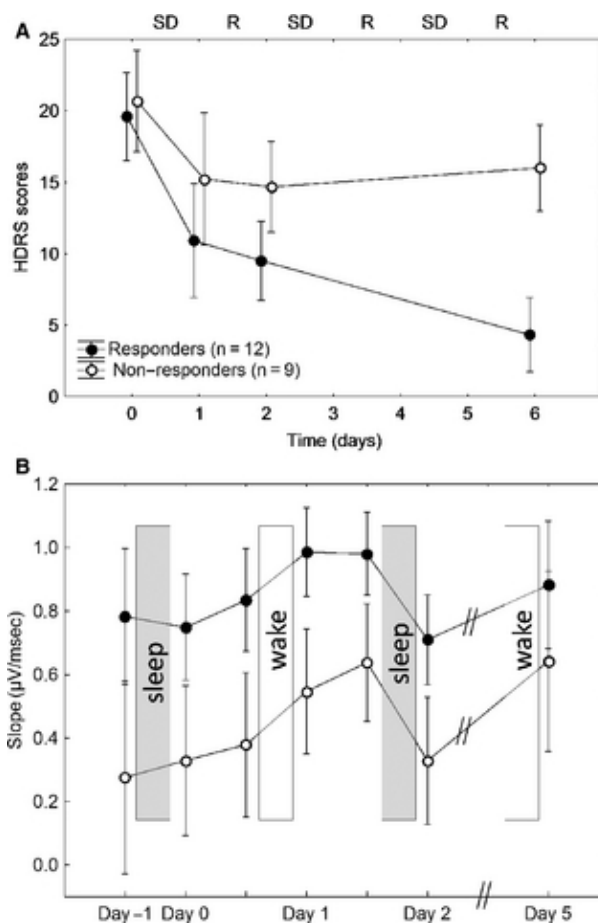
Figure 2.2.5. - Changes of Hamilton Depression Rating Scale (HDRS) scores of depression severity (A) and of the slope of the first-evoked component (µV/ms) (B) during treatment in the sample divided according to final response to treatment (HDRS 50% reduction).

Cortical excitability: changes of GMFP and LMFP and effects of treatment

Baseline cortical excitability (GMFP and LMFP) was significantly higher in responders than in non-responders (LMFP: $F = 2.08$; $df = 20,340$; $p = 0.00445$; GMFP: $F = 1.64$; $df = 20,320$; $p = 0.04199$).

These differences were maintained during the day (Day 0: morning and evening), with a similar pattern of circadian change from morning to evening among patients but with higher values in responders than in non-responders (LMFP: F = 2.49; df = 20,240; p = 0.00057; GMFP: F = 2.10; df = 20,240; p = 0.00471).

Two ANOVAs were conducted separately for the effects of the first sleep deprivation (Day 0–1) and of the whole treatment week. The analyses of the pattern of change of the evoked GMFP response before/after the first sleep deprivation cycle (Figure 2.2.6) showed that: (i) the evoked response over time (msec) was overall higher in responders than in non-responders (time × response interaction: F = 2.54; df = 20,180; p = 0.000577); (ii) there was a significant interaction effect of circadian timing (morning versus evening) and response to treatment on the pattern of GMFP, due to a better enhancement during the day in responders (F = 1.7; df = 20,180; p = 0.03557); and (iii) after sleep deprivation, responders tended to increase the GMFP response and its circadian fluctuations, while non-responders did not (four-way interaction of sleep deprivation treatment, response to treatment, and circadian timing on the GMFP pattern of response: F = 1.94; df = 20,180; p = 0.01215).

Similar effects were observed when analysing all sessions (seven TMS/EEG sessions) in the subgroup of patients with a complete data recording (n = 12). A two-way repeated ANOVA confirmed a significant interaction of time and response (LMFP: time, F = 1.48; df = 6,36; p = 0.21009; response, F = 6.75; df = 1,6; p = 0.04069; interaction, F = 1.36; df = 120,720; p = 0.0095; GMFP: time, F = 0.47; df = 6,36; p = 0.8235; response, F = 5.88; df = 1,6; p = 0.0515; interaction, F = 1.24; df = 120,720; p = 0.04938), meaning that the pattern of increasing cortical excitability after the sleep deprivation treatment did not follow parallel slopes of time-course in responders and in non-responders to treatment.

Additional analyses were performed using, as a dependent variable, the integral of the LMFP within the first two components of the EEG response, and gave similar results. Finally, EEG theta power increased after sleep deprivation and decreased after sleep during the experimental period, with a significantly lower increase in responders to treatment, in agreement with previous studies showing less night sleep after sleep deprivation in responders than in non-responders (Benedetti et

al., 2007b). Changes in measures of cortical excitability did not significantly differ between patients on ongoing lithium and those newly started on lithium treatment).
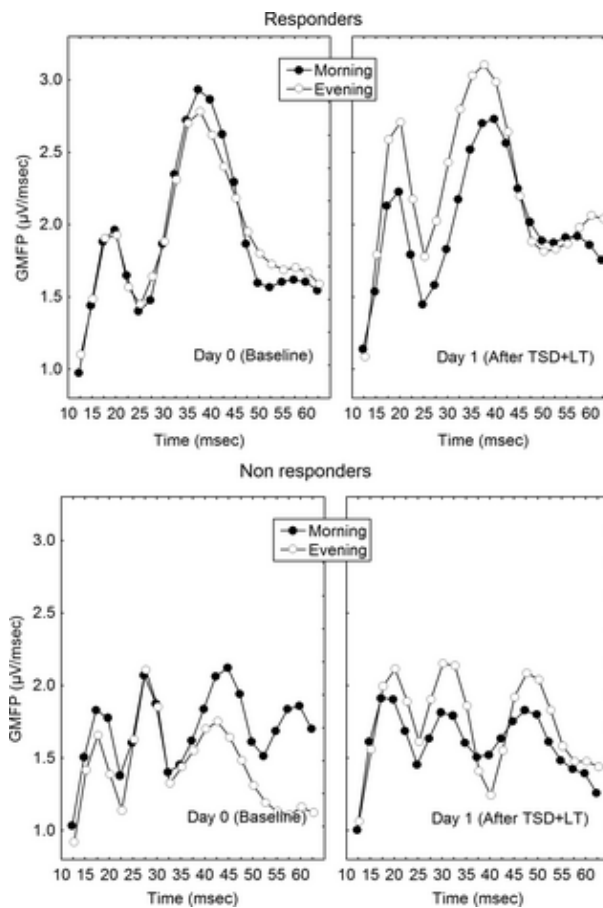
Figure 2.2.6. - Global mean field power (GMFP) values (μV/ms) before and after the first sleep deprivation cycle. Black circles are mornings; white circles are evenings. TSD + LT = total sleep deprivation + light therapy.

2.2.2.3 Discussion

Our patients showed a sawtooth pattern of increased cortical excitability during wake and decreased cortical excitability during sleep. Despite a similar pattern of variation in responders and non-responders, measures of synaptic strength were markedly lower at baseline in non-responders, and after treatment did not even reach the baseline values of responders. This fluctuation of cortical excitability around a lower mean value is a new biological correlate of non-response, independent of comparable baseline severity of depression and clinical characteristics. This effect suggests that the baseline status of the brain could be a major factor affecting

antidepressant response, and that mechanisms underlying cortical excitability can be involved in the biological changes needed to recover from depression.

In comparison with observations in healthy subjects (Huber et al., 2013), the circadian pattern of progressive increase of cortical excitability during wake, which has been proposed as a neurophysiological correlate of synaptic homeostasis (Tononi and Cirelli, 2006), was absent at baseline in our patients, in agreement with current perspectives on impaired sleep homeostasis in patients with bipolar disorder (Harvey, 2008) and in animal models of depression (Savelyev et al., 2012). Moreover, the relative circadian increase showed a higher individual variability in our patients than in healthy subjects (Huber et al., 2013), which needs direct case–control comparisons to be clarified.

Cortical excitability has been proposed as a physiological correlate of process S, and our findings then confirm hypotheses of process Sincrease as a core mechanism of action of antidepressant sleep deprivation (Vyazovskiy et al., 2008; Wirz-Justice and Van den Hoofdakker, 1999). Given that changes of synaptic strength during the sleep–wake cycle suggest that sleep deprivation is associated with synaptic potentiation (Bushey et al., 2011; Cirelli, 2009; Liu et al., 2010; Rao et al., 2007; Tononi and Cirelli, 2006), it is tempting to surmise that the progressive enhancement in cortical excitability after sleep deprivation in bipolar depression may capture changes of synaptic efficiency and neuroplasticity.

Definite conclusions on this topic are hampered by a lack of basic data on the neurobiological meaning of these neurophysiological measures in humans. In animal models and in vitro, the slope of early local field potential, which is induced by electrical intra-cortical stimulation, is a clear-cut correlate of synaptic building and homeostatic sleep pressure (Vyazovskiy et al., 2008); and long-term potentiation (LTP) increased local field potential slope (Bliss and Collingridge, 1993; Glazewski et al., 1998; Iriki et al., 1991), while long-term depression (LTD) reduced it (Kirkwood et al., 1993). In humans, the delivery of repeated TMS (rTMS) over the motor cortex provided the first demonstration of LTP, which was measured as the increased EEG cortical response to TMS using our same TMS/EEG method (Esser et al., 2006). This suggests that the combination of TMS and EEG provides a means of approximating the classical stimulation protocols available for animal

models. This hypothesis is supported by the convergent findings on the circadian cyclicity of cortical excitability, observed with direct intra-cortical stimulation and recordings in rodents, and with TMS/EEG in humans (Huber et al., 2013; Vyazovskiy et al., 2008).

Several non-alternative mechanisms can contribute to the effects of chronotherapeutics on measures of synaptic homeostasis. Sleep deprivation directly targets the glutamatergic system, by reducing N-methyl-D-aspartate (NMDA) sensitivity (Novati et al., 2012) and increasing the circadian peaks of glutamate production (Dash et al., 2009), with changes of glutamate/glutamine concentrations after sleep deprivation being proportional to mood improvements (Benedetti et al., 2009). Moreover, sleep deprivation can promote a rapid and robust expression of plasticity related factors, including brain-derived neurotrophic factor (BDNF), its receptor tropomyosin related kinase B (TrkB) and cyclic adenosine monophosphate response element-binding protein (CREB) (Duman et al., 2000), with the increase of BDNF levels positively correlating with antidepressant response to sleep deprivation (Gorgulu and Caliyurt, 2009). Sleep deprivation potentiates the serotonin, noradrenaline, and dopamine neurotransmitter systems, which can contribute to circadian changes of cortical excitability by boosting synaptic plasticity (Connor et al., 2012), regulating neuronal excitability and synaptic transmission, integration and plasticity (Tritsch and Sabatini, 2012), and maintaining the neocortical activity-dependent excitatory–inhibitory balance(Moreau et al., 2013). Finally, sleep deprivation targets the circadian pattern of the secretion of pro-inflammatory cytokines (Voderholzer et al., 2012, 2004), which are key mediators of the homeostatic response to sleep loss (Krueger et al., 2001; Wisor et al., 2011).

Whatever the exact mechanism, our observation suggests that TMS/EEG measures of cortical excitability could be proposed as novel biomarkers of antidepressant response. In a previous pilot study, using this same TMS/EEG method, we observed an increase in the slope after electroconvulsive therapy in patients affected by severe major depression resistant to drug treatments (Casarotto et al., 2013); remarkably, similar to our present observations, non-responders showed significantly lower baseline slope values than responders (0.11 ± 0.09 versus 0.50 ± 0.24, respectively; $t = 2.57$, $p = 0.042$), and post-treatment values of non-responders did not reach the baseline values of responders.

Patients with bipolar disorder spend a substantial proportion of their time ill (Altshuler et al., 2010), with depression representing their predominant abnormal mood state (Kupka et al., 2007), despite prolonged and highly complex medication regimens to achieve a stable response in bipolar disorder (Post et al., 2010). Hence the interest in novel biomarkers which could speed up the investigation of new treatments, by providing surrogate indices of clinical endpoints and promoting the identification of new targets (Zarate et al., 2013). Albeit technically demanding, the TMS/EEG procedure is now established, and can thus be tested in different clinical settings to be validated with further research using other antidepressant treatments (Canali, 2014).

This study, which was correlational in nature, has several limitations, including the rather small sample size, and issues of generalizability, patients being non-drug-naïve, the lack of a placebo control, and possible population crypto-stratification. Our measures closely resemble those obtained with electrophysiological studies in rodents, where, however, the slope of the early LFP was measured after having been induced by direct electrical stimulation: the interpretation of the different absolute values obtained using a TMS/EEG method in responders and non-responders thus requires further basic research in humans. Nevertheless, considering the close link between cortical excitability and both synaptic neurobiology and clinical response to treatment, further exploration of these biomarkers in depression is warranted.

2.2.3 Shared reduction of oscillatory natural frequencies in bipolar disorder, major depressive disorder and schizophrenia

High-frequency gamma oscillations are critical for communication among brain areas, thus allowing integration among cortical modules (Nikolić et al., 2013; Rodriguez et al., 1999; M. A Whittington et al., 2000). In the last decade clinical research on oscillatory brain dynamics reported altered neuronal oscillations in neuropsychiatric disorders (Başar, 2013; Başar and Güntekin, 2008; Herrmann and Demiralp, 2005; Uhlhaas and Singer, 2010), suggesting that reduced gamma oscillations could be common to bipolar disorder (BPD), major depressive disorder (MDD) and schizophrenia (SCZ) (Maharajh et al., 2007; B. F O'Donnell et al., 2004).

Frontal cortical gamma activity (30–50 HZ), as indexed through electroencephalography (EEG), is reduced in patients with SCZ (Uhlhaas et al., 2008), in response to odd-ball paradigm (Gallinat et al., 2004; Haig et al., 2000; Symond et al., 2005) or cognitive control task (Cho et al., 2006). EEG power and phase synchronization in beta/gamma frequencies bands after to 40 Hz auditory stimulation are also reduced (Kwon et al., 1999; Light et al., 2006). Findings in mood disorders are similar. BPD patients in the manic or mixed state show hampered auditory EEG synchronization in beta/gamma band (20–50 Hz) during a click trains paradigm (B.F. O'Donnell et al., 2004), and reported significantly reduced long distance gamma coherence in a visual odd-ball paradigm (Özerdem et al., 2011). A recent study reported a decrease of frontal gamma oscillations in patients with MDD and BPD in response to implicit emotional tasks (Lee et al., 2010; Liu et al., 2012). A reduced phase locking and evoked power at 40-Hz auditory steady-state stimulation in first episode psychosis of patients with either schizophrenia or affective disorders has also been reported (Spencer et al., 2008).

The combination of transcranial magnetic stimulation with high-density electroencephalographic recording (TMS/EEG) represents a provocative approach useful to identify the integrity of thalamocortical circuits by directly challenging the brain's capacity to produce and sustain oscillatory activity (Buzsáki and Watson, 2012; Canali, 2014; Rosanova et al., 2012). By combining TMS/EEG we previously demonstrated that each cortical region perturbed by TMS tend to oscillate at specific natural frequency (Rosanova et al., 2009), and we found a deficit in the oscillatory properties in schizophrenia resulting in a reduction of frontal natural frequencies (Ferrarelli et al., 2012, 2008). Here we hypothesized impairments of the thalamocortical system to produce fast oscillations in bipolar disorder and major depression. We then aimed at investigating the oscillatory properties of the premotor cortex by employing TMS/EEG in two groups of patients with bipolar disorder and major depression, and using a group of healthy subjects as negative controls and a group of patients with schizophrenia as positive controls.

2.2.3.1 Methods

We studied 12 healthy subjects as controls (HC), and 36 consecutively admitted in patients suffering from three different psychiatric disorders (DSM-IV criteria, SCID interview): either major depressive episode, without psychotic features, in course of BPD (n=12) or in course of MDD (n=12), or chronic undifferentiated schizophrenia (n=12). Inclusion criteria were the absence of other diagnoses on axis I and of mental retardation on axis II; absence of pregnancy, history of epilepsy, or major medical and neurologic disorders; absence of a history of drug or alcohol dependency or abuse within the last 6 months. Six BPD were taking lithium salts. All MDD patients were on antidepressanttreatment, also with benzodiazepines (n=8) or mood stabilizers (n=3). SCZ patients were taking antipsychotics (typical neuroleptics: n=5; a typical antipsychotics: n=7). A written informed consent was obtained for all study participants. The local ethics committee approved the experimental protocol.

The experimental setup included a TMS compatible 60-channel EEG amplifier (Nexstim) equipped with sample-and-hold circuits that prevents the recording from the powerful TMS-related artifact (Virtanen et al., 1999). Accuracy and reproducibility of TMS/EEG responses were controlled with a Navigated Brain Stimulation (NBS) system (Nexstim) and a 3D-infrared Tracking Position Sensor Unit (Northem Digital Inc). TMS was delivered on the convexity of the middle caudal portion of the superior frontal gyrus close to the midline (Broadmann's areas 6), with the current perpendicular to its main axis. To ensure significant EEG responses (Casali et al., 2010; Komssi et al., 2007; Rosanova et al., 2009) intensity of TMS induced electric field was always >90 V/m as estimated by the NBS system, for each study participant. We delivered about 200–300 stimuli for each session at a frequency randomly jittered between 1.5 and 1.8 s (equivalent to about 0.5–0.6 Hz). Data analysis was carried out using Matlab with the EEGLAB toolbox (Delorme and Makeig, 2004). Each TMS-evoked response was obtained by averaging 150–250 artifact free trials.

In order to quantify the responses in the time-frequency domain (Delorme and Makeig, 2004), from each TMS/EEG session, we measured the event-related spectral perturbation (ERSP) changes in the power spectrum using wavelet decomposition (3.5 oscillation cycles) across single-trials at the

channel closest to the stimulation site. The ERSP was normalized by subtracting the mean baseline power spectrum. Significant ERSP were evaluated by applying a bootstrap statistical method based on a surrogate distribution randomly derived from the pre-stimulus onset (ranging from −700 to −50 ms). Statistical significance level was set at $p<0.01$ and only significant values were considered in the analysis. Averaged ERSP values across all trials of a session were calculated between 8 and 50 Hz (1 Hz bin resolution) over a 20–300 milliseconds time window, corresponding to the main EEG activity evoked by TMS. The natural frequency was computed as the frequency bin with the largest cumulated ERSP over time (Rosanova et al., 2009). Differences between the frontal natural frequencies of the four study groups were analyzed with one-way ANOVA followed by post-hoc Newman–Keuls's tests. Pearson correlation analysis between medications doses, clinical variables and natural frequency were performed. Analyses were carried out using a commercial available software (StatSoft Statistica) and following standard computational procedures (Hill and Lewicki, 2006).

2.2.3.2 Results

Clinical and demographic characteristics of the sample divided according to diagnosis, and the evoked natural frequencies, are resumed in table 2.4.

Table 2.4 - Demographic and Clinical Characteristics of the study groups

	Healthy subjects	Bipolar disorder	Major depression	Schizophrenia	*F*	*P*
Gender (m/f)	5/7	2/10	4/8	9/3		
Age (yrs)	39 (15)	36 (7)	46 (8)	38 (9)	2.1	0.1
Age at onset (yrs)		25 (6)	29 (9)	25 (6)	1.1	0.3
Duration of illness (yrs)		11 (9)	18 (10)	13 (6)	0.1	0.1
PANSS (positive)				18 (4)		
PANSS (negative)				18 (4)		
PANSS (general)				37 (5)		
HDRS (baseline)		26 (6)	24 (7)		1.1	0.8
Frontal natural frequency (Hz)	27.25 (3.22)	20.30 (3.72)	19.24 (5.03)	20.30 (4.22)		

Values are expressed as mean and standard deviations.

All four groups were closely age-matched. Patients with bipolar or unipolar depression had a similar age at onset and duration of illness and did not differ on the Hamilton Depression Rating Scale (HDRS) score. Patients with schizophrenia reported positive and negative symptoms as measured by PANSS.

Data obtained with the TMS/EEG procedure are resumed in Figure 2.2.7.
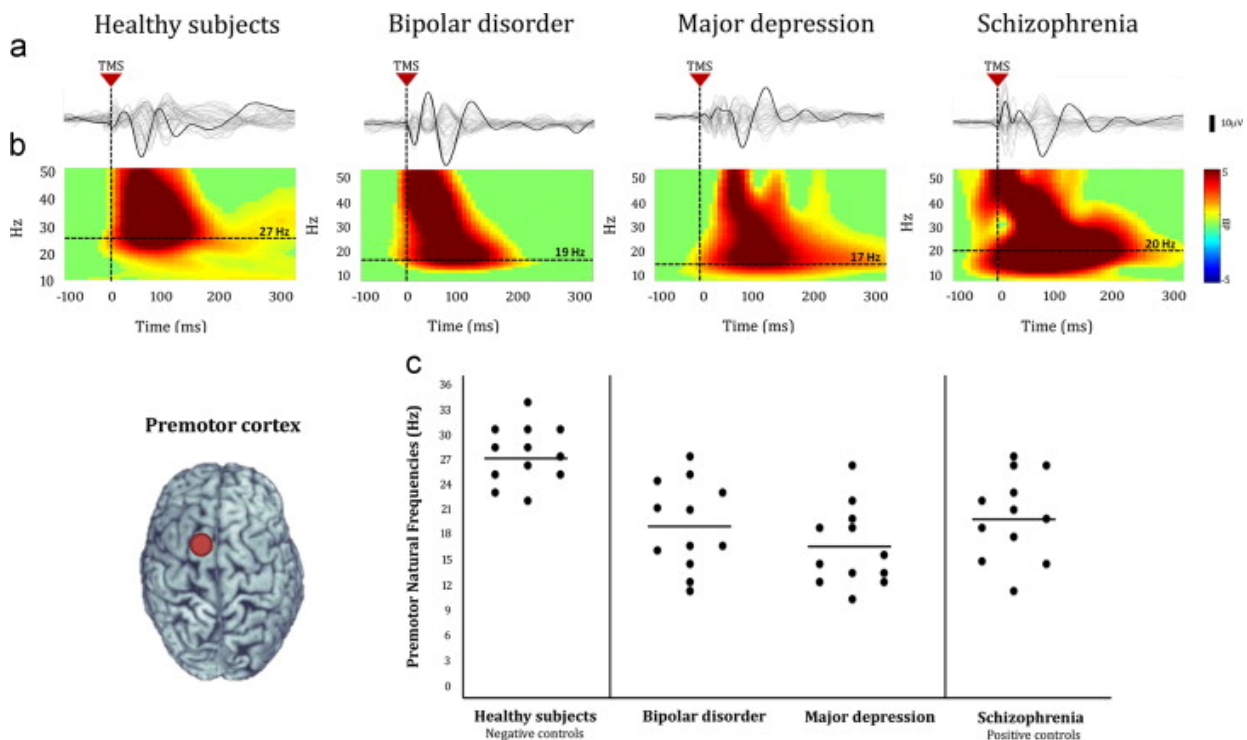
Figure 2.2.7. - Top panel: (a) average EEG responses to TMS (grey traces represent the 60 recording channels) for the channel closest to the stimulation site (black trace) over the premotor area; **(b)** color-coded: event-related spectral perturbation (ERSP) plots reflect the significant TMS related changes in amplitude and their duration. Dotted lines show the frequency with the highest activity (natural frequency). Data are shown from a representative subject from each of the four groups. Bottom panel: individual natural frequencies values for healthy control subjects (negative controls) and patients with bipolar disorder, major depressive disorder and schizophrenia (positive controls).

TMS significantly activated the beta/gamma band response (range 21–50 Hz) to frontal cortical perturbation in HC. The main frequencies of frontal EEG responses to TMS were significantly reduced in patients with either BPD, MDD or SCZ (range 11–27 Hz; one-way ANOVA: F=12.31; df=3,44; p=0.000006) (Figure 2.2.7c). Frontal natural frequencies were markedly faster in healthy subjects compared to all the patient groups (post-hoc:p=0.000485 vs SCZ, p=0.000171 vs MDD, and p=0.000290 vs BP, respectively), which did not significantly differ among themselves.

Correlational analyses between natural frequencies and HDRS, PANSS scores and medication doses did not show significant effects.

2.2.3.3. Discussion

This is the first study to provide a TMS/EEG direct measure of frontal natural oscillations in patients with either BPD or MDD, compared to HC and SCZ. We extended the finding of reduced gamma oscillations, previously reported in SCZ, to mood disorders. All the three diagnostic conditions were

associated with significantly slower gamma-band oscillations compared to healthy controls, and did not differ among themselves.

Common to these psychiatric conditions, a biological underpinning of slower gamma-band oscillations could be found in abnormal Ɣ-aminobutyric acid (GABA) neurotransmission.

TMS/EEG can assess cortical inhibition due to inhibitory GABA interneurons (Daskalakis et al., 2002b), and short cortical inhibition, interhemispheric inhibition and cortical silent period are decreased in SCZ (Daskalakis et al., 2002a; Fitzgerald and Daskalakis, 2008), MDD (Lefaucheur et al., 2008; Levinson et al., 2010) and BPD (Levinson et al., 2007). Gamma oscillations may reflect the activity of GABA inhibitory interneurons (Brenner et al., 2009; Gonzalez-Burgos and Lewis, 2008; Gray and McCormick, 1996; Traub et al., 2005), which produce and sustain complex large-scale network oscillations in fast frequency bands (40–100 Hz) (Benes and Berretta, 2001), also generating inhibitory potentials in excitatory pyramidal neurons (Whittington et al., 2011). GABAa receptor agonizts activate, and antagonists block, high frequency oscillations (Whittington et al., 1995). Fast parvalbumin-expressing GABA interneurons are necessary for high-frequency oscillations (Bartos et al., 2007; Uhlhaas et al., 2008), and recent animal studies demonstrated that their inhibition resulted in gamma suppression (Sohal et al., 2009). Similarly, decreasing fast-spiking interneuron activity reduced power and synchronization of gamma oscillations (Spencer, 2009), while its activation induced gamma power increase (Cardin et al., 2009).

GABA-ergic neurotransmission has been extensively studied in psychiatry (Başar, 2013). Post-mortem, low GABA levels were found in SCZ (Volk and Lewis, 2002) and MDD (Rajkowska et al., 2007), and the GABA-synthesizing enzyme GAD1 and GAD67 were altered in SCZ and BPD (Akbarian and Huang, 2006; Gonzalez-Burgos and Lewis, 2008). In depressed suicide victims GABAa receptor mRNA expression was reduced in hippocampus, amygdala and frontal cortex (Merali et al., 2004; Poulter et al., 2010). Reduced density of gabaergic neurons was found in the cortex of patients with either BPD or SCZ (Benes and Berretta, 2001), with reduced GABA synthesis in PV-interneurons (Lewis et al., 2005) in SCZ, suggesting a considerable overlap in inhibitory interneuron abnormalities in neuropsychiatric disorders. Brain magnetic resonance spectroscopy revealed low GABA levels in prefrontal cortex of patients with MDD (Hasler et al.,

2007; Price et al., 2009) and BPD (Bhagwagar et al., 2007). Altogether, these data support the hypothesis that abnormal GABAergic neurotransmission could be critical to explain the abnormal ϒ-oscillations observed in our patients (Sohal et al., 2009; M. A. Whittington et al., 2000).

GABAergic neurotransmission is a therapeutic target in mood disorders and in SCZ. GABA levels increase with mood-stabilizing medications such as valproate and lithium in BPD (Malhi et al., 2013). High-frequency repetitive transcranial magnetic stimulation (rTMS) enhances GABA-inhibitory mechanisms (Daskalakis et al., 2006), and increases gamma-oscillations in HC (Barr et al., 2009). Indeed, rTMS has been shown to improve cognitive deficits in MDD (Downar and Daskalakis, 2013) involving synaptic modulation and plasticity (Esser et al., 2006). Deficits in the modulations of the dopamine system may trigger the appearance of a defective GABA (Benes and Berretta, 2001). Recent studies reported that clozapine treatment may potentiate GABA receptors in schizophrenia patients (Liu et al., 2009).

However, patients with MDD and BPD showed reduced gamma activity even after complete remission (Özerdem et al., 2011; Shaw et al., 2013), suggesting that successful treatment is unable to normalize these core biological features of the disorders. A recent study reported a deficit to produce frontal fast oscillations, independent of medication status (Minzenberg et al., 2010). Here we did not find any correlation between medication doses and natural frequencies. We also previously reported that the natural frequencies of different cortical areas, other than the frontal ones, were not altered in medicated SCZ patients, while if medications would affect neuronal oscillations one would expect a generalized effect (Ferrarelli et al., 2012).

Strengths of the present study include a focused research question, state-of-the-art TMS/EEG methods, and straightforward effects. However, our experimental setting did not allow to directly assess the role of deeper structures, such as hippocampus, which contribute to gamma oscillations (Başar et al., 2001). We obtained an excellent power to study group differences, but could not consider other biological markers, gene variants, and their interaction with clinical variables. Patients were non drug-naïve. Recruitment was in a single ethnic group, thus raising the possibility of population stratifications limiting the generalizability of the findings.

In conclusion, these limitations do not bias the main finding of significantly lower natural frequency of frontal cortico-thalamocortical circuits in patients with BPD, MDD, and SCZ, which suggest their possible relevance as an endophenotype common to major psychoses.

2.3 – Quantifying cortical EEG responses to TMS in (un)consciousness.

Excitability and effective connectivity are key parameters of cortical circuits' functioning. Moreover, alterations of these parameters have been suggested to underlie neurologic and psychiatric conditions.

Some recent studies employed TMS/EEG to measure cortical excitability and effective connectivity in healthy subjects during wakefulness, slow-wave sleep, REM sleep, and benzodiazepine induced anesthesia.

In a first set of experiments (Rosanova et al., 2009) TMS was targeted over three different cortical sites (one occipital, one parietal and one frontal region) of six healthy subjects and the ensuing EEG oscillations were recorded. Indeed, TMS consistently evoked dominant alpha-band oscillations (8–12 Hz) in the occipital cortex, beta-band oscillations (13–20 Hz) in the parietal cortex, and fast beta/gamma-band oscillations (21–50 Hz) in the frontal cortex. In a second series of experiments, Massimini and colleagues (Massimini et al., 2005a; M. Rosanova et al., 2012) recorded TMS-evoked brain responses in healthy subjects whose level of consciousness was experimentally manipulated under both physiological (Massimini et al., 2010, 2007, 2005b) and pharmacological (Ferrarelli et al., 2010) conditions, and compared the obtained responses to those recorded during wakefulness. They then extended these initial observations to the study of pathological conditions in which consciousness was impaired and performed TMS/EEG measurements in brain-injured patients with a broad spectrum of clinical diagnoses, ranging from the vegetative state (VS)/unresponsive wakefulness syndrome (UWS) to the minimally conscious state (MCS) and locked-in syndrome (LIS).

Most important, they show that the EEG response to TMS, once all confounding factors are controlled for, reflects only the intrinsic properties of targeted cortical circuits rather than physical or biological artifacts.

NREM Sleep

In a first series of studies, Massimini and colleagues investigated the changes in TMS-evoked EEG responses during the transition from wakefulness to NREM sleep early in the night, when consciousness fades (Massimini et al., 2005b). During wakefulness, TMS triggers a sequence of low-amplitude, high-frequency (ranging from 10 to 30 Hz) waves associated with a differentiated (in both space and time) pattern of cortical activations (Rosanova et al., 2009) that propagate along long-range ipsilateral and transcallosal connections (Figures 2.3.1A and 2.3.1B, left). Thus, in line with the theoretical requirements, during conscious wakefulness a direct cortical perturbation resulted in complex activity patterns that are, at once, distributed within a system of interacting cortical areas (integrated) and differentiated in space and time (information-rich).

In contrast, during NREM sleep, TMS delivered, with the same stimulation parameters, invariably produces a simple wave of activation that remains localized to the site of stimulation, indicating a breakdown of communication and a loss of integration within thalamocortical networks (Massimini et al., 2005b) (Figure 2.3.1A, middle). In other words, when subjects lose consciousness during NREM sleep, TMS triggers a low-frequency wave, associated with a strong initial cortical activation, which does not propagate to connected brain regions and dissipates rapidly. Interestingly, the disappearance of a complex spatiotemporal pattern of cortical activation is not simply due to a reduction of responsiveness of hyperpolarized cortical neurons. In fact, when TMS is applied at progressively higher intensity the initial activation is followed by a larger negative wave that spreads like an oil spot to vast regions of the cortex. Particularly, when TMS is applied over the parietal cortex this wave reaches period-amplitude criteria of a full-fledged sleep slow wave (Massimini et al., 2007). Thus, during NREM sleep an increase of the spread of the response (integration) comes with the price of a loss of differentiation (Figure 2.3.1A, middle).

Overall, these results demonstrated that during NREM the thalamocortical system, despite being active and reactive, loses its ability to engage in complex activity patterns (Casarotto et al., 2010; Rosanova et al., 2009) that are, at once, distributed within a system of interacting cortical areas (integrated) and differentiated in space and time (information-rich); it either breaks down in casually independent modules (loss of integration) or bursts in an explosive response (loss of differentiation/information).
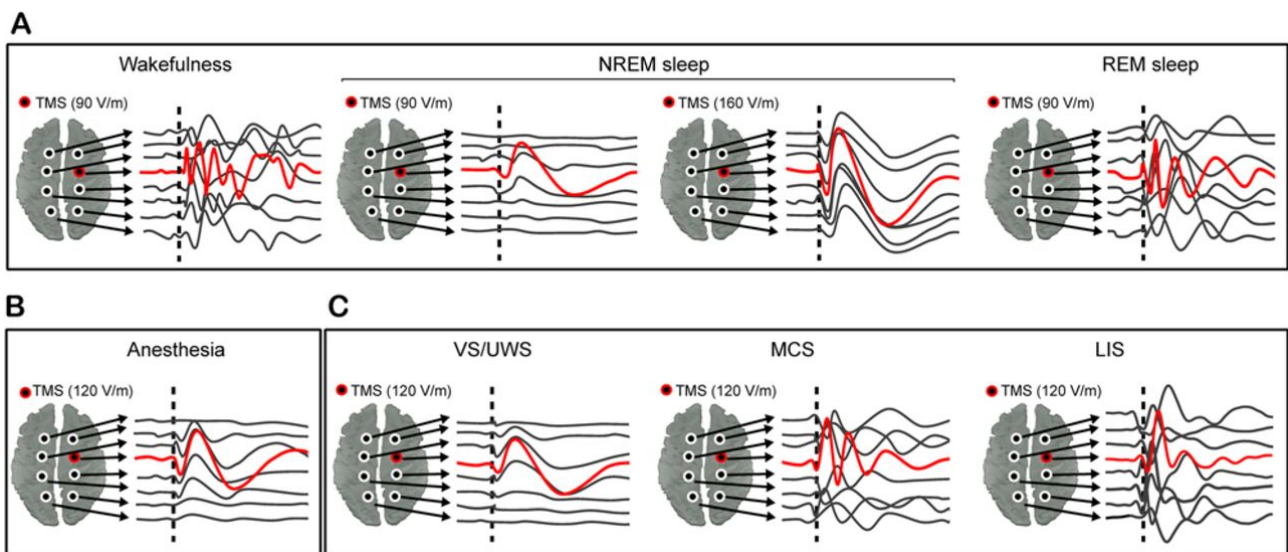
Figure 2.3.1 - Loss and recovery of integration and information in thalamocortical networks. During wakefulness (A, left), TMS triggers a sustained response made of recurrent waves of activity associated with spatially and temporally differentiated patterns of activation (brain complexity). During NREM sleep (A, middle), anesthesia (B), and vegetative state (C, left) the thalamocortical system, despite being active and reactive, loses its ability to engage in complex activity patterns and either breaks down in casually independent modules (loss of integration) or it bursts in an explosive response (loss of differentiation/information). During REM sleep (A, right) and in MCS (C, middle) and LIS patients (C, right), the TMS response shows a recovery of recurrent waves of activity associated with spatially and temporally differentiated patterns of activation.

Midazolam Anesthesia

These observations have been replicated in a recent set of experiments where it has been tested whether cortical effective connectivity would show a breakdown, similar to the one observed in deep NREM sleep, during LOC induced by a pharmacological agent, midazolam, delivered to healthy participants at anesthetic concentrations (Ferrarelli et al., 2010). Similar to NREM while during wakefulness TMS triggered complex responses involving multiple cortical areas distant from the site of stimulation, during midazolam-induced LOC, TMS evoked a positive–negative response

that was initially larger but that remained local (Figure 2.3.1B, right). As during NREM sleep, also during midazolam anesthesia, this stereotypical response evolved into a full-fledged slow oscillation when the cerebral cortex was stimulated at higher intensity(Massimini et al., 2012).

Dreaming

One of the most striking paradoxes sleep can offer is represented by dreaming. A person lying down with eyes closed—as during NREM sleep—disconnected from the external environment, almost completely paralyzed and unresponsive, is consciously experiencing something that closely resembles waking activity, and upon awakening is able to verbally report its content. Dreamlike consciousness occurs during various phases of sleep, including sleep onset and late night, especially during rapid eye movement (REM) sleep. Thus, to probe the internal dialogue of the thalamocortical system even in the absence of any behavioral cue, it has been recorded the TMS-evoked responses during REM sleep in healthy subjects whose consciousness regained in the form of long and vivid dreams (Massimini et al., 2010). Consistent with the theoretical predictions, the recovery of conscious experience during REM was accompanied by a widespread and differentiated pattern of cortical activation similar to those observed during wakefulness (Figure 2.3.1A, right).

Severe Brain Injury

Finally, it has been investigated whether a stereotypical pattern of cortical responses (similar to NREM sleep and midazolam anesthesia) was present also when consciousness was lost due to brain insults (Rosanova et al., 2012). To do so, it has been employed TMS/EEG to measure cortical responses at the bedside of VS/UWS patients (ie, awake, but entirely unaware). To minimize the possibility of a misdiagnosis due to fluctuations in behavioral responsiveness, clinical assessment was performed by means of the Coma Recovery Scale–Revised (CRS-R)(Giacino et al., 2004) repeated 4 times a week, every other day. Invariably, the EEG response to TMS was characterized by a local, stereotypical positive–negative wave similar to those obtained during NREM sleep and anesthesia (Figure 2.3.1C, left). Interestingly, the same stimulation performed in

noncommunicative brain-injured patients capable of purposeful behaviors, such as visual tracking or response to simple commands (therefore diagnosed as MCS), was characterized by regaining a complex spatiotemporal pattern of cortical activations, closely resembling those obtained during wakefulness and REM sleep (Figure 2.3.1C, right). This similarity was even more explicit when TMS was performed in LIS patients, who were totally paralyzed except for vertical eye movements through which they could signal their awareness and establish a nonambiguous, functional communication with the external world. Along these lines, in a recent study, Ragazzoni and colleagues (Ragazzoni et al., 2013) reported reduced cortical connectivity following TMS in VS/UWS patients, as compared to MCS patients and healthy controls.

## 2.3.1 - Consciousness and Complexity: From Theory to Practice

Theoretical measures based on the idea that consciousness relies on the joint presence of differentiation and integration in neural systems have been proposed over the past decade (Seth et al., 2011; Tononi, 2008; Tononi et al., 1994). For example, neural complexity (Tononi et al., 1994) is high when small subsets of elements tend to show independence (differentiation), but large subsets show increasing dependence (integration). Φ (Tononi, 2008) is based on perturbing a system in all possible ways to count the number of different states (differentiation) that can be discriminated through causal interactions within the system as a whole (integration). A related measure, called causal density (Seth et al., 2011), is based on Granger causality and is high if a system's elements are both globally integrated (they predict each other's activity) and differentiated (they contribute to these predictions in different ways). Unlike other measures based on the entropy of spontaneous signals (Pincus et al., 1991), these theoretical measures share the insight that the kind of complexity that is relevant for consciousness should be based on the interactivity among different parts of the brain (Seth et al., 2008; Tononi, 2004). Unfortunately, the application of neural complexity, Φ and causal density to actual brains presents substantial practical challenges, such as extraordinary computational demands.

The results outlined in the previous section demonstrated that during LOC the thalamocortical system, despite being active and reactive, loses its ability to engage in complex activity patterns

that are, at once, distributed within a system of interacting cortical areas (integrated) and differentiated in space and time (information-rich); it invariably either breaks down in casually independent modules (Massimini et al., 2005b) (loss of integration) or it bursts in an explosive response (Massimini et al., 2007) (loss of differentiation/information). The aforementioned TMS/EEG empirical measurements thus provide qualitative support to basic theoretical predictions and pave the way toward a quantification of brain complexity across subjects and conditions, a key requirement for a reliable, unified measurement scale.

The Perturbational Complexity Index

In order to capture brain complexity by means of a synthetic, quantitative index, have been recently developed a theory-driven empirical measure, the so called Perturbational Complexity Index (PCI), which can be practically employed at the patient's bedside (Casali et al., 2013). In agreement with the relevant theoretical requirements for consciousness, PCI gauges the amount of information contained in the integrated response of the thalamocortical system to a direct perturbation. The idea is that the level of consciousness could be estimated empirically by perturbing the cortex ("zapping") to engage distributed interactions and measuring the information content of the ensuing responses by algorithmic compressibility ("zipping"). Operationally, PCI is defined as the normalized Lempel–Ziv algorithmic complexity (Lempel and Ziv, 2006) of the overall spatiotemporal pattern of significant cortical activation measured by EEG and triggered by a direct cortical perturbation with TMS (Figure 2.3.2). In practice, PCI is expected to be low whenever causal interactions among cortical areas are reduced (loss of integration), since the matrix of activation engaged by TMS is spatially restricted; PCI will also be low if many interacting areas react to the perturbation, but they do so in a stereotypical way (loss of differentiation). In this case, the resulting matrix would be large but redundant and could be effectively compressed. It derives that PCI will be high only if the initial perturbation is transmitted to a large set of integrated areas that react in a differentiated way, giving rise to a complex spatiotemporal pattern of deterministic activation that cannot be easily reduced.
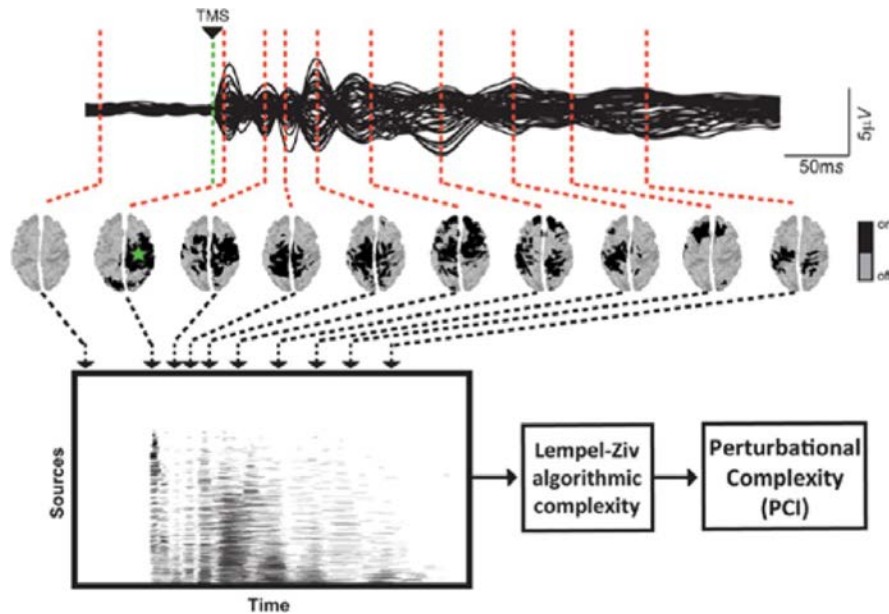
Figure 2.3.2 - Calculating the PCI. A binary spatiotemporal matrix of significant cortical activation triggered by TMS (green star) is compressed ("zipped") by Lempel–Ziv algorithmic complexity. Modified from Casali et al (Casali et al., 2013).

PCI was tested on a large data set of TMS-evoked potentials recorded in healthy subjects (N = 32) during wakefulness, dreaming, NREM sleep, and different levels of sedation induced by different anesthetic agents (midazolam, xenon, and propofol), as well as in a group of patients (N = 20) who emerged from coma and recovered consciousness to a variable extent. As shown in Figure 2.3.3A, experimentally, PCI was reproducible within and across subjects and depended exclusively on the level of consciousness in all conditions. Specifically, PCI was always high in wakefulness, irrespectively of TMS stimulation site and intensity, but dropped drastically when subjects lost consciousness in NREM sleep, after administration of midazolam, and during general anesthesia with propofol and xenon. In all these conditions, PCI was invariably reduced resulting in a clear-cut distinction between the distributions of the conscious and unconscious states. Crucially, PCI was as low as in NREM sleep and anesthesia in patients with a stable clinical diagnosis of VS/UWS, but was invariably higher in subjects who regained consciousness, including MCS, emerging from MCS (EMCS) and LIS patients (Figure 2.3.3B and 2.3.3C).
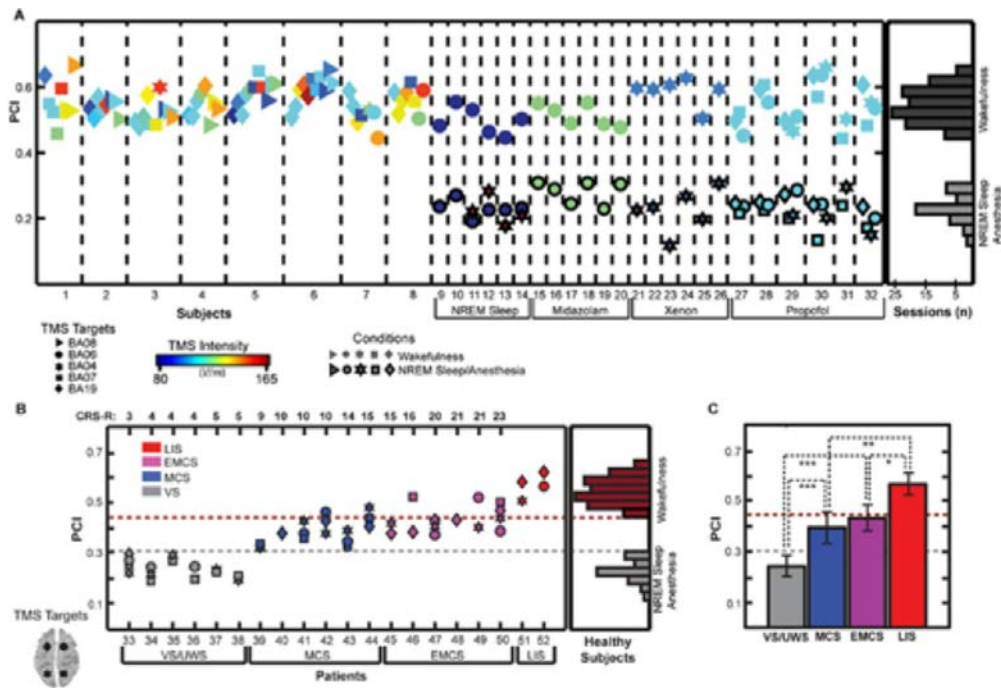
Figure 2.3.3 - Testing the PCI. (A) PCI values are shown for 152 TMS sessions collected from 32 healthy subjects. The histograms on the right display the distributions of PCI across subjects during alert wakefulness (dark gray bars) and loss of consciousness (LOC; light gray bars). PCI calculated during wakefulness (110 sessions) ranged between 0.44 and 0.67 (mean = 0.55 ± 0.05), whereas the PCI calculated after LOC (42 sessions) ranged between 0.12 and 0.31 (mean = 0.23 ± 0.04). (B) PCI values are shown for 48 TMS sessions collected from 20 severely brain-injured patients. PCI followed the level of consciousness (as clinically assessed with CRS-R) progressively increasing from VS/UWS through MCS and recovery of functional communication (EMCS) and attaining levels of healthy awake subjects in LIS. Patient results are directly compared with the ones obtained in healthy individuals. (C) Box plots for PCI in brain-injured patients are presented with the statistical significance between pairs of conditions (dashed black lines). *P < .005. **P < .0005. Modified from Casali et al (Casali et al., 2013).

These results indicate that PCI provides an entirely data-driven metric that is reproducible across different conditions (wakefulness, dreaming, LIS, MCS, EMCS, NREM sleep, midazolam sedation, xenon and propofol anesthesia, VS/UWS) and comparable within and across single subjects in the same coordinate space. The main reason for this unprecedented result may reside in the fact that perturbational complexity gauges, at the same time, both the information content and the integration of brain activations. Indeed, PCI combines measures of algorithmic complexity with a perturbational approach, a method that detects large-scale activations that are intrinsically causal. Unlike other measures of complexity that are commonly applied to spontaneous brain signals, PCI accounts only for the information that is generated through deterministic interactions within the thalamocortical system. In this way, the resulting complexity is not affected by random processes, such as noise and muscle activity, or by patterns that are not genuinely integrated, such as the

ones generated by isolated neuronal sources or common drivers. Most important, PCI establishes a reliable measurement scale by defining a range of values between various conditions in which consciousness is known to be present (wakefulness, dreaming, LIS), and absent (NREM sleep, different types of anesthesia, stable diagnosis of VS/UWS).

Finally, another clear advantage of this metric is the fact that it can be assessed on the basis of the complexity of cortical interactions, thus independent of the subjects' capacity or willingness to react to external stimuli/commands.

CHAPTER 3 – CORTICAL BISTABILITY UNDERLIES PHYSIOLOGICAL AND PATHOLOGICAL LOSS OF CONSCIOUSNESS

Why do complex, long-range cortical interactions collapse into a simple response whenever consciousness is lost?

The striking similarity between TMS-evoked EEG responses during sleep, under anesthesia, and in VS/UWS patients suggests common neuronal mechanisms for LOC in these conditions. In all cases, the complex TMS-evoked activation observed during wakefulness is replaced by a stereotypical positive–negative deflection, which, when TMS is delivered at high intensities, evolves into a graphoelement that matches the EEG criteria for a sleep slow wave, or a K-complex (Massimini et al., 2007). Animal (Steriade et al., 2001) and human (Cash et al., 2009) intracranial recordings have shown that both spontaneous EEG sleep slow waves and K-complexes are underpinned by the occurrence of a silent, hyperpolarized down-state in cortical neurons, which is preceded and followed by a period of activation (up-state). This bimodal alternation between up- and down-states reflects an intrinsic bistability in thalamocortical circuits that is thought to depend on neuronal as well as network properties (Hill and Tononi, 2005; Mann et al., 2009; Sanchez-Vives and McCormick, 2000; Timofeev et al., 2000, Sarasso et al., 2014).

Our proposition is that, due to bistability, portions of the thalamocortical system, which are otherwise healthy, would not be able to sustain balanced patterns of activations; thus, the inescapable occurrence of a stereotypical down-state after an initial activation would prevent the emergence of complex, long-range patterns of activation in response to a direct stimulation.

In order to test this hypothesis , experimentally, one should first demonstrate that the slow wave-like graphoelement triggered by TMS during NREM, anesthesia and in VS/UWS patients truly reflect a neuronal down-state (i.e., a long lasting period of membrane hyperpolarization). To this aim, ideally, one could measure modulation of high-frequencies (gamma-range), which is considered a good proxy of the hyperpolarization of cortical neurons.

In the following paragraphs this problem has been addressed first from an intracerebral perspective, then using TMS/EEG. First, in the paragraph 3.1 the results obtained by Pigorini et al. are reported (Pigorini et al., 2015). Here intracranial electrical stimulation and recordings have been employed to demonstrate that during NREM sleep (a physiological model of LOC), a perturbation of thalamo-cortical system induced a widespread suppression of high frequencies (i.e. cortical downstates) that impairs the ability of thalamocortical circuits to engage in causal interactions, a theoretical requirement for consciousness (Tononi, 2004). Second, a recently submitted paper by Fecchio et al. is reported in the paragraph 3.2. Here, the results obtained invasively by using intracranial stimulation and recordings were confirmed non-invasively using TMS/EEG in NREM sleep. More important, they were extended at VS/UWS patients suggesting that bistability could be an important neurophysiological mechanisms underlying both physiological and pathological loss of consciousness.

3.1 – Bistability breaks-off deterministic responses to intracortical stimulation during non-REM sleep

Once awakened from NREM stage N3 early in the night people often deny that they were experiencing anything at all (Stickgold et al., 2001). Experimentally, this reduction of consciousness upon falling into NREM is associated with a significant impairment of the ability of distributed groups of cortical neurons to sustain reciprocal interactions. This alteration has been detected by analyzing functional connectivity within cortical networks in resting condition (Boly et al., 2012; Spoormaker et al., 2011; Tagliazucchi et al., 2013) and becomes obvious when one applies perturbations directly to the cerebral cortex. Hence, measurements performed with transcranial magnetic stimulation (TMS) and electroencephalography (EEG) have shown that a single magnetic pulse triggers a complex chain of causal interactions that propagate through a distributed network of cortical areas during wakefulness, but a simple response that remains either local (Massimini et al., 2005b) or spreads like an oil-spot (Massimini et al., 2007) during NREM. This altered response to TMS has been subsequently observed in other conditions in which

consciousness is lost, such as general anesthesia and the vegetative state (Casali et al., 2013; Rosanova et al., 2012). Also in these cases, a differentiated pattern of deterministic interactions is replaced by the occurrence of a stereotypical slow wave. Yet, the neurophysiological mechanisms underlying this reduction of the brain's capacity to sustain complex patterns of cortical activation remain unclear.

The most obvious feature of spontaneous brain activity during NREM is the appearance of EEG slow waves associated with brief periods of hyperpolariziation and neuronal silence (down-states) (Steriade et al., 1993). In principle, the spontaneous occurrence of cortical down-states may in itself be enough to prevent reliable information transmission among cortical areas. However, while this mechanism may be crucial in the case of general anesthesia, during which cortical activity is frequently interrupted by long hyperpolarized down-states (Lewis et al., 2005), it may not be sufficient in other conditions such as sleep. In fact, intracellular recordings in cats show that even during deep NREM, cortical neurons can spend most of their time in a depolarized, wakefulness-like up-state, which is only occasionally interrupted by hyperpolarized, silent down-states (Chauvette et al., 2011). Local field potentials (LFP) and multiunit recordings in humans have also demonstrated that most slow waves and the associated down-states are local (Hangya et al., 2011; Nir et al., 2011), and that some brain areas may be active for long stretches while others are asleep (Nobili et al., 2011). Finally, the active periods observed during NREM share several fundamental features with ongoing activity during wakefulness, e.g. mean firing rate (Destexhe et al., 1999; Hobson and McCarley, 1971; Steriade et al., 2001), spectral profile (Csercsa et al., 2010) and synchronization level (Destexhe et al., 1999; Steriade and Amzica, 1996) so much so that the depolarized states of the sleep slow oscillation have been referred to as "fragments of wakefulness" (Destexhe et al., 2007, 1999). Thus, it is not obvious that the spontaneous occurrence of silent periods may substantially impair the brain's capacity for internal communication.

Besides changes in spontaneous activity, cortical neurons undergo a more profound modification upon falling asleep as they become bistable upon changes in their intrinsic properties (Compte et al., 2003; Sanchez-Vives and McCormick, 2000; Timofeev et al., 2001). Due to underlying

bistability, cortical networks have the tendency to fall into a silent down-state in response to transient increases in activity (Compte et al., 2003; Sanchez-Vives and McCormick, 2000). An intriguing possibility is that this tendency may specifically impair the emergence of stable patterns of causal interactions among cortical areas. Specifically, we hypothesize that (i) during NREM a group of neurons that receives a cortical input rapidly plunges into a down-state and that (ii) this period of silence breaks-off the causal effects of the initial input.

Intracranial single-pulse electrical stimulation (SPES) and simultaneous stereotactic EEG (SEEG) recordings offer a unique opportunity to test this hypothesis. First, intracranial recordings allow a reliable, although indirect, detection of cortical down-states as a significant suppression of high frequency power above 20 Hz in the LFP (Cash et al., 2009; Valderrama, 2012). Second, intracranial perturbations with SPES permit to assess cortico-cortical and/or cortico-subcortico-cortical interactions from a causal perspective by calculating the phase locking factor (PLF) (Sinkkonen et al., 1995). We thus analyzed by means of time–frequency decomposition and phase-locking analysis the SEEG responses to SPES in 8 patients undergoing neurosurgical evaluation for intractable epilepsy.

Materials and methods

Patients and data acquisition

Data included in the present study derived from a dataset collected during the pre-surgical evaluation of eight neurosurgical patients with a history of drug-resistant, focal epilepsy (Table 3.1). All subjects were candidates for surgical removal of the epileptic focus. During the pre-surgical evaluation all patients underwent individual investigation with simultaneous single pulse electrical stimulation (SPES) and recordings performed by stereotactically implanted depth multi-lead electrodes (Stereo-EEG, SEEG) for the precise localization of the epileptogenic zone and connected areas (Cossu et al., 2005). The investigated hemisphere, the duration of implantation and the location and number of stimulation sites were determined based on the non-invasive clinical assessment.

Table 3.1 Demographic and clinical information for each patient

Subject	Gender (Age, years)	Medications (mg/day)	Number of electrodes	Number of contacts [after contact rejection]	Epileptic zone location
1	F (31)	Carbamazepine 600 mg/day	17	189 [68]	**
2	M (21)	Levetiracetam 3000 mg/day; Carbamazepine 800 mg/day	14	147 [64]	Right central cingulate gyrus
3	F (21)	Levetiracetam 3000 mg/day; Topiramate 500 mg/day	12	146 [44]	Left posterior medial frontal gyrus
4	M (36)	Oxcarbamazepine 1200 mg/day; Phenobarbital 100 mg/day; Lamotrigine 150 mg/day	14	170 [44]	Right temporal neocortex
5	M (31)	Carbamazepine 800 mg/day; Phenobarbital 100 mg/day; Levetiracetam 3000 mg/day	15	179 [58]	Right orbital gyrus
6	M (18)	Carbamazepine 800 mg/day	14	165 [56]	Right genus cinguli
7	M (20)	Carbamazepine 800 mg/day; Levetiracetam 3000 mg/day	14	186 [48]	Right posterior mesial frontal gyrus
8	M (25)	Phenytoin 400 mg/day; Topiramate 500 mg/day	12	143 [40]	Right superior frontal gyrus

**SEEG assessment in this patient was unrevealing (no contact showed interictal/ictal signatures).

SEEG activity was recorded from platinum–iridium semiflexible multi-contact intracerebral electrodes, with a diameter of 0.8 mm, a contact length of 1.5 mm, an inter-contact distance of 2 mm and a maximum of 18 contacts per electrode (Dixi Medical, Besancon France—Figures 3.1.1A–B). The individual placement of the electrodes was ascertained by post-implantation tomographic imaging (CT) scans (Figure 3.1.1B). In addition scalp EEG activity was recorded from two platinum needle electrodes placed during surgery on the scalp at standard "10–20" positions Fz and Cz. Electro-ocular activity was recorded from the outer canthi of both eyes, and submental electromyographic activity was also recorded. Both EEG and SEEG signals were recorded using a 192-channel recording system (NIHON-KOHDEN NEUROFAX-110) with a sampling rate of 1000 Hz. Data were recorded and exported in EEG Nihon-Kohden format. Recordings were referenced to a contact located entirely in the white matter.
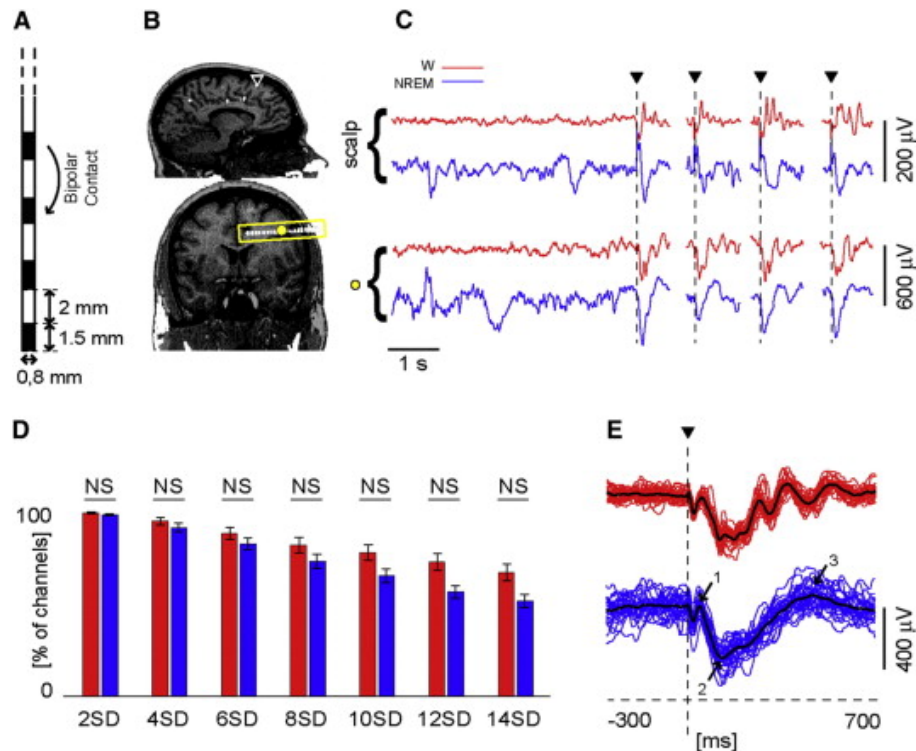
Figure 3.1.1. - Experimental setup and methods for SPES and recordings. Panel A. Outline of a multi-lead intracerebral electrode. Panel B. Sagittal and coronal sections of Subject 1 MRI showing an example of a multi-lead intracerebral electrode (yellow rectangle). White dots identify recording contacts whereas a black triangle indicates the stimulation site. Panel C. Scalp EEG recorded during wakefulness (W-red) and NREM (NREM-blue) and concurrent raw intracerebral signal recorded from one bipolar contact (indicated by the yellow circle in Panel B). The first 5 s of each trace display spontaneous EEG activity followed by evoked responses to SPES (dashed lines and black triangles). Panel D. Percentage of contacts (± standard error) showing significant CCEPs during wakefulness (red) and NREM (blue). At the level of individual contacts, we tested different thresholds (from 2 to 14 standard deviation of the mean baseline activity) calculated from the rectified, mean amplitude of the CCEPs. Panel E. Colored traces represent single trials collected in W and NREM (red and blue respectively) at a given recording site (black circle onto the MRI coronal section of Panel B). Average responses are overlaid in black. The numbers and the arrows indicate the three components (1, 2 and 3) that characterize the response to SPES during NREM.

SPES is a clinical procedure increasingly employed for the identification of abnormal cortical excitability in patients with epilepsy (David et al., 2010; Valentín et al., 2002). In the present dataset, SPES was performed five days after electrode implantation both during wakefulness and during NREM (Silber et al., 2007) given the possible nocturnal nature of the seizures. Specifically, a 5 mA current was applied through one pair of adjacent contacts, while SEEG activity was simultaneously recorded from all other bipolar contacts. A single stimulation session consisted of 30 consecutive single pulses delivered at varying inter-stimulus intervals (1 to 5 s). The stimulation, recording and data treatment procedures were approved by the local Ethical Committee (protocol number: ID 939, Niguarda Hospital, Milan, Italy). All patients provided written informed consent.

Selection of recording contacts and stimulation session

In each subject the dataset derived from the pre-surgical exploration included several sessions (up to 20), in which different contacts were stimulated, and multiple contacts (up to 189) were recorded. For the present analysis, selection of recording sites and stimulation sessions was based on the following criteria; we excluded from the analysis those contacts that (i) were located in the epileptogenic zone (as confirmed by post-surgical assessment), (ii) were located over regions of documented alterations of the cortical tissue (e.g. Taylor Dysplasia) as measured by the radiographic assessment, or (iii) exhibited spontaneous or evoked (Valentín et al., 2002) epileptiform SEEG activity during wakefulness or NREM (visual inspection performed by L.N. and P.P.). Also contacts located in white matter, as assessed by means of MRI, were excluded (by two of the authors: L.N. and C.S.) from further analysis. Anatomical locations of bipolar derivations were confirmed by means of customized MATLAB scripts, using Destrieux ATLAS.

With the given contact selection, we analyzed the stimulation sessions that: (i) were delivered through a contact far from the epileptogenic zone (as confirmed by post-surgical assessment); (ii) were delivered through a contact that did not show spontaneous interictal activity (by visual inspection); (iii) did not evoke epileptic responses (Valentín et al., 2002) either in wakefulness or NREM; (iv) did not elicit muscle twitches, sensations or evident motor/cognitive effects (e.g. language comprehension/production or complex motor sequences) during presurgical evaluation, including single pulse and repetitive (50 Hz) stimulation (Cossu et al., 2005); (v) occurred during a period of N3 sleep; and (vi) did not disrupt sleep depth as assessed by comparing the power spectra of scalp EEG spontaneous activity before and after the stimulation train. If in a given subject more than one stimulation session fulfilled these criteria, we selected the one that triggered significant cortico-cortical evoked potentials (CCEPs, Matsumoto et al., 2004) in the largest number of contacts as in Keller et al. (2011).

Data preprocessing

Data recorded during both wakefulness and NREM were imported from EEG Nihon Kohden format into Matlab and converted using a customized Matlab-based script. Data were subjected to linear detrend and bandpass filtering (0.5 – 300 Hz), using a third order Butterworth filter. Bipolar montages were calculated by subtracting the signals from adjacent contacts of the same depth-electrode to minimize common electrical noise and to maximize spatial resolution (Cash et al., 2009; Gaillard et al., 2009) (see Figure 3.1.1A). Single trials were obtained by using a digital trigger simultaneous to each SPES delivery. Finally, stimulation artifact was reduced by applying a Tukey-windowed median filtering, as in Chang et al. (2012), between − 5 and 5 ms.

Methodological rationale and data analysis

First we assessed the number of contacts showing significant response to SPES by applying the same methodology as in Keller et al. (2011). Specifically, at the level of individual contacts, we tested different thresholds (from 2 to 14 standard deviations of the mean baseline activity) calculated from the rectified, mean amplitude of the CCEPs. Then, in order to assess quantitatively the differences in the dynamics triggered by SPES in wakefulness and NREM, we quantified (1) the amplitude of the low frequency components (< 4 Hz), (2) the suppression of high frequency power (> 20 Hz) and (3) the PLF. Indeed, these three measures indicate respectively the possible presence of SPES-evoked slow waves, the correspondent occurrence of a cortical down-state (Cash et al., 2009; Csercsa et al., 2010; Valderrama, 2012) induced by SPES and the causal effects of SPES at the level of individual contacts. In the following, as in previous works (Nir et al., 2011; Vyazovskiy et al., 2009), we use the terms "OFF" periods instead of "down" (or "hyperpolarized") states (Steriade et al., 2001) because silent periods were defined on the basis of extracellular activity (suppression of high frequency in the LFP) rather than based on a direct measure of membrane potential.

Amplitude of low frequency component

To assess and quantify the presence of SPES-evoked slow waves we calculated, both for wakefulness and NREM, the amplitude of low frequency components (< 4 Hz) (Figure 3.1.2) for each contact as the average of absolute value of filtered (4 Hz low-pass, third order Chebyshev filtering) single trials. We rectified the slow components because slow waves could be either positive or negative, depending on contacts locations. Then we set to zero all the non-significant time points using a trial-based bootstrap statistical analysis (α < 0.01, number of permutations = 1000) with respect to baseline (from $-$ 300 ms to $-$ 50 ms).

High-frequency suppression

To assess and quantify the presence of SPES-evoked cortical OFF-periods we calculated the amount of significant (bootstrap method; α < 0.05, number of permutations = 1000) high-frequency (> 20 Hz) suppression, an established extracellular marker of the neuronal down-state that characterizes sleep bistability (Cash et al., 2009; Csercsa et al., 2010; Mukovski et al., 2007; Nir et al., 2011; Valderrama, 2012; Vyazovskiy et al., 2009). Hence, as in Cash et al. (2009), we calculated for each contact the mean value of the ERSP above 20 Hz (Figure 3.1.2) over a peri-stimulus time-window ranging between $-$ 300 and + 700 ms.

Phase locking factor

To quantify and compare the duration of the deterministic effects of SPES during both wakefulness and NREM for each contact, the instantaneous PLF was calculated as in Palva et al. (2005). PLF is an adimensional (range 0–1) index defined as the absolute value of the average of the Hilbert Transform of all single trials; in the case of evoked potentials (here CCEPs), it reflects the ability of an external stimulus (here SPES) to affect the phase of ongoing oscillations across trials. Statistical differences from baseline (from $-$ 300 ms to $-$ 50 ms) were assessed (for each contact) by assuming a Rayleigh distribution of the values of the baseline. Then, given a statistical threshold set at α < 0.05, those PLF values below threshold were set to zero (Figure 3.1.2B).

Before calculating PLF, single trials were filtered (8–100 Hz) with a combination of high-pass and low-pass third-order Butterworth filters in order to minimize time-domain spread of PLF (Palva et al., 2005). To verify that the drop in PLF above 8 Hz was not trivially due to the absence of power in the same frequency range, we computed the average of the squared absolute value of filtered single trials (8 Hz high-pass, third order Butterworth filtering). Within the investigated frequency range, we also explored the contribution of the three classical EEG bands by measuring PLF of signals filtered in the alpha (8–13 Hz), beta (13–30 Hz) and gamma (above 30 Hz) ranges.
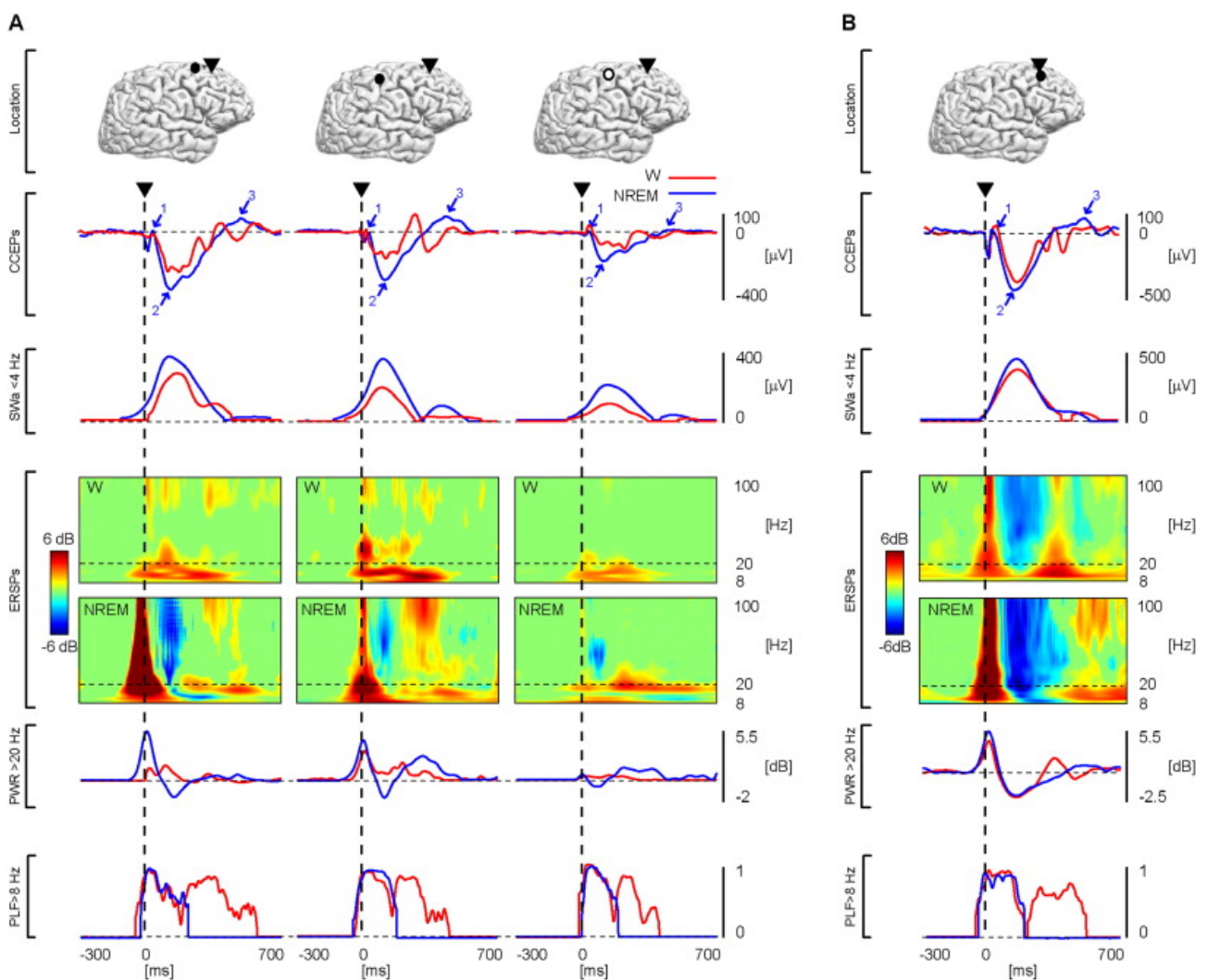
Figure 3.1.2. - During NREM, SPES triggers a slow-wave-like response that is associated with high frequency suppression followed by decay of PLF. In Panel A the following measures are reported for three representative contacts in one subject. Location: the position of the stimulating contact is depicted (black triangle) over a 3D brain reconstruction (lateral view) of the individual's brain (Subject 1). Black circles and white circles show the position of three representative recording bipolar derivations from right and left hemisphere, respectively. CCEPs: the corresponding average responses from these contacts during wakefulness (W-red) and NREM (NREM-blue). As in Figure 3.1.1E, blue arrows and numbers indicate the three components of CCEPs evoked during NREM. SWa < 4 Hz: amplitude of the slow (< 4 Hz) wave component calculated as squared absolute value

70

of the CCEPs after 4 Hz low-pass third order Chebyshev filtering. After bootstrap statistic (α < 0.05), non-significant time points (with respect to baseline, from − 300 to − 50 ms) were set to zero. ERSPs: time-frequency power spectra of CCEPs recorded in W and NREM. Time-frequency decomposition is applied at a single trial level using Wavelet Trasform (Morlet, 3 cycles) and significance for bootstrap statistics is set with α < 0.05. Blue color indicates a significant reduction compared to the baseline, while red indicates significant increase. The dashed horizontal line indicates 20 Hz. PWR > 20 Hz: time series of high frequency power (> 20 Hz). PLF > 8 Hz: PLF calculated on a single trial level both for W (red) and NREM (blue) after high-pass filtering (> 8 Hz). Statistical differences from baseline are assessed (for each contact) by assuming a Rayleigh distribution of the values of the baseline (from − 300 to − 50 ms). Then, given a statistical threshold set at α < 0.05, those PLF values below threshold were set to zero. Dashed vertical lines and triangles represent stimulus onset. Panel B. Same measures of Panels A but referred to a contact close to the stimulation site.

Results

In all patients (Table 3.1) SPES was delivered both during wakefulness and NREM through one pair of adjacent (2 mm apart) contacts pertaining to the same depth-electrode, while SEEG recordings were obtained from all other bipolar contacts (Figures 3.1.1A–B; see Materials and methods for a detailed description of the number and location of the stimulating and recording contacts). In each individual, depending on clinical needs, a number of cortical sites were stimulated with 30 pulses at frequencies between 0.2 and 1 Hz during wakefulness preceding lights off as well as during NREM (scored according to Silber et al., 2007). Off-line sleep scoring using one scalp EEG derivation, together with one bipolar electrooculographic (EOG) and one electromyographic (EMG) derivation confirmed that all considered sessions were recorded during NREM N3. The stability of stage N3 throughout each stimulation session was further assessed by comparing the power spectra of the scalp EEG recorded immediately (40-s epochs) before and after the SPES train.

As illustrated in Figure 3.1.1C, CCEPs were highly reproducible from trial to trial and were characterized by a high signal-to-noise ratio in intracranial recordings. As a first step, we asked whether the ability of SPES to trigger significant activations across recording contacts differed in NREM compared to wakefulness. To do so, we detected at each contact the presence of significant CCEPs employing the same criteria described by Keller et al. (2011); for each individual contact, we tested different thresholds applied to the rectified amplitude of the CCEPs calculated on the mean amplitude signal. Across patients, the percentage of significantly active contacts in both wakefulness and NREM decreased monotonically with increasing thresholds (from ~ 100% at 2SD to ~ 50% at 14SD) and tended to be lower during NREM (Figure 3.1.1D). However, no

significant difference was observed between the two conditions at any applied threshold. Despite this similarity in the number of contacts affected by the initial stimulation, the CCEPs recorded during wakefulness and NREM were substantially different in terms of their wave shape.

SPES evokes a slow wave-like response in NREM but not in wakefulness

Generally, during wakefulness SPES evoked a composite response made of recurrent waves of activity that persisted until ~ 500 ms (Figure 3.1.1E). Conversely, during NREM, CCEPs consisted of a simpler and slower wave, composed of three consecutive events, which we will henceforth call components 1, 2 and 3 (Figures 3.1.1E and 3.1.2). The polarity of these components could be inverted depending on the location of the recording contacts. In all cases, component 1 was a sharp peak (between 10 and 50 ms), component 2 was a prominent rebound of opposite polarity (peaking ~ 200 ms), and component 3 was an ensuing, smoother deflection in the same direction as component 1. Quantitatively, cortical responses to SPES during NREM were characterized by a prevalent low frequency (0.5–4 Hz) oscillation that was invariably reduced during wakefulness (Figure 3.1.2A). Overall, both in terms of period and peak amplitude, the CCEPs recorded during NREM closely resembled spontaneously occurring sleep slow waves.

SPES induces suppression of high-frequency power in NREM but not in wakefulness

To further explore the relationships between the CCEPs obtained during NREM and sleep slow waves, we capitalized on previous animal and human intracranial recordings. These studies show that the silent hyperpolarized state that characterizes the cortical OFF-period of spontaneously occurring sleep slow oscillations is marked by a suppression of high-frequency power (> 20 Hz) in the LFP (Amzica and Steriade, 2002; Cash et al., 2009; Csercsa et al., 2010; Mukovski et al., 2007; Nir et al., 2011; Steriade et al., 1993). Hence, we performed time–frequency decomposition of CCEPs (Cash et al., 2009) to compare the power modulation (as assessed by event-related spectral perturbation—ERSP) during wakefulness and NREM. Results obtained in one patient at three representative cortical targets during wakefulness and NREM are shown Figure 3.1.2A.

While the composite CCEPs recorded during wakefulness corresponded to increases in spectral power as compared to baseline, the slow wave-like response elicited in NREM was associated with an alternation of positive and negative significant power modulations (see Methods, bootstrap statistics, $\alpha < 0.05$). Specifically, component 1 of the NREM response coincided with a transient broad-band increase of spectral power. Component 2 was associated with a significant suppression of high-frequency oscillations (> 20 Hz) (Figure 3.1.2), irrespective of stimulation frequency and of the level of background activity. Finally, during component 3 spectral power recovered and rebounded to a level comparable to wakefulness in a broad range of frequencies (between 8 Hz and 100 Hz), including alpha, spindle and beta rhythms (Figure 3.1.2A).

Phase-locking is short-lasting during NREM but sustained during wakefulness

Next, we tested our main hypothesis, i.e. that bistability break-off the causal effect of cortical inputs during NREM. To quantify and compare the duration of the deterministic effects of SPES during both wakefulness and NREM, we employed PLF applied to the LFP activity in the 8–100 Hz frequency band, the same range characterizing (i) wakefulness activity (Steriade et al., 2001; Timofeev et al., 2001), (ii) cortical activity during the up-state of spontaneous sleep slow oscillation (Destexhe et al., 2007; Mölle et al., 2002; Steriade, 2006), and (iii) the power increase observed, in our experiment, during component 3 of the NREM response (see Figure 3.1.2A). As shown in Figure 3.1.2A, compared to wakefulness, NREM CCEPs were characterized by an early dampening of PLF, which remained below significance level (Rayleigh, $\alpha < 0.05$) throughout component 3, despite the persistence/recovery of power in the 8–100 Hz range (Figure 3.1.2A). Notably, during wakefulness PLF was long lasting and remained significant until ~ 500 ms even for the few contacts adjacent to the stimulation site, which reacted with a slow wave and a suppression of high frequency similar to NREM (Figure 3.1.2B).

Amplitude, power and phase-locking modulations of cortical responses are reproducible across contacts and patients

Overall, the results obtained for low frequency amplitude, high-frequency power suppression, duration of PLF and their differences between wakefulness and NREM were reproducible across cortical contacts (Figure 3.1.3B), significant across contacts at the single subject level (Figure 3.1.3B, histograms—Wilcoxon ranksum test, $p < 0.05$) and consistent at the population level (Figure 3.1.3C—Wilcoxon ranksum test, $p < 0.05$). Hence, cortical responses to SPES during NREM were characterized by a prominent low frequency (0.5–4 Hz) oscillation, by a significant suppression of high-frequency (20–100 Hz) activity and by an early (~ 200 ms) obliteration of phase-locked, deterministic effects. By contrast, during wakefulness, when the low frequency component was reduced and the suppression of high frequency was absent, the PLF remained significant until ~ 500 ms after SPES.
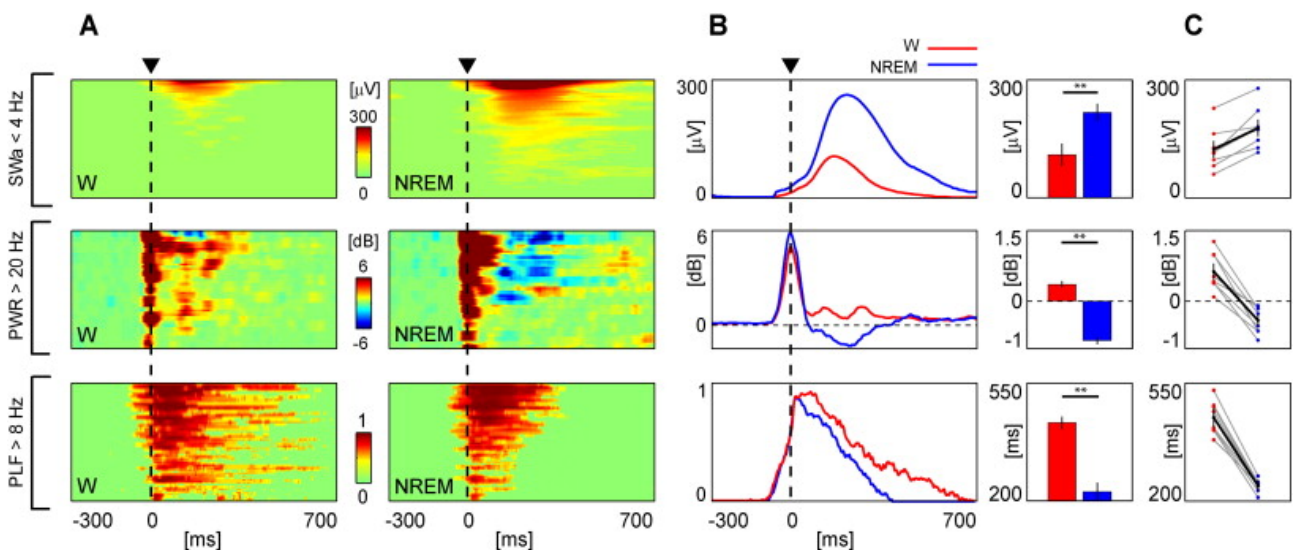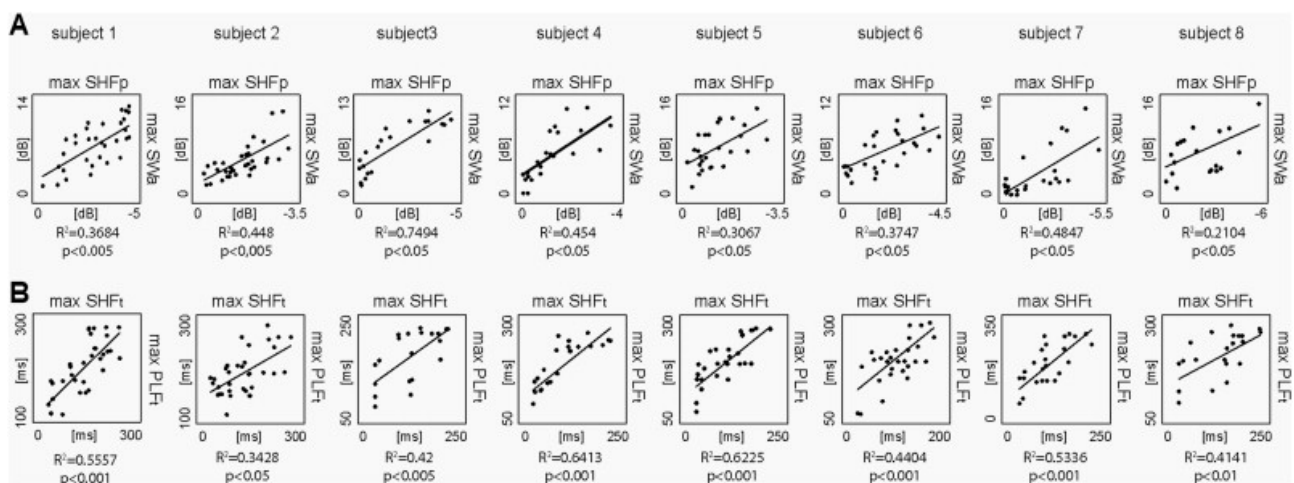

Figure 3.1.3. - Amplitude, power and phase-locking modulation are consistent across contacts and subjects. Panel A: for the same representative subject, color coded plots of amplitude of the slow (< 4 Hz) wave component, high frequency power (> 20 Hz) and PLF (> 8 Hz) are calculated as a function of time for all contacts both for wake (W—left column) and NREM (NREM—right column). For each plot the responses to SPES are ranked based on the amount of low frequency power during NREM. Panel B. On the left, the same three measures as in Panel A averaged across contacts for W (in red) and NREM (in blue). On the right, the top and the middle histograms indicate the average values for low frequency amplitude and high frequency power respectively (black bars indicate standard error of the mean) calculated over the time interval between − 50 ms and + 50 ms around the maximum of the low frequency wave detected at each contact (Panel A—top left box). The bottom histogram shows the average duration of phase-locking (black bars indicate standard error of the mean) calculated from the time of the latest statistically significant non-zero PLF for each contact, in W and NREM. ** indicates significant differences (Wilcoxon ranksum test $p < 0.01$). Panel C. The same three measures shown in Panels A and B are tested across all subjects (W in red, NREM in blue). Black lines indicate the grand average across subjects. Black vertical bars indicate the standard errors. Differences between W and NREM at the population level were tested using a Wilcoxon ranksum test ($p < 0.01$) and were significant for all three measures.

Amplitude, power and phase-locking modulations of cortical responses are related during NREM

We finally asked whether the three distinctive features of the NREM response (i.e. the presence of a slow wave-like response, high frequency suppression and shorter PLF duration) were related. To this aim, for each subject, we selected the contacts showing the largest (top 50%) power in the slow wave frequency band (0.5–4 Hz). We then computed (i) the correlation between the maximum amplitude of the evoked slow wave (max SWa) and the maximum level of suppression of high-frequency power with respect to baseline (max SHFp) as well as (ii) the correlation between the timing of the maximum high frequency suppression (max SHFt) and the latency at which PLF dropped below significance level (max PLFt). This analysis detected significant correlations in each single subject showing (i) that larger evoked slow waves corresponded to more pronounced suppressions of high frequencies and (ii) that earlier suppressions corresponded to an earlier dampening of PLF (Figure 3.1.4).

Figure 3.1.4. - Amplitude, power and phase-locking modulation are related during NREM. Panel A. For each subject the correlation between the maximum amplitude (converted in dB) of the evoked slow wave (max SWa) and the maximum level of high-frequency power suppression with respect to baseline (max SHFp) is shown. Below, the coefficient of determination R2 and the significance level p of the correlation are indicated for each subject. Panel B. For each subject the correlation between the timing of the maximum high frequency suppression (max SHFt) and the latency at which PLF fell below the threshold for significance (max PLFt) is shown. Below, the coefficient of determination R2 and the significance level p of the correlation are indicated for each subject. For each subject, both correlations were calculated considering the contacts that showed the highest (top 50%) low frequency amplitude during NREM.

Discussion

In the present work we compared CCEPs recorded during wakefulness and NREM by means of time–frequency analysis and PLF in 8 epileptic patients implanted with SEEG electrodes for clinical evaluation. We observed that during wakefulness SPES triggers a chain of sustained effects, as indicated by a phase-locked response that lasted for about half a second. During NREM the same initial activation induces a slow wave and a cortical OFF-period in its cortical targets after which the phase-locked response breaks-off, in spite of restored levels of cortical activity.

Bistability, cortical down-states and break-off of phase-locked responses

Intracortical stimulation/recordings can be used to study cortico-cortical interactions from a causal perspective. SPES delivered to the grey matter is thought to elicit direct depolarization of the initial segment of the axons, which travels through direct or indirect cortico-cortical pathways generating CCEPs in adjacent and remote areas (Keller et al., 2011; Matsumoto et al., 2004). Accordingly, in the present work, we observed evoked responses to SPES in targets both near and far from the stimulating contact, in ipsi-lateral and contro-lateral areas (see Figure 3.1.2A). Significant responses to SPES could be elicited in a large number of contacts during both wakefulness and NREM (Figure 3.1.1D). This finding is in agreement with previous animal studies (Richardson and Fetz, 2012) and with the hypothesis that the breakdown of complex interactions observed during NREM by means of TMS/EEG is not due to the interruption of structural cortico-cortical and/or cortico-subcortico-cortical connections but rather to changes in the dynamics of neuronal responsiveness (Massimini et al., 2012). Indeed, we observed that the initial activation triggered by SPES in its cortical targets was followed by a composite set of waves during wakefulness, but by a stereotypical slow wave that was associated with an extracellular marker of a neuronal down-state during NREM. Interestingly, slow waves and cortical OFF-periods could be triggered even on the background of a low-amplitude, wakefulness-like activated LFP. This observation is consistent with in vivo and in vitro studies showing that, due to bistability, networks that can display wakefulness-like activity tend to fall into a silent down-state upon transient increases in activation (Compte et al.,

2003; Sanchez-Vives and McCormick, 2000; Timofeev et al., 2001). At the neuronal level, the bistability of NREM sleep is thought to be primarily due to the dynamics of activity-dependent potassium (K +) currents, which become prominent when the neuromodulating milieu changes upon falling asleep (Compte et al., 2003; Sanchez-Vives and McCormick, 2000; Timofeev et al., 2001). In this condition, the stronger is the initial activation, the more K +-currents will tend to drive neurons into a hyperpolarized, silent state (Compte et al., 2003). Accordingly, in the present study, the degree of high frequency suppression was significantly correlated with the amplitude of the SPES-evoked potentials (Figure 3.1.4A), indicating that larger responses were associated with stronger OFF-periods (i.e deeper down-states).

We also found that the timing of the occurrence of the OFF-period was correlated with the timing of the drop of PLF (Figure 3.1.4B) pointing to a specific role of the down-state in the early disruption of causal interactions. Importantly, PLF values dropped below significance level after the OFF-period despite power recovering to levels comparable to wakefulness in the 8 to 100 Hz frequency band. Different neuronal mechanisms may account for this phenomenon. Indeed, in vivo, in vitro and in computo studies seem to suggest that the resumption of cortical activity after the silent down-state of the slow oscillation is a stochastic process (Chauvette et al., 2011; Compte et al., 2003; Sanchez-Vives and McCormick, 2000) possibly due to spontaneous neurotransmitter release (Timofeev et al., 2000), intrinsic properties leading to spontaneous firing of layer V neurons (Sanchez-Vives and McCormick, 2000), or selective synchronization of small neuronal ensembles (Cossart et al., 2003; Luczak et al., 2007).

An additional finding that is worth discussing is that the PLF measured during wakefulness remained significant up to ~ 500 ms even in the contacts adjacent to the stimulation site, which, unlike distant targets, displayed a large slow wave with a concurrent significant suppression of high frequency activity, possibly due to the local paraphysiological effects of intracranial electrical stimulation (Borchers et al., 2012). A plausible explanation for the persistence of deterministic effects induced by SPES following this local OFF-period is the feedback of phase-locked activity from the rest of the network during wakefulness. A recent study employing cortical microstimulation in the monkey visual cortex demonstrated that, while feed-forward interactions mainly occur in the

gamma band, feed-backs are carried by alpha oscillations (Van Kerkoerle et al., 2014). Interestingly, in the present study we found that phase-locking in the gamma band was short-lasting (~ 70 ms) and comparable between wakefulness and NREM, whereas phase-locking in the beta and alpha bands was sustained (~ 500 ms) only during wakefulness. In future studies it will be important to elucidate the relative contribution of feed-forward versus feed-back network dynamics to the persistence of phase-locking during wakefulness as compared to NREM.

Bistability and loss of consciousness

Growing evidence suggest that the sleeping brain can still process sensory inputs at least to some extent (Bastuji et al., 2002; Kouider et al., 2014) and that it can actively support restorative functions (Tononi and Cirelli, 2014) and memory consolidation (Destexhe et al., 2007; Inostroza and Born, 2013). Indeed, compared to general anesthesia, during which a saturation of slow waves (Purdon et al., 2013) and frequent down-states may lead to a complete fragmentation of neuronal networks (Lewis et al., 2012), the impairment of cortico-cortical and/or cortico-subcortico-cortical interactions indicated by the present measurements in NREM is more likely to be relative and graded. In practice, the dynamics revealed by SPES point to a general mechanism by which the brain's potential to sustain large-scale, specific patterns of causal interactions may be impaired during NREM compared to wakefulness; due to bistability cortical circuits, upon receiving an input, tend to respond briefly, then hush and forget. We argue that, while this dynamics still allows a certain degree of deterministic interactions, it may specifically affect the level of consciousness. For example, stimulation (Libet, 1982) as well as recording (King et al., 2014) experiments in humans have shown that conscious perception requires the activity of cortical neurons to be stable in time for hundreds of milliseconds. The occurrence of a cortical OFF-period (i.e. down-state) observed here as early as 100 ms after SPES, may act on this time factor by curtailing the duration of stable neuronal responses. At the network level, bistability may interfere directly with the efficacy of recurrent processes among distributed cortical areas, another mechanism that is thought to be important for consciousness (Lamme et al., 1998; Tononi and Edelman, 1998). To the extent that reentry relies on the amplification of coherent activity across distributed set of neurons, the

scrambling of phases operated by the down-states at each node may critically impair the emergence of this large-scale phenomenon (Lumer et al., 1997). Finally, the present data fit nicely with the postulate that consciousness depends on the brain's ability to integrate information which, in turn, relays on effective information (EI) among different group of neurons (Hoel et al., 2013). EI is a perturbation-based general measure of causal interactions that captures how effectively causes produce effects in the system and how selectively causes can be identified from effects. Thus, EI is maximal for systems that are deterministic (i.e. a given initial state produces a given effect) and not degenerate (i.e. different initial states produce different effects); EI decreases with degeneracy (i.e. different initial states produce the same effect) and/or indeterminism (i.e. when a given initial state produce different effects) (Hoel et al., 2013). Our results suggest that, when cortical neurons become bistable, any input invariably converges into a stereotypical down-state (degeneracy), after which the causal effects of the input are obliterated (loss of determinism).

In this perspective, cortical bistability seem to be in a key position to selectively impair the level of consciousness.

Practically, the present results provide a mechanistic account for the collapse of complex spatiotemporal interactions revealed by non-invasive TMS/EEG experiments during NREM and other conditions (Casali et al., 2013). A particularly interesting possibility is that bistability may play a role in pathological states in which TMS invariably triggers a stereotypical EEG slow wave, such as the vegetative state/unresponsive wakefulness syndrome (Casali et al., 2013; Rosanova et al., 2012). Indeed, brain lesions may indirectly induce bistability in intact cortical tissue in several ways such as by (i) impairing the function of brainstem activating systems, thus enhancing K+-conductances at the cortical level (Englot et al., 2010), by (ii) reducing the excitatory drive of thalamostriatal circuits on cortical neurons (Schiff, 2010), by (iii) altering the excitation/inhibition balance in favor of inhibition (Murase et al., 2004), and by (iv) severing subcortical white matter fibers (Timofeev et al., 2000). To the extent that bistability—a process that is in principle reversible—is involved in these conditions, it may represent a suitable target for novel therapeutic approaches in patients in whom consciousness is impaired despite preserved cortical activity.

Limitations

Our observations were derived from a population of epileptic patients whose clinical condition and ongoing treatment may affect the SEEG recordings. To minimize this confound, our results did not include any contact (i) located in the epileptic zone as verified by surgical resection, (ii) located over regions of documented structural brain damage, nor (iii) exhibiting interictal activity (see Material and methods).

Another potential limitation is that our data did not include multi-unit activity recordings, thus preventing a direct observation of neuronal silence. However, previous studies in animals (Mukovski et al., 2007; Vyazovskiy et al., 2009) and humans (Cash et al., 2009; Csercsa et al., 2010; Nir et al., 2011) have provided solid evidence that the typical down-state characterized by sleep slow oscillations can be reliably detected based on spectral modulation in the high-frequency (20–100 Hz) range of the LFP signal.

The number of session and recording contacts included in this study was constrained by clinical needs and exclusion criteria. However, the recording contacts included in the present analysis showed a widespread distribution across the cerebral cortex and the stimulations were applied to different cortical areas including frontal, parietal, cingular and insular cortex. Thus, while we cannot rule out specific regional differences that may only become significant through a more intensive and systematic mapping of CCEPs during wakefulness and sleep, we may safely conclude that our results could be generalized to different cortical areas.

Finally, it is known that awakening from NREM sleep (especially stages N1 and N2) and from Rapid Eyes Movement sleep (REM) result in dream report (McNamara et al., 2010). Although bistability per se does not index directly the level of consciousness, it would be important to assess its degree in all these conditions. In the present work we focused on comparing the responses obtained during wakefulness and N3 early in the night because (1) our primary goal was to parallel previous experiments employing non-invasive stimulation and recordings with TMS/EEG, (2) because we observed that NREM sleep N2 was less stable and much more affected by spontaneous interictal activity and paraphysiological pattern compared to N3 and (3) because,

since we couldn't wake up subjects to obtain a report during the clinical protocol, we capitalized on previous works showing that the most extreme reduction of conscious experience occurs during the first N3 episode of the night (McNamara et al., 2010; Stickgold et al., 2001). This specific focus represents a limitation of this study and future works should definitively try to assess differences among sleep stages with special regards on REM sleep.

3.2 – Sleep-like cortical bistability in vegetative state patients

The results presented in paragraph 3.1 reveal a general neurophysiological mechanism (bistability and the associated down-states) by which reliable deterministic interactions within thalamo-cortical system may be impaired even in the presence of intact cortical connections and preserved levels of neuronal activity. In essence, cortical circuits, upon receiving an input, tend to respond briefly, then hush and forget. In this paragraph has been presented a study that investigate whether the same mechanism may account for the collapse of thalamo-cortical complexity detected by TMS/EEG in pathological conditions such as the vegetative state/unresponsive wakefulness syndrome.

Materials and methods

Study participants

Twenty-one severely brain-injured patients (8 females; mean age±SD: 53.47±21.47) and thirty-three healthy subjects (14 females; mean age±SD: 28.93 ±7.56) participated in the study. Patients were diagnosed as VS (n=13) and MCS (n=8) by means of the Coma Recovery Scale-Revised (CRS-R)(Giacino et al., 2004). In order to avoid diagnostic errors due to fluctuations in responsiveness and to obtain a stable clinical diagnosis, nineteen out of twenty-one patients underwent CRS-R assessments four times a week, every other day. The remaining two patients (Patient 20 and 21 of Table 3.2) were recruited from intensive care and underwent longitudinal behavioral and TMS/EEG assessments as they awakened from coma and progressed towards recovery of consciousness evolving from a VS, through a MCS to emergence from the MCS

(EMCS). The VS and MCS subgroups of patients did not systematically differ in etiology and time from injury. In Table 3.2 single patient's details about etiology and CRS-R performed before the TMS/EEG experiment are reported.

Study design

All study participants underwent at least one TMS/EEG session during wakefulness. Eight healthy subjects and participated in one TMS/EEG session during sleep. Patients 20 and 21 that underwent longitudinal assessments, three TMS/EEG sessions (Session 1, Session 2 and Session 3) were performed as they awakened from coma and progressed towards different clinical states (see *Study participants*). Session 1 was performed at least 48 h after withdrawal of sedation, when patients exited from coma and entered the VS. In these subjects who recovered, Session 2 was performed on the day after they transitioned from VS to MCS (however, Patient 21 temporarily slipped back into a vegetative state); Session 3 was performed after they regained functional communication and emerged from a minimally conscious state (emergence from minimally conscious state). The experimental procedures were approved respectively by the ethical committees of the Medicine Faculty of the University of Liège, Niguarda Hospital and Institute Don Gnocchi for the patients and by Hospital Luigi Sacco for the healthy subjects.

Table 3.2 *Clinical information*

	Clinical features			**CRS-R**						
Patient	**Gender (age, years)**	**Etiology**	**Time of TMS/EEG (days after insult)**	**Diagnosis at time of TMS/EEG**	**Auditory function**	**Visual function**	**Motor function**	**Oromotor/ Verbal function**	**Communication**	**Arousal**	**Total score**
1	M (81)	CVA	19	VS	0	0	2	1	0	2	5
2	M (68)	Trauma	21	VS	0	0	2	0	0	2	4
3	F (83)	Trauma	6	VS	1	0	1	0	0	1	3
4	M (19)	Trauma	172	VS	1	0	1	1	0	2	5
5	F (77)	Subarachnoid hemorrhage	44	VS	1	0	2	1	0	1	5
6	M (67)	Hemorrhage	247	VS	2	0	1	1	0	2	6
7	M (34)	CRA	7809	VS	1	1	2	1	0	2	7
8	F (19)	Trauma	1316	VS	1	1	1	2	0	1	6
9	M (55)	CVA	50	VS	2	1	0	0	0	2	5
10	M (57)	CRA	895	VS	1	0	2	1	0	2	6
11	F (44)	CVA	2891	VS	1	0	2	2	0	2	7
12	M (28)	Trauma	2410	MCS	2	3	5	2	0	2	14
13	F (76)	Subarachnoid hemorrhage	28	MCS	1	3	2	2	0	2	10
14	M (72)	CVA	38	MCS	3	5	2	2	1	1	14
15	M (20)	Trauma	1334	MCS	3	3	1	1	0	2	10
16	F (38)	Trauma	12	MCS	3	3	5	2	1	1	15
17	M (62)	Subarachnoid hemorrhage	20	MCS	1	3	2	1	0	2	9
18	M (32)	CRA	35	MCS	2	3	5	2	0	2	14
19	M (71)	CVA	18	MCS	2	2	5	2	0	2	13
20	F (60)	CVA	15	VS	0	0	2	2	0	1	5
			23	MCS	3	0	2	1	1	1	8
			31	EMCS	4	5	6	2	2	1	20
21	F (60)	CVA	35	VS	0	0	1	1	0	1	3
			46	MCS	3	1	1	1	0	1	7
			56	EMCS	3	3	4	3	2	1	16

CRA cardio respiratory arrest, CVA cerebrovascular accident

Transcranial Magnetic Stimulation targeting and stimulation parameters

A single TMS/EEG session consisted in different measurements that differed either for the site or the intensity of stimulation.

Patients' cortical targets were identified on CT or structural MRI scans acquired respectively with a Siemens Senatom Sensation 16 and a using a 3T scanner. In healthy subjects TMS targets were identified on anatomical magnetic resonance imaging (MRI) scans that were acquired using a 3T scanner. We employed a Focal Bipulse figure-of-eight coil for the stimulation (mean/outer winding

diameter ~50/70 mm, biphasic pulse shape, pulse length ~280 ms, focal area of the stimulation 0.68 cm^2) driven by a Mobile Stimulator Unit (eXimia TMS Stimulator, Nexstim Ltd.). We controlled TMS parameters by means of a Navigated Brain Stimulation (NBS) system (Nexstim Ltd.) that employed a 3D, frameless infrared tracking position sensor unit to locate the relative positions of the coil and subject's head within the reference space of individual CT or MRI scans. NBS estimates online, the distribution and the intensity (expressed in V/m) of the intracranial electric field induced by TMS. The location of the maximum electric field induced by TMS on the cortical surface (hot spot) was always kept on the convexity of the targeted gyrus with the induced current perpendicular to its main axis. At least 300 trials were collected for each stimulation site. Stimulation was delivered with an interstimulus interval randomly jittering between 2000 and 2300 ms (0.4–0.5 Hz), at an intensity ranging from 90 V/m up to 200 V/m on the cortical surface, that is largely above the threshold (50 V/m) for a significant TMS/EEG response (Casali et al., 2010; Komssi et al., 2007). The CT/MRI-guided intracranial electric field estimation is a crucial step during the experimental procedure; due to shifts of intracranial volumes in brain-injured patients, it is difficult to assess whether TMS is on target and effective based on extra-cranial landmarks alone and this may result in false-negatives (absence of EEG response due to missed target or sub-threshold stimulation)(Gosseries et al., 2015). NBS also guaranteed the reproducibility of the stimulation coordinates, within and across sessions in Patient 20 and 21, as it indicates, in real-time, any deviation from the designated target >3 mm.

By means of the NBS, TMS was targeted to the premotor and the posterior parietal cortex as well as its interactions with more frontal areas, is thought to be particularly relevant for consciousness (Laureys et al., 2004). In practice, all cortical sites were not always accessible in all patients due to skull breaches or external drain derivations. In these cases, we avoided stimulating over focal cortical lesions that were clearly visible in CT scans, since the EEG response of these areas may be absent or unreliable (Gosseries et al., 2015).

EEG recordings

TMS-evoked EEG measurements were recorded using a TMS compatible 60-channel amplifier (Nexstim). This device prevents amplifier saturation and reduces, or abolishes, the magnetic artefacts induced by the coil's discharge (Virtanen et al., 1999). The EEG signals were referenced to a forehead electrode, filtered (0.1-500 Hz), and sampled at 1450 Hz. Two additional sensors were applied to record the electro-oculogram (EOG). In the present experiments, as in previous studies, in order to abolish the evoked auditory potentials due to the click associated with the TMS discharge, a sound masking the TMS click was generated and played via earphones throughout the TMS/HD-EEG sessions.

During off-line data processing, an automatic algorithm was used in order to reject all trials that contained spontaneous blinks, eye movement, or muscle artefacts (Casali et al., 2010). After artefact rejection, 86 good TMS/EEG measurements were further analyzed and were included in the present study. For each patient we considered a single TMS/EEG measurement per area based on the maximum intensity of stimulation, for a total of 38 TMS/EEG session (9 premotor and 11 parietal in VS patients, 9 in premotor and 9 in parietal in MCS patients) in patient population, 40 TMS/EEG session (20 premotor and 20 parietal) for awake healthy subjects and 8 during sleep (3 premotor and 5 parietal).

General experimental procedures

During the experiment, patients were lying on their beds, awake and with their eyes open. If signs of drowsiness appeared, recordings were momentarily interrupted and subjects were stimulated using the CRS-R arousal facilitation protocols. Each healthy subject was sitting in an adjustable chair with a headrest that ensured a stable head position. As for patients, healthy subjects were asked to keep their eyes open to ensure wakefulness throughout the recording sessions. The stability of the stimulation coordinates was continuously monitored throughout all acquisitions by means of the NBS system. If the virtual aiming device was signaling a displacement from the cortical target greater than 4 mm, the TMS/EEG measurement was interrupted and the coil was

repositioned. At the end of the experiment, the stimulation coordinates were recorded and the electrode positions were digitized.

Data analysis and statistic

Data analysis was performed using Matlab R2012a (The MathWorks). TMS/EEG trials containing noise, muscle activity or eye movements were automatically rejected (Casali et al., 2010) and then visually inspected for an additional check. After that, EEG data were band-pass filtered (1-45 Hz), down-sampled to half of the original sampling rate (725 Hz) and then segmented in window of ± 600 ms around the stimulus. Then, trials were average referenced and baseline corrected over 500 ms prestimulus. Independent component analysis (ICA) was then applied in order to remove residual artifacts. Each TMS-evoked response was obtained by averaging 100-250 artifact-free trials.

Methodological rationale and data analysis

In order to assess quantitatively the differences in the dynamics triggered by TMS in patients and healthy subjects, we quantified (1) the amplitude of the low frequency components (< 4 Hz), (2) the suppression of high frequency power (> 20 Hz) and (3) the phase locking factor (PLF). Indeed, these three measures indicate respectively the possible presence of TMS-evoked slow waves, the correspondent occurrence of a cortical down-state (Cash et al., 2009; Csercsa et al., 2010; Pigorini et al., 2015; Valderrama, 2012) induced by TMS and the causal effects of TMS at the level of individual EEG electrode.

Analysis of TMS/EEG measurements in the frequency domain

We calculated in order to assess and quantify the presence of TMS-evoked slow waves the amplitude of low frequency components (< 4 Hz) for each electrode as the absolute value of filtered (4 Hz low-pass, third order Chebyshev filtering) evoked response after re-referencing to the mathematically linked mastoids. We re-referenced the TMS-evoked response to the mastoids because the slow components in the single channels average referenced could be either positive

or negative. Then, the amplitude of low frequency component was calculated by the integral of the signal from 8 to 350 ms. In order to calculate the EEG high frequency (>20 Hz) power suppression to assess and quantify the presence of TMS-evoked cortical OFF-periods, an established extracellular marker of the neuronal down-state, TMS evoked potentials were analyzed using *newtimef,* an EEGlab function. Specifically, time-frequency decomposition using Wavelet transform (Morlet, 3.5 cycles) and absolute spectra normalization was firstly applied at single trial level (Grandchamp et al., 2012) for a baseline included in the time range between -400 ms and -100 ms. Finally, non-significant activity is set to zero (green) using bootstrap statistic method ($\alpha < 0.05$, number of permutations = 500) with respect to baseline. As in Pigorini et al. (2015), we calculated for each electrode the mean value of the event-related spectral perturbation (ERSP) above 20 Hz over a time-window ranging between − 350 and + 350 ms. Then, the average between 100 and 350ms was carried out in order to quantify the high frequency power suppression.

In order to calculate TMS time-locked activity and compare the duration of the deterministic effects of TMS, PLF was calculated as in Pigorini et al. (2015) across trials after high pass filtering (>8 Hz, Butterworth, 3rd order). Specifically, PLF was calculated as the absolute value of the average of the Hilbert transform of all single trials. Statistical differences from baseline (from -400 ms to -50 ms) were assessed (for each channel) by assuming a Rayleigh distribution of the values of the baseline. Then, given a statistical threshold set at $\alpha < 0.05$, those PLF values below threshold were set to zero. In the case of evoked potentials, PLF reflects the ability of an external stimulus to affect the phase of ongoing oscillations across trials.

Results

Overall, we performed 212 TMS/EEG measurements in 21 patients and 33 healthy subjects using a TMS-compatible 60-channels EEG amplifier. Specifically, for each subject/patient we performed up to 9 TMS/EEG measurements in which cortical areas in the parietal or the in the frontal lobe were targeted and stimulated at 120 V/m. In total, 86 TMS/EEG measurements were included in the present study. For each session we consider the 4 channels closest to the stimulation site.

TMS/EEG recordings were analyzed in the frequency domain both for power and phase parameters (see Materials and Methods).

In vegetative state patients TMS triggers a simple EEG response associated with a suppression of high-frequency oscillations and a short-lasting PLF

Fig. 3.2.1 displays a typical EEG response to TMS of the right premotor cortex in an awake healthy subject (left side of panels A and B). As shown in previous works, this response is composed by a series of several positive and negative deflections corresponding to different voltage scalp topographies that initially involve the stimulation site (right premotor) and then other cortical locations (Massimini et al., 2005b; Rosanova et al., 2009). On the contrary, the TMS applied over the premotor cortex in an awake VS patient is characterized by a simple, large positive-negative deflection (right side of panels A and B) (Rosanova et al., 2012) that remains local.

Notably, time-frequency analysis reveals a widespread and long-lasting increase of power for broadband (8-45 Hz) EEG oscillations triggered by TMS in healthy wakefulness, while in awake VS condition TMS evokes an early increase of power immediately followed by a significant suppression in the same frequency range (8-45 Hz)(left side of panel C). EEG scalp topographies of time-frequency power values cumulated between 8 and 45 Hz reveal that, after a global activation, this phenomenon has a very precise spatial distribution confined under the coil (right side of panel C).

In order to quantify and compare the duration of the deterministic effects of TMS in both awake healthy subjects and awake VS patients, we calculated PLF of TMS-evoked potentials in the 8-45 Hz frequency band as in Pigorini et al. (2015). Figure 3.2.1D shows that TEPs recorded in VS patients were characterized by an early drop (about 200 ms) of PLF below the level of statistical significance (Rayleigh, $\alpha<0.05$) despite the recovery of high-frequency EEG power (>20 Hz) at the baseline level (right side of panel D). In fact, in awake healthy subjects TEPs show a significant PLF lasting up to 430 ms in the same frequency interval (left side of panel D)
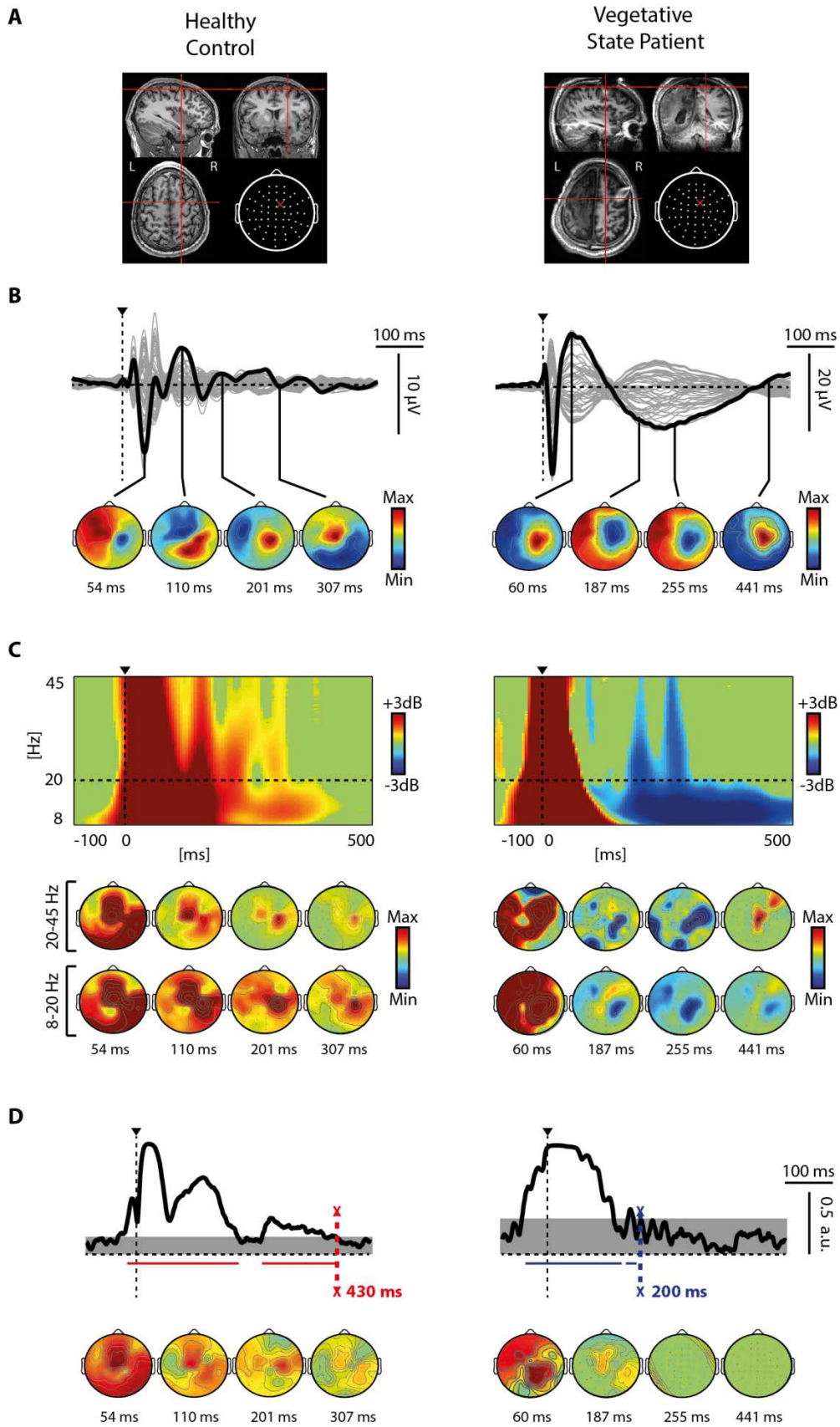
Figure 3.2.1 – Comparison of TMS-evoked responses, time-frequency power spectra and PLF time course obtained during wakefulness in healthy subjects and in vegetative state patients: TMS evokes a stereotypical slow-wave-like response that is associated with high-frequency suppression followed by a drop of PLF in VS

patients but not in healthy subjects. A representative healthy subject (HC - Left) and a representative vegetative state patient (VS - Right) are shown.
Panel A. Structural MRIs (T1-weighted) and cortical TMS target as estimated by NBS.
**Panel B.** TMS-evoked cortical responses (the dashed vertical line indicates the onset of the TMS pulse). The grey traces show the butterfly plot of the superimposed averaged TMS-evoked responses recorded from all 60 channels; the black trace represents the evoked potential recorded at one of the selected four electrode under the coil. Instantaneous voltage topographies at selected peaks are shown in the lower part of the panel (auto-scaled color-coded maps between the maximum and the minimum of instantaneous voltages): of note, in the VS, the stimulus-evoked response remains local while, in the HC, the TMS stimulus results in a complex pattern of activation which initially involves the stimulation site and then spreads to other cortical areas.
Panel C. Time-frequency power spectra of TMS-evoked potentials. For time-frequency decomposition, the Wavelet Transform (Morlet, 3.5 cycles) has been applied at a single trial level. Significance for bootstrap statistics is set at $\alpha<0,05$ (absence of any significant activations is green-colored): red color indicates a significant power increase compared to the baseline, while blue color represents a significant power decrease. The dashed horizontal lines mark the 20 Hz frequency.
In the lower part of the panel, the corresponding power topographies are depicted and subdivided in two main frequency bands, respectively a lower (from 8 to 20 Hz) and a higher band (from 20 to 45 Hz) (auto-scaled color-coded maps between the maximum and the minimum of power). In the awake healthy subject, the TMS-related global power increase, for both bands, is typically sustained in time, whereas in the awake VS patient, an initial global power increase is replaced by a rapid power decrease followed by a recovery of the high frequency band (20-45 Hz) to the baseline level at the stimulation site. Conversely the power suppression of the low frequency band (8-20 Hz) persists over time up to 400-500 msec.
Panel D. PLF-time course calculated on a single trial level after high-pass filtering (>8 Hz). To assess for each electrode the statistical difference from the baseline (from -500 to − 100 ms) a Rayleigh distribution of the baseline values was assumed. Then, those PLF values below a statistical threshold ($\alpha<0,01$) were set to zero. In the lower part of the panel, the corresponding PLF topographies are depicted. Of note, in the VS patient, the PLF is short-lasting and sharply drops below the significance level concurrently with the high-frequency power suppression (see panel C), whereas in healthy subjects the global PLF activity is long-lasting and remains significant until ~400 ms.

Figure 3.2.2A shows significant differences at the group level (Wilcoxon ranksum test, p<0.01) obtained for power in the low frequency range (<4 Hz) corresponding to spontaneous EEG delta waves, high-frequency EEG power suppression and duration of PLF (>8 Hz). These results show that across VS patients TMS/EEG cortical responses were characterized by a larger power in low frequency band (<4 Hz), by a significant suppression of high-frequency EEG activity (20-45 Hz) and by an early drop (~175 ms) of PLF. On the other hand, TMS delivered in awake healthy subjects evokes complex, sustained increase of power of the EEG responses in high-frequency and a PLF that remains significant until ~250 ms after the TMS pulse. Interestingly, as shown in Figure 3.2.2B, in VS patients the correlation between the maximum amplitude of the evoked slow wave (max SWa) and the maximum level of suppression of high frequency power (max SHFp) were significantly correlated. Similarly, also the latency at which PLF drops below the statistical significance level (max PLFt) and the timing of the maximum high frequency suppression (max SHFt). These correlations strongly suggest that a larger TMS-evoked slow wave corresponds to a deeper suppression of high frequencies. Moreover, the earlier this suppression occurs the earlier the PLF drops down.
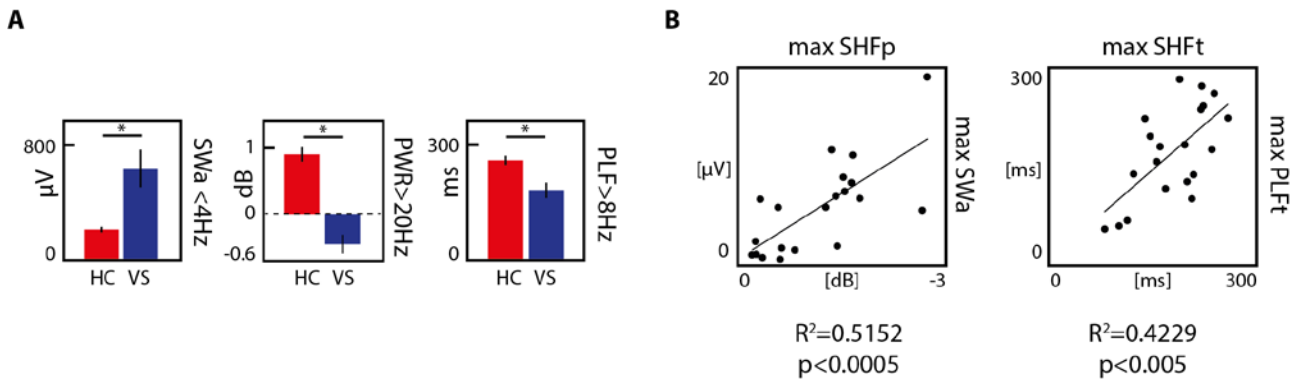
Figure 3.2.2 - Panel A. Differences at the group level between awake HC and VS patients. Slow wave amplitude (SWa<4 Hz), high frequency power (PWR>20 Hz) and duration of PLF (>8 Hz) between HC (red column) and VS patients (blue column) are significantly different (p<0.01). The three measures are calculated on the average across the four channels closest to the stimulation site. For each individual, SWa is calculated as the sum of the absolute value of the filtered (4 Hz low-pass, third order Chebyshev filtering) TMS-evoked response between 8 and 350 ms after re-referencing to the mathematically linked mastoids. PWR is the mean power of high frequency (>20Hz) between 100 and 350 ms. The duration of PLF of frequencies above 8Hz is computed from the latest statistically significant time point and averaged across the four selected electrodes. Histograms indicate the average values between subject in each group (awake HC and VS), the black bars indicate the standard error of the mean and the asterisk * denotes the statistical significant differences (Wilcoxon ranksum test, p<0.01). Panel B. Amplitude, power and phase-locking modulation are related in VS patients. The correlation between the maximum amplitude of the evoked slow wave (max SWa) and the maximum level of high-frequency power suppression with respect to baseline (max SHFp) computed in each patient is shown on the left. The correlation between the timing of the maximum high frequency suppression (max SHFt) and the latency at which PLF fell below the threshold for significance (max PLFt) computed in each patient is shown on the right. Below each correlation, the coefficient of determination R^2 and the significance level p of the correlation are indicated.

TEPs in vegetative state and NREM sleep are similar in terms of waveform and spectral properties

TEPs recorded in awake VS patients closely resemble EEG responses to TMS recorded during NREM sleep in healthy subjects (Rosanova et al., 2012). In order to further characterize this similarity we have performed TMS/EEG measurements in a subset of healthy controls (HC) during NREM sleep (stage N3). Figure 3.2.3A confirms that TMS evokes similar responses in awake VS patients and in healthy subjects during NREM sleep in terms of waveforms. However, time-frequency analysis shows that the high-frequency EEG suppression associated with the negative phase of the wave is smaller in NREM sleep compared to VS. Furthermore, in NREM sleep this high- frequency suppression is followed by an increase of power in the frequency range of the sleep spindles that occurs, as expected, during the rising phase of the wave. Interestingly, as shown in Figure 3.2.3B, baseline power spectra (PWRb) above 20 Hz (average of single trial baseline from -600 to -100 ms) are significantly different, although the comparison of high-

frequency suppression calculated in VS patients and healthy subjects in NREM sleep does not result in a statistically significant difference.
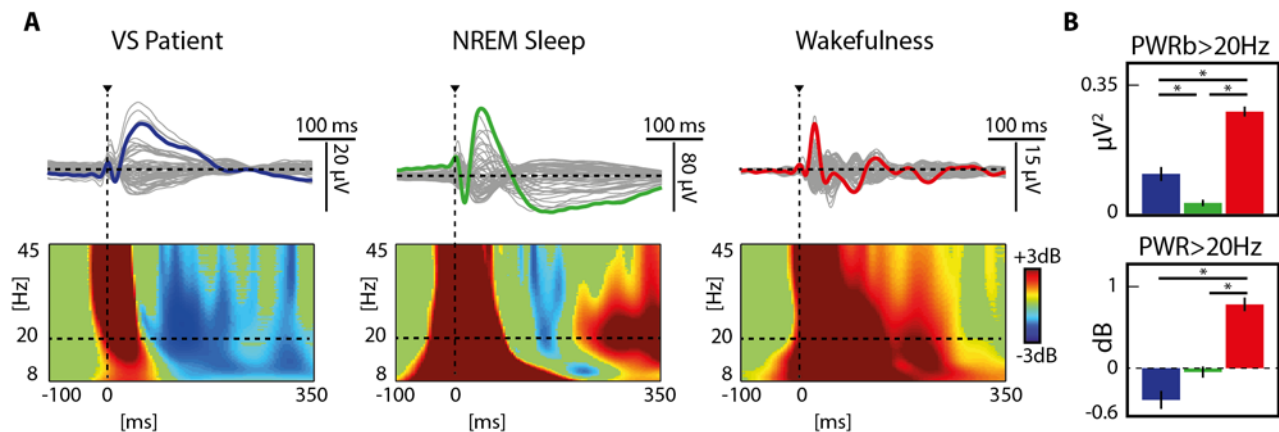
Figure 3.2.3 – Panel A. Comparison of TMS-evoked potentials and time-frequency analyses between VS patients during wakefulness and healthy subjects during NREM sleep and wakefulness.
The TMS-evoked cortical responses of three representative individuals in each condition are shown (top panel). As in figure 3.2.1, the grey traces represent the butterfly plot of TMS-evoked responses from all 60 channels; in each condition (awake VS patients in blue, healthy subjects during NREM sleep in green and awake healthy subjects in red), the colored traces show the evoked potential recorded at the channel closest to the stimulation. On the bottom, the corresponding time-frequency analyses of the selected channels are shown. Despite the similar positive-negative slow wave evoked by the TMS, awake VS patients are characterized by a greater and more prolonged high-frequency EEG suppression compared to the NREM sleep of healthy subjects. Specifically, even if both conditions present a suppression of high frequencies (>20Hz) following the initial global power increase, in the VS patients the power reduction slowly recovers to the baseline whereas in the NREM sleep of healthy subjects it is replaced by a late increase of power.
Panel B. Group-level comparison of the high-frequency mean power computed during the pre-stimulus (baseline spectra) and post-stimulus period in the three conditions (same color-coding of panel A). Both computations (baseline and post-stimulus) are performed, in each individual, on the same four channels closest to the stimulation site. The top histograms represent the mean of normalized spectra (PWRb) above 20 Hz obtained applying Fast Fourier Transform on the baseline (from -600 to -100 ms) The bottom histograms represent the mean of high-frequency power (PWR>20 Hz) from 100 and 350 ms.

Resurgence of consciousness is paralleled by a recovery of TMS-evoked high-frequency oscillations and by a longer PLF

Finally, we wanted to understand whether the suppression in TMS-evoked high frequency oscillations would be possibly modulated in those VS patients who spontaneously recover consciousness. To this aim, we longitudinally monitored by means of TMS/EEG 2 VS patients who progressively evolved through the Minimally Conscious State (MCS) and eventually regain consciousness. As shown in figure 3.2.4A, in these patients, TMS/EEG responses recorded at different stages of the clinical evolution were characterized by a progressive recovery of TMS-evoked EEG high-frequency oscillations and by an increase of PLF duration.

In figure 3.2.4B, VS patients are compared with MCS and HC subjects in terms of PWRb>20 Hz, SWa<4 Hz, PWR>20 Hz and duration of PLF. PWRb and SWa values are comparable between

VS and MCS patients, while the two groups differ in terms of EEG high-frequency suppression and PLF. On the contrary, PLF duration is similar between HC and MCS conditions.
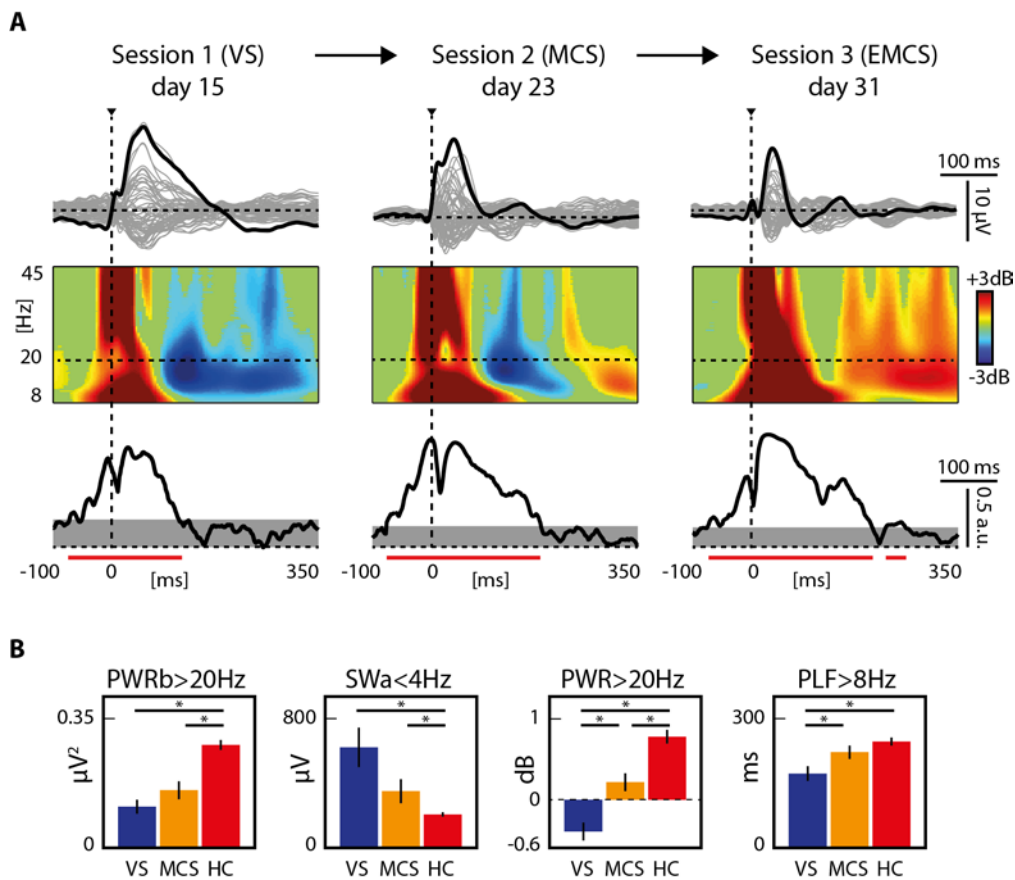
Figure 3.2.4 – Panel A. Longitudinal TMS-EEG evaluations in a single patient who gradually recovered consciousness evolving from a vegetative state (VS), through a minimally conscious state (MCS) to emergence from a MCS (EMCS). The butterfly plot of the TMS-evoked potentials, the corresponding time-frequency analysis and the PLF time course in each clinical status (VS, MCS and EMCS) are shown. TMS/EEG responses are characterized by a progressive recovery of high-frequency EEG power and by a parallel increase of the PLF duration which closely match the clinical evolution of the patient as assessed by the Coma Recovery Scale-Revised (CRS-R).
Panel B. Group-level comparison of high frequency baseline spectra (PWRb), slow wave amplitude (SWa), post-stimulus high-frequency power (PWR) and duration of PLF (PLF) between VS patients (in blue), MCS patients (in yellow) and healthy subjects (in red). For computation details, refer to previous figures. Statistically significant differences are depicted by an the asterisk * (Wilcoxon rank sum test, p<0.01).

Discussion

In the work presented in this paragraph we compared TMS/EEG response recorded in awake severely brain-injured patients affected by disorders of consciousness and healthy subjects during NREM sleep and wakefulness by means of time-frequency analysis and PLF. We observed that while during wakefulness different cortical areas react to TMS with a pattern of activation which has a characteristic shape and frequency content and a sustained phase-locked response, in vegetative state patients TMS evokes a simple positive-negative wave and a cortical OFF-period

followed by a drop of phase-locking, similarly to healthy subjects during NREM sleep. Moreover, two patients who evolved from vegetative state to minimally conscious state, and emerged from minimally conscious state show a progressive recovery of EEG high frequency power and an increase of PLF duration, closely matching their clinical evolution.

Bistability, cortical down-states and break-off of phase locked responses in VS patients

TMS/EEG has been employed to measure cortical responses in healthy subjects as controls (HC) during wakefulness and at the bedside of awake VS/UWS patients. Coma Recovery Scale-Revised (CRS-R) has been performed 4 times a week, every other day, to minimize the possibility of a misdiagnosis due to fluctuations in behavioral responsiveness. In line with Rosanova et al 2009 and 2012, the EEG response to TMS in HC during wakefulness resulted in complex activity patterns depending on the area stimulated, but in a local, stereotypical positive-negative wave in awake VS patients. We observed that this slow wave was associated with an OFF-period, possibly reflecting the neuronal down-state observed in animal intracellular (Steriade et al., 2001) and human intracranial (Cash et al., 2009; Pigorini et al., 2015) recordings during NREM sleep, suggesting that also in the case of pathological LOC bistability may play a role. These studies have shown that both spontaneous EEG sleep slow waves and K-complexes are underpinned by the occurrence of a silent, hyperpolarized down-state in cortical neurons, which is preceded and followed by a period of activation (up-state). This bimodal alternation between up- and down-states reflects an intrinsic bistability in thalamocortical circuits that is thought to depend on neuronal as well as network properties (Hill and Tononi, 2005; Mann et al., 2009; Sanchez-Vives and McCormick, 2000; Timofeev et al., 2000). During NREM sleep, bistability may be mainly caused by increased activity of leak K+ channels, brought about by decreased brainstem cholinergic activity (McCormick et al., 1993). On the other hand, increased inhibition within thalamocortical networks may play a crucial role in inducing bistability (Mann et al., 2009). Similarly, in brain injured patients brain lesions themselves may indirectly induce bistability in intact cortical tissue in several ways such as by (i) impairing the function of brainstem activating systems, thus enhancing K+-conductances at the cortical level (Englot et al., 2010), by (ii) reducing the excitatory drive of

thalamostriatal circuits on cortical neurons (Schiff, 2010), by (iii) altering the excitation/inhibition balance in favor of inhibition (Murase et al., 2004), and by (iv) severing subcortical white matter fibers (Timofeev et al., 2000). In all cases, brain lesion may induce cortical bistability to various extents. The presence of an evoked slow wave associated with high frequency EEG suppression shown here in VS patients seems to confirm this possibility. A challenging relevant scientific question is then regarding the effects of such cortical dynamics on the overall brain complexity and in turn of the ability to sustain consciousness. Our proposition, is that following brain injury, due to bistability intact portions of thalamo-cortical system would not be able to sustain long-range patterns of causal activations in response to a direct stimulation. In order to verify this hypothesis we first performed a set of controlled experiments exploiting NREM sleep as a model to demonstrate a specific role of the down-state in the early disruption of causal cortico-cortical interaction following direct stimulation (see chapter 3.1, Pigorini et al., 2015). In brief, at odds with wakefulness during NREM sleep due to bistability cortical circuits, upon receiving an input, tend to respond briefly (thus showing the preserved reactivity of the sleeping brain) but then hush and forget. Specifically, PLF values dropped below significance after the occurrence of an OFF-period. Notably, the timing of occurrence of the OFF-period was correlated with the timing of the drop of PLF (see figure 3.1.2). Similarly, here we show that in awake VS patients the occurrence of TMS evoked OFF-periods was associated with an early drop of causal cortico-cortical interactions as reflected by short PLF durations as compared to wakefulness. More importantly, also in the case of awake VS patients the timing of the drop PLF was correlated with the occurrence of the OFF-period thus providing for the first time a mechanistic account for the collapse of long-range causal cortico-cortical interaction following brain injury.

Altogether these results suggest that in both physiological and pathological states consciousness may be impaired due to the occurrence of a silent OFF-period disrupting the emergence of long-range causal brain dynamics. In order to demonstrate the causal role of bistability in the loss of consciousness following brain injury one should demonstrate that a reduction of TMS evoked slow waves and the associated down-states would follow the clinical progression towards the recovery of consciousness and that this is paralleled by a recovery of long-range causal interaction. Here we

explicitly addressed this account and performed longitudinal TMS/EEG measurements in brain injured patients who gradually recovered consciousness evolving from a vegetative state, through a minimally conscious state (MCS) to emergence from a MCS (EMCS). Our results showed a progressive reduction of the TMS evoked slow wave accompanied by a progressive recovery of high-frequency EEG power and by a parallel increase of the PLF duration (matching that off HC) which closely followed the clinical evolution of the patient as assessed by the Coma Recovery Scale-Revised (CRS-R).

Brain complexity is related with high frequency EEG power suppression in VS patients

This set of empirical evidences regarding the mechanism responsible for the collapse of long-range causal interactions during LOC may also partially explain the collapse of brain complexity (a theoretically relevant aspect for consciousness) across different conditions such as sleep, anesthesia and VS following severe brain injury, as measured by PCI (Casali et al., 2013). Indeed, PCI captures the complexity of the spatiotemporal pattern of deterministic activation following a direct perturbation. As such the overall brain complexity should be low during LOC conditions due to the occurrence of a silent OFF-periods that breaks-off causal cortico-cortical interactions therefore preventing the emergence of complex large-scale deterministic activations. In an attempt to illustrate this possibility here we perform preliminary analysis correlating the timing of the occurrence of the evoked OFF-period with the temporal evolution of PCI. Interestingly, we found a significant positive correlation showing that build-up of algorithmic complexity ceased to occur soon after the occurrence of the evoked OFF-period. Far from been conclusive these results highlight the tight link between a basic neurophysiological mechanism (i.e. bistability) and a theoretically based index of consciousness.
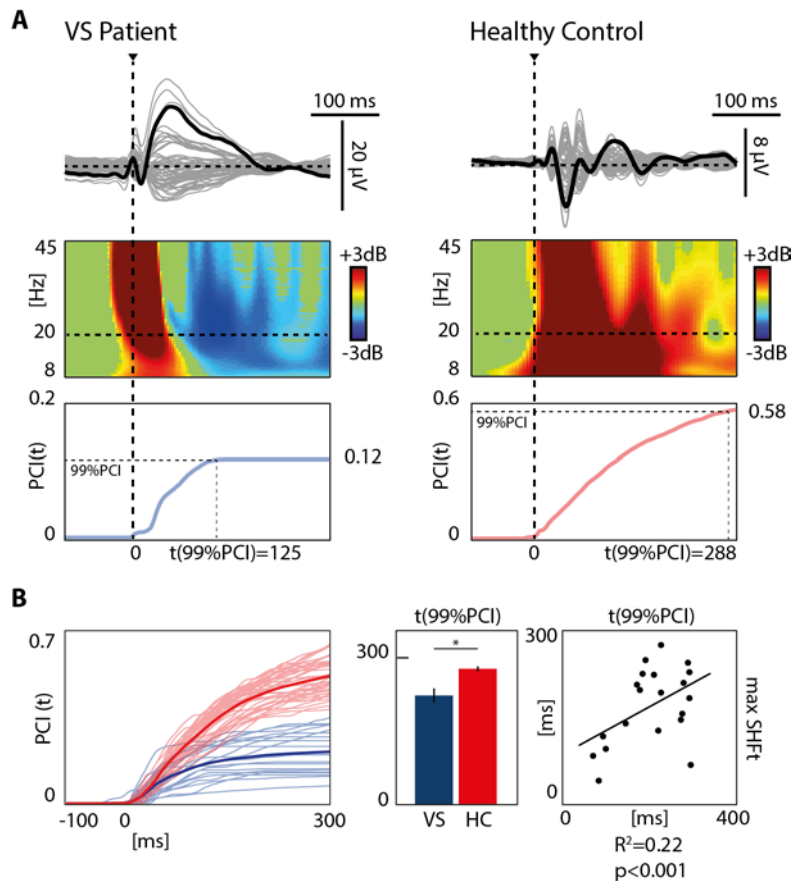
Figure 3.2.5 – Panel A. TMS-evoked cortical responses (top of the panel, a selected channel in bold) of a representative VS patient and a representative healthy subject, the time-frequency analysis of the corresponding bold channel (middle of the panel), and the temporal evolution of PCI (bottom of the panel) are shown. In the bottom graphs representing the time course of PCI, the light-dashed vertical line marks the exact time when PCI reach the 99% (t(99%PCI)) of its maximum value (indicated by a number at the end of each temporal evolution) while the light-dashed horizontal line indicates the corresponding 99% of PCI value. Panel B. On the left, the temporal evolution of PCI, PCI(t), calculated during wakefulness (light-red lines) and pathological loss of consciousness (light-blue lines) at the single-subject level. The dark blue and red lines represent averaged PCI(t). In the middle of the panel, the group-level comparison of t(99%PCI) computed in VS patients (blue column) and healthy subjects (red column) shows that they are significantly different (Wilcoxon ranksum test, $p < 0.01$). On the right, the correlation between the time of the maximum high frequency suppression (max SHFt) and the time (t(99%PCI)) when PCI reach the 99% of its maximum value. The relationship between the two time measures could indicate that the occurrence of an OFF-period can prevent the further growing of PCI. The coefficient of determination R^2 and the significance p level are reported.

Following these lines of evidence, further studies should aim at deepening the understanding of the cellular/molecular aspects of such mechanisms since bistability is in principle reversible and may represent a suitable pharmacological target for novel therapeutic approaches aimed at promoting brain complexity and in turn recovery of consciousness following brain injury.

REFERENCES

Akbarian, S., Huang, H.-S., 2006. Molecular and cellular mechanisms of altered GAD1/GAD67 expression in schizophrenia and related disorders. Brain Res. Rev. 52, 293–304. doi:10.1016/j.brainresrev.2006.04.001

Altar, C.A., Laeng, P., Jurata, L.W., Brockman, J.A., Lemire, A., Bullard, J., Bukhman, Y.V., Young, T.A., Charles, V., Palfreyman, M.G., 2004. Electroconvulsive Seizures Regulate Gene Expression of Distinct Neurotrophic Signaling Pathways. J. Neurosci. 24, 2667–2677. doi:10.1523/JNEUROSCI.5377-03.2004

Altshuler, L.L., Kupka, R.W., Hellemann, G., Frye, M.A., Sugar, C.A., McElroy, S.L., Nolen, W.A., Grunze, H., Leverich, G.S., Keck, P.E., Zermeno, M., Post, R.M., Suppes, T., 2010. Gender and depressive symptoms in 711 patients with bipolar disorder evaluated prospectively in the Stanley Foundation bipolar treatment outcome network. Am. J. Psychiatry 167, 708–715. doi:10.1176/appi.ajp.2009.09010105

Amzica, F., Steriade, M., 2002. The functional significance of K-complexes. Sleep Med. Rev. 6, 139–149. doi:10.1053/smrv.2001.0181

Arthuis, M., Valton, L., Régis, J., Chauvel, P., Wendling, F., Naccache, L., Bernard, C., Bartolomei, F., 2009. Impaired consciousness during temporal lobe seizures is related to increased long-distance cortical-subcortical synchronization. Brain J. Neurol. 132, 2091–2101. doi:10.1093/brain/awp086

Bajbouj, M., Lang, U.E., Niehaus, L., Hellen, F.E., Heuser, I., Neu, P., 2006. Effects of right unilateral electroconvulsive therapy on motor cortical excitability in depressive patients. J. Psychiatr. Res. 40, 322–327. doi:10.1016/j.jpsychires.2005.07.002

Bajbouj, M., Luborzewski, A., Danker-Hopfe, H., Lang, U.E., 2005. Motor cortical excitability in depressive patients after electroconvulsive therapy and repetitive transcranial magnetic stimulation. J. ECT 21, 243–245.

Barr, M.S., Farzan, F., Rusjan, P.M., Chen, R., Fitzgerald, P.B., Daskalakis, Z.J., 2009. Potentiation of Gamma Oscillatory Activity through Repetitive Transcranial Magnetic Stimulation of the Dorsolateral Prefrontal Cortex. Neuropsychopharmacology 34, 2359–2367. doi:10.1038/npp.2009.79

Bartos, M., Vida, I., Jonas, P., 2007. Synaptic mechanisms of synchronized gamma oscillations in inhibitory interneuron networks. Nat. Rev. Neurosci. 8, 45–56. doi:10.1038/nrn2044

Başar, E., 2013. Brain oscillations in neuropsychiatric disease. Dialogues Clin. Neurosci. 15, 291–300.

Başar, E., Güntekin, B., 2008. A review of brain oscillations in cognitive disorders and the role of neurotransmitters. Brain Res., Brain Oscillations in Cognition and Cognitive Disorders 1235, 172–193. doi:10.1016/j.brainres.2008.06.103

Başar, E., Schürmann, M., Başar-Eroglu, C., Demiralp, T., 2001. Selectively distributed gamma band system of the brain. Int. J. Psychophysiol. 39, 129–135. doi:10.1016/S0167-8760(00)00136-7

Bastuji, H., Perrin, F., Garcia-Larrea, L., 2002. Semantic analysis of auditory input during sleep: studies with event related potentials. Int. J. Psychophysiol., Event-related Potential Measure of Information Processing During Sleep 46, 243–255. doi:10.1016/S0167-8760(02)00116-2

Baxter, L.R., 1985. Can lithium carbonate prolong the antidepressant effect of sleep deprivation? Arch. Gen. Psychiatry 42, 635.

Ben Achour, S., Pascual, O., 2010. Glia: The many ways to modulate synaptic plasticity. Neurochem. Int., Glia as Neurotransmitter Sources and Sensors 57, 440–445. doi:10.1016/j.neuint.2010.02.013

Benedetti, F., 2012. Antidepressant chronotherapeutics for bipolar depression. Dialogues Clin. Neurosci. 14, 401–411.

Benedetti, F., Barbini, B., Bernasconi, A., Fulgosi, M.C., Dallaspezia, S., Gavinelli, C., Locatelli, C., Lorenzi, C., Pirovano, A., Radaelli, D., Smeraldi, E., Colombo, C., 2010. Acute antidepressant response to sleep deprivation combined with light therapy is influenced by the catechol-O-methyltransferase Val(108/158)Met polymorphism. J. Affect. Disord. 121, 68–72. doi:10.1016/j.jad.2009.05.017

Benedetti, F., Barbini, B., Campori, E., Colombo, C., Smeraldi, E., 1996. Dopamine agonist amineptine prevents the antidepressant effect of sleep deprivation. Psychiatry Res. 65, 179–184.

Benedetti, F., Barbini, B., Fulgosi, M.C., Colombo, C., Dallaspezia, S., Pontiggia, A., Smeraldi, E., 2005. Combined total sleep deprivation and light therapy in the treatment of drug-resistant bipolar depression: acute response and long-term remission rates. J. Clin. Psychiatry 66, 1535–1540.

Benedetti, F., Bernasconi, A., Blasi, V., Cadioli, M., Colombo, C., Falini, A., Lorenzi, C., Radaelli, D., Scotti, G., Smeraldi, E., 2007a. Neural and genetic correlates of antidepressant response to sleep deprivation: a functional magnetic resonance imaging study of moral valence decision in bipolar depression. Arch. Gen. Psychiatry 64, 179–187. doi:10.1001/archpsyc.64.2.179

Benedetti, F., Calabrese, G., Bernasconi, A., Cadioli, M., Colombo, C., Dallaspezia, S., Falini, A., Radaelli, D., Scotti, G., Smeraldi, E., 2009. Spectroscopic correlates of antidepressant response to sleep deprivation and light therapy: a 3.0 Tesla study of bipolar depression. Psychiatry Res. 173, 238–242. doi:10.1016/j.pscychresns.2008.08.004

Benedetti, F., Colombo, C., 2011. Sleep deprivation in mood disorders. Neuropsychobiology 64, 141–151. doi:10.1159/000328947

Benedetti, F., Colombo, C., Barbini, B., Campori, E., Smeraldi, E., 1999. Ongoing lithium treatment prevents relapse after total sleep deprivation. J. Clin. Psychopharmacol. 19, 240–245.

Benedetti, F., Colombo, C., Serretti, A., Lorenzi, C., Pontiggia, A., Barbini, B., Smeraldi, E., 2003. Antidepressant effects of light therapy combined with sleep deprivation are influenced by a functional polymorphism within the promoter of the serotonin transporter gene. Biol. Psychiatry 54, 687–692.

Benedetti, F., Dallaspezia, S., Fulgosi, M.C., Barbini, B., Colombo, C., Smeraldi, E., 2007b. Phase advance is an actimetric correlate of antidepressant response to sleep deprivation and light therapy in bipolar depression. Chronobiol. Int. 24, 921–937. doi:10.1080/07420520701649455

Benedetti, F., Riccaboni, R., Locatelli, C., Poletti, S., Dallaspezia, S., Colombo, C., 2014. Rapid treatment response of suicidal symptoms to lithium, sleep deprivation, and light therapy (chronotherapeutics) in drug-resistant bipolar depression. J. Clin. Psychiatry 75, 133–140. doi:10.4088/JCP.13m08455

Benedetti, F., Smeraldi, E., 2009. Neuroimaging and genetics of antidepressant response to sleep deprivation: implications for drug development. Curr. Pharm. Des. 15, 2637–2649.

Benedetti, F., Terman, M., 2013. Much ado about…a moody clock. Biol. Psychiatry 74, 236–237. doi:10.1016/j.biopsych.2013.05.037

Benes, F.M., Berretta, S., 2001. GABAergic Interneurons: Implications for Understanding Schizophrenia and Bipolar Disorder. Neuropsychopharmacology 25, 1–27. doi:10.1016/S0893-133X(01)00225-1

Berthomier, C., Drouot, X., Herman-Stoïca, M., Berthomier, P., Prado, J., Bokar-Thire, D., Benoit, O., Mattout, J., d'Ortho, M.-P., 2007. Automatic analysis of single-channel sleep EEG: validation in healthy individuals. Sleep 30, 1587–1595.

Bhagwagar, Z., Wylezinska, M., Jezzard, P., Evans, J., Ashworth, F., Sule, A., Matthews, P.M., Cowen, P.J., 2007. Reduction in Occipital Cortex γ-Aminobutyric Acid Concentrations in Medication-Free Recovered Unipolar Depressed and Bipolar Subjects. Biol. Psychiatry 61, 806–812. doi:10.1016/j.biopsych.2006.08.048

Bhattacharjee, Y., 2007. Psychiatric research. Is internal timing key to mental health? Science 317, 1488–1490. doi:10.1126/science.317.5844.1488

Biedermann, S., Weber-Fahr, W., Zheng, L., Hoyer, C., Vollmayr, B., Gass, P., Ende, G., Sartorius, A., 2012. Increase of hippocampal glutamate after electroconvulsive treatment: A quantitative proton MR spectroscopy study at 9.4 T in an animal model of depression. World J. Biol. Psychiatry 13, 447–457. doi:10.3109/15622975.2011.580778

Bliss, T.V., Collingridge, G.L., 1993. A synaptic model of memory: long-term potentiation in the hippocampus. Nature 361, 31–39. doi:10.1038/361031a0

Bliss, T.V.P., Lømo, T., 1973. Long-lasting potentiation of synaptic transmission in the dentate area of the anaesthetized rabbit following stimulation of the perforant path. J. Physiol. 232, 331–356.

Blumenfeld, H., Taylor, J., 2003. Why do seizures cause loss of consciousness? Neurosci. Rev. J. Bringing Neurobiol. Neurol. Psychiatry 9, 301–310.

Boly, M., Perlbarg, V., Marrelec, G., Schabus, M., Laureys, S., Doyon, J., Pélégrini-Issac, M., Maquet, P., Benali, H., 2012. Hierarchical clustering of brain activity during human nonrapid eye movement sleep. Proc. Natl. Acad. Sci. U. S. A. 109, 5856–5861. doi:10.1073/pnas.1111133109

Borchers, S., Himmelbach, M., Logothetis, N., Karnath, H.-O., 2012. Direct electrical stimulation of human cortex-the gold standard for mapping brain functions? Nat. Rev. Neurosci. 13, 63–70. doi:10.1038/nrn3140

Boroojerdi, B., Meister, I.G., Foltys, H., Sparing, R., Cohen, L.G., Töpper, R., 2002. Visual and motor cortex excitability: a transcranial magnetic stimulation study. Clin. Neurophysiol. 113, 1501–1504. doi:10.1016/S1388-2457(02)00198-0

Boylan, L.S., Devanand, D.P., Lisanby, S.H., Nobler, M.S., Prudic, J., Sackeim, H.A., 2001. Focal prefrontal seizures induced by bilateral ECT. J. ECT 17, 175–179.

Brefel-Courbon, C., Payoux, P., Ory, F., Sommet, A., Slaoui, T., Raboyeau, G., Lemesle, B., Puel, M., Montastruc, J.-L., Demonet, J.-F., Cardebat, D., 2007. Clinical and imaging evidence of zolpidem effect in hypoxic encephalopathy. Ann. Neurol. 62, 102–105. doi:10.1002/ana.21110

Brenner, C.A., Kieffaber, P.D., Clementz, B.A., Johannesen, J.K., Shekhar, A., O'Donnell, B.F., Hetrick, W.P., 2009. Event-related potential abnormalities in schizophrenia: A failure to "gate in" salient information? Schizophr. Res. 113, 332–338. doi:10.1016/j.schres.2009.06.012

Bushey, D., Tononi, G., Cirelli, C., 2011. Sleep and synaptic homeostasis: structural evidence in Drosophila. Science 332, 1576–1581. doi:10.1126/science.1202839

Buzsáki, G., Watson, B.O., 2012. Brain rhythms and neural syntax: Implications for efficient coding of cognitive content and neuropsychiatric disease. Dialogues Clin. Neurosci. 14, 345–367.

Canali, P., 2014. A role for TMS/EEG in neuropsychiatric disorders. Neurol. Psychiatry Brain Res. 20, 37–40. doi:10.1016/j.npbr.2014.02.001

Cardin, J.A., Carlén, M., Meletis, K., Knoblich, U., Zhang, F., Deisseroth, K., Tsai, L.-H., Moore, C.I., 2009. Driving fast-spiking cells induces gamma rhythm and controls sensory responses. Nature 459, 663–667. doi:10.1038/nature08002

Casali, A.G., Casarotto, S., Rosanova, M., Mariotti, M., Massimini, M., 2010. General indices to characterize the electrical response of the cerebral cortex to TMS. NeuroImage 49, 1459–1468. doi:10.1016/j.neuroimage.2009.09.026

Casali, A.G., Gosseries, O., Rosanova, M., Boly, M., Sarasso, S., Casali, K.R., Casarotto, S., Bruno, M.-A., Laureys, S., Tononi, G., Massimini, M., 2013. A Theoretically Based Index of Consciousness Independent of Sensory Processing and Behavior. Sci. Transl. Med. 5, 198ra105–198ra105. doi:10.1126/scitranslmed.3006294

Casarotto, S., Bianchi, A.M., Cerutti, S., Chiarenza, G.A., 2004. Principal component analysis for reduction of ocular artefacts in event-related potentials of normal and dyslexic children. Clin. Neurophysiol. 115, 609–619. doi:10.1016/j.clinph.2003.10.018

Casarotto, S., Canali, P., Rosanova, M., Pigorini, A., Fecchio, M., Mariotti, M., Lucca, A., Colombo, C., Benedetti, F., Massimini, M., 2013. Assessing the effects of electroconvulsive therapy on cortical excitability by means of transcranial magnetic stimulation and electroencephalography. Brain Topogr. 26, 326–337. doi:10.1007/s10548-012-0256-8

Casarotto, S., Romero Lauro, L.J., Bellina, V., Casali, A.G., Rosanova, M., Pigorini, A., Defendi, S., Mariotti, M., Massimini, M., 2010. EEG Responses to TMS Are Sensitive to Changes in the Perturbation Parameters and Repeatable over Time. PLoS ONE 5, e10281. doi:10.1371/journal.pone.0010281

Cash, S.S., Halgren, E., Dehghani, N., Rossetti, A.O., Thesen, T., Wang, C., Devinsky, O., Kuzniecky, R., Doyle, W., Madsen, J.R., Bromfield, E., Eross, L., Halász, P., Karmos, G., Csercsa, R., Wittner, L., Ulbert, I., 2009. The human K-complex represents an isolated cortical down-state. Science 324, 1084–1087. doi:10.1126/science.1169626

Chauvette, S., Crochet, S., Volgushev, M., Timofeev, I., 2011. Properties of slow oscillation during slow-wave sleep and anesthesia in cats. J. Neurosci. 31, 14998–15008. doi:10.1523/JNEUROSCI.2339-11.2011

Chen, G., Henter, I.D., Manji, H.K., 2010. Translational research in bipolar disorder: emerging insights from genetically based models. Mol. Psychiatry 15, 883–895. doi:10.1038/mp.2010.3

Chistyakov, A.V., Kaplan, B., Rubichek, O., Kreinin, I., Koren, D., Hafner, H., Feinsod, M., Klein, E., 2005. Effect of electroconvulsive therapy on cortical excitability in patients with major depression: a transcranial magnetic stimulation study. Clin. Neurophysiol. 116, 386–392. doi:10.1016/j.clinph.2004.09.008

Cho, R.Y., Konecky, R.O., Carter, C.S., 2006. Impairments in frontal cortical γ synchrony and cognitive control in schizophrenia. Proc. Natl. Acad. Sci. U. S. A. 103, 19878–19883. doi:10.1073/pnas.0609440103

Cirelli, C., 2009. The genetic and molecular regulation of sleep: from fruit flies to humans. Nat. Rev. Neurosci. 10, 549–560. doi:10.1038/nrn2683

Classen, J., Schnitzler, A., Binkofski, F., Werhahn, K.J., Kim, Y.S., Kessler, K.R., Benecke, R., 1997. The motor syndrome associated with exaggerated inhibition within the primary motor cortex of patients with hemiparetic. Brain 120, 605–619. doi:10.1093/brain/120.4.605

Compte, A., Sanchez-Vives, M.V., McCormick, D.A., Wang, X.-J., 2003. Cellular and network mechanisms of slow oscillatory activity (<1 Hz) and wave propagations in a cortical network model. J. Neurophysiol. 89, 2707–2725. doi:10.1152/jn.00845.2002

Connor, S.A., Maity, S., Roy, B., Ali, D.W., Nguyen, P.V., 2012. Conversion of short-term potentiation to long-term potentiation in mouse CA1 by coactivation of β-adrenergic and muscarinic receptors. Learn. Mem. Cold Spring Harb. N 19, 535–542. doi:10.1101/lm.026898.112

Cossart, R., Aronov, D., Yuste, R., 2003. Attractor dynamics of network UP states in the neocortex. Nature 423, 283–288. doi:10.1038/nature01614

Cossu, M., Cardinale, F., Castana, L., Citterio, A., Francione, S., Tassi, L., Benabid, A.L., Lo Russo, G., 2005. Stereoelectroencephalography in the presurgical evaluation of focal epilepsy: a retrospective analysis of 215 procedures. Neurosurgery. 57, 706–718; discussion 706–718.

Cruse, D., Chennu, S., Chatelle, C., Bekinschtein, T.A., Fernández-Espejo, D., Pickard, J.D., Laureys, S., Owen, A.M., 2011. Bedside detection of awareness in the vegetative state: a cohort study. Lancet 378, 2088–2094. doi:10.1016/S0140-6736(11)61224-5

Csercsa, R., Dombovári, B., Fabó, D., Wittner, L., Erss, L., Entz, L., Sólyom, A., Rásonyi, G., Szcs, A., Kelemen, A., Jakus, R., Juhos, V., Grand, L., Magony, A., Halász, P., Freund, T.F., Maglóczky, Z., Cash, S.S., Papp, L., Karmos, G., Halgren, E., Ulbert, I., 2010. Laminar analysis of slow wave activity in humans. Brain 133, 2814–2829. doi:10.1093/brain/awq169

Dash, M.B., Douglas, C.L., Vyazovskiy, V.V., Cirelli, C., Tononi, G., 2009. Long-term homeostasis of extracellular glutamate in the rat cerebral cortex across sleep and waking states. J. Neurosci. Off. J. Soc. Neurosci. 29, 620–629. doi:10.1523/JNEUROSCI.5486-08.2009

Daskalakis, Z.J., Christensen, B.K., Chen, R., Fitzgerald, P.B., Zipursky, R.B., Kapur, S., 2002a. Evidence for impaired cortical inhibition in schizophrenia using transcranial magnetic stimulation. Arch. Gen. Psychiatry 59, 347–354.

Daskalakis, Z.J., Christensen, B.K., Fitzgerald, P.B., Chen, R., 2002b. Transcranial magnetic stimulation: A new investigational and treatment tool in psychiatry. J. Neuropsychiatry Clin. Neurosci. 14, 406–415. doi:10.1176/appi.neuropsych.14.4.406

Daskalakis, Z.J., Möller, B., Christensen, B.K., Fitzgerald, P.B., Gunraj, C., Chen, R., 2006. The effects of repetitive transcranial magnetic stimulation on cortical inhibition in healthy human subjects. Exp. Brain Res. 174, 403–412. doi:10.1007/s00221-006-0472-0

David, O., Bastin, J., Chabardès, S., Minotti, L., Kahane, P., 2010. Studying network mechanisms using intracranial stimulation in epileptic patients. Front. Syst. Neurosci. 4, 148. doi:10.3389/fnsys.2010.00148

Davidson, R.J., Irwin, W., 1999. The functional neuroanatomy of emotion and affective style. Trends Cogn. Sci. 3, 11–21. doi:10.1016/S1364-6613(98)01265-0

Delorme, A., Makeig, S., 2004. EEGLAB: an open source toolbox for analysis of single-trial EEG dynamics including independent component analysis. J. Neurosci. Methods 134, 9–21. doi:10.1016/j.jneumeth.2003.10.009

Destexhe, A., Contreras, D., Steriade, M., 1999. Spatiotemporal analysis of local field potentials and unit discharges in cat cerebral cortex during natural wake and sleep states. J. Neurosci. 19, 4595–4608.

Destexhe, A., Hughes, S.W., Rudolph, M., Crunelli, V., 2007. Are corticothalamic "up" states fragments of wakefulness? Trends Neurosci., July INMED/TINS special issue—Physiogenic and pathogenic oscillations: the beauty and the beast 30, 334–342. doi:10.1016/j.tins.2007.04.006

Downar, J., Daskalakis, Z.J., 2013. New Targets for rTMS in Depression: A Review of Convergent Evidence. Brain Stimulat. 6, 231–240. doi:10.1016/j.brs.2012.08.006

Drevets, W.C., 2000. Neuroimaging studies of mood disorders. Biol. Psychiatry 48, 813–829. doi:10.1016/S0006-3223(00)01020-9

Duman, R.S., Malberg, J., Nakagawa, S., D'Sa, C., 2000. Neuronal plasticity and survival in mood disorders. Biol. Psychiatry 48, 732–739.

Duman, R.S., Voleti, B., 2012. Signaling pathways underlying the pathophysiology and treatment of depression: novel mechanisms for rapid-acting agents. Trends Neurosci., Special Issue: Neuropsychiatric Disorders 35, 47–56. doi:10.1016/j.tins.2011.11.004

Dwivedi Y, Rizavi HS, Conley RR, Roberts RC, Tamminga CA, Pandey GN, 2003. ALtered gene expression of brain-derived neurotrophic factor and receptor tyrosine kinase b in postmortem brain of suicide subjects. Arch. Gen. Psychiatry 60, 804–815. doi:10.1001/archpsyc.60.8.804

Edelman, G.M., 2007. Second Nature: Brain Science and Human Knowledge, 1 edition. ed. Yale University Press, Amsterdam ; New York.

Englot, D.J., Yang, L., Hamid, H., Danielson, N., Bai, X., Marfeo, A., Yu, L., Gordon, A., Purcaro, M.J., Motelow, J.E., Agarwal, R., Ellens, D.J., Golomb, J.D., Shamy, M.C.F., Zhang, H., Carlson, C., Doyle, W., Devinsky, O., Vives, K., Spencer, D.D., Spencer, S.S., Schevon, C., Zaveri, H.P., Blumenfeld, H., 2010. Impaired consciousness in temporal lobe seizures: Role of cortical slow activity. Brain 133, 3764–3777. doi:10.1093/brain/awq316

Eranti, S., Mogg, A., Pluck, G., Landau, S., Purvis, R., Brown, R.G., Howard, R., Knapp, M., Philpot, M., Rabe-Hesketh, S., Romeo, R., Rothwell, J., Edwards, D., McLoughlin, D.M., 2007. A randomized, controlled trial with 6-month follow-up of repetitive transcranial magnetic stimulation and electroconvulsive therapy for severe depression. Am. J. Psychiatry 164, 73–81. doi:10.1176/appi.ajp.164.1.73

Esser, S.K., Huber, R., Massimini, M., Peterson, M.J., Ferrarelli, F., Tononi, G., 2006. A direct demonstration of cortical LTP in humans: A combined TMS/EEG study. Brain Res. Bull. 69, 86–94. doi:10.1016/j.brainresbull.2005.11.003

Fava, M., 2003. Diagnosis and definition of treatment-resistant depression. Biol. Psychiatry 53, 649–659. doi:10.1016/S0006-3223(03)00231-2

Ferrarelli, F., Massimini, M., Peterson, M.J., Riedner, B.A., Lazar, M., Murphy, M.J., Huber, R., Rosanova, M., Alexander, A.L., Kalin, N., Tononi, G., 2008. Reduced evoked gamma oscillations in the frontal cortex in schizophrenia patients: A TMS/EEG study. Am. J. Psychiatry 165, 996–1005. doi:10.1176/appi.ajp.2008.07111733

Ferrarelli, F., Massimini, M., Sarasso, S., Casali, A., Riedner, B.A., Angelini, G., Tononi, G., Pearce, R.A., 2010. Breakdown in cortical effective connectivity during midazolam-induced loss of consciousness. Proc. Natl. Acad. Sci. U. S. A. 107, 2681–2686. doi:10.1073/pnas.0913008107

Ferrarelli, F., Sarasso, S., Guller, Y., Riedner, B.A., Peterson, M.J., Bellesi, M., Massimini, M., Postle, B.R., Tononi, G., 2012. Reduced natural oscillatory frequency of frontal thalamocortical circuits in schizophrenia. Arch. Gen. Psychiatry 69, 766–774. doi:10.1001/archgenpsychiatry.2012.147

Fitzgerald, P.B., Brown, T.L., Marston, N.A.U., Daskalakis, Z.J., De Castella, A., Kulkarni, J., 2003. Transcranial magnetic stimulation in the treatment of depression: a double-blind, placebo-controlled trial. Arch. Gen. Psychiatry 60, 1002–1008. doi:10.1001/archpsyc.60.9.1002

Fitzgerald, P.B., Daskalakis, Z.J., 2008. A review of repetitive transcranial magnetic stimulation use in the treatment of schizophrenia. Can. J. Psychiatry 53, 567–576.

Freeman, C.P.L., Basson, J.V., Crighton, A., 1978. DOUBLE-BLIND CONTROLLED TRIAL OF ELECTROCONVULSIVE THERAPY (E.C.T.) AND SIMULATED E.C.T. IN DEPRESSIVE ILLNESS. The Lancet, Originally published as Volume 1, Issue 8067 311, 738–740. doi:10.1016/S0140-6736(78)90857-7

Gaillard, R., Dehaene, S., Adam, C., Clémenceau, S., Hasboun, D., Baulac, M., Cohen, L., Naccache, L., 2009. Converging intracranial markers of conscious access. PLoS Biol. 7.

Gallinat, J., Winterer, G., Herrmann, C.S., Senkowski, D., 2004. Reduced oscillatory gamma-band responses in unmedicated schizophrenic patients indicate impaired frontal network processing. Clin. Neurophysiol. 115, 1863–1874. doi:10.1016/j.clinph.2004.03.013

G E Alexander, M R DeLong, Strick, P.L., 1986. Parallel Organization of Functionally Segregated Circuits Linking Basal Ganglia and Cortex. Annu. Rev. Neurosci. 9, 357–381. doi:10.1146/annurev.ne.09.030186.002041

George, M.S., Ketter, T.A., Post, R.M., 1994. Prefrontal cortex dysfunction in clinical depression. Depression 2, 59–72. doi:10.1002/depr.3050020202

Gershon, A.A., Dannon, P.N., Grunhaus, L., 2003. Transcranial Magnetic Stimulation in the Treatment of Depression. Am. J. Psychiatry 160, 835–845. doi:10.1176/appi.ajp.160.5.835

Gerwig, M., Kastrup, O., Meyer, B.-U., Niehaus, L., 2003. Evaluation of cortical excitability by motor and phosphene thresholds in transcranial magnetic stimulation. J. Neurol. Sci. 215, 75–78. doi:10.1016/S0022-510X(03)00228-4

Giacino, J.T., Kalmar, K., Whyte, J., 2004. The JFK Coma Recovery Scale-Revised: measurement characteristics and diagnostic utility. Arch. Phys. Med. Rehabil. 85, 2020–2029.

Gibbons, R.D., Hedeker, D., Elkin, I., Waternaux, C., Kraemer, H.C., Greenhouse, J.B., Shea, M.T., Imber, S.D., Sotsky, S.M., Watkins, J.T., 1993. Some conceptual and statistical issues in analysis of longitudinal psychiatric data. Application to the NIMH treatment of Depression Collaborative Research Program dataset. Arch. Gen. Psychiatry 50, 739–750.

Gillin, J.C., Buchsbaum, M., Wu, J., Clark, C., Bunney, W., 2001. Sleep deprivation as a model experimental antidepressant treatment: Findings from functional brain imaging. Depress. Anxiety 14, 37–49. doi:10.1002/da.1045

Glazewski, S., Herman, C., McKenna, M., Chapman, P.F., Fox, K., 1998. Long-term potentiation in vivo in layers II/III of rat barrel cortex. Neuropharmacology 37, 581–592.

Gonzalez-Burgos, G., Lewis, D.A., 2008. GABA neurons and the mechanisms of network oscillations: Implications for understanding cortical dysfunction in schizophrenia. Schizophr. Bull. 34, 944–961. doi:10.1093/schbul/sbn070

Gorgulu, Y., Caliyurt, O., 2009. Rapid antidepressant effects of sleep deprivation therapy correlates with serum BDNF changes in major depression. Brain Res. Bull. 80, 158–162. doi:10.1016/j.brainresbull.2009.06.016

Gosseries, O., Sarasso, S., Casarotto, S., Boly, M., Schnakers, C., Napolitani, M., Bruno, M.-A., Ledoux, D., Tshibanda, J.-F., Massimini, M., Laureys, S., Rosanova, M., 2015. On the cerebral origin of EEG responses to TMS: insights from severe cortical lesions. Brain Stimulat. 8, 142–149. doi:10.1016/j.brs.2014.10.008

Grandchamp, R., Braboszcz, C., Makeig, S., Delorme, A., 2012. Stability of ICA decomposition across within-subject EEG datasets. Conf. Proc. Annu. Int. Conf. IEEE Eng. Med. Biol. Soc. IEEE Eng. Med. Biol. Soc. Annu. Conf. 2012, 6735–6739. doi:10.1109/EMBC.2012.6347540

Gray, C.M., McCormick, D.A., 1996. Chattering cells: Superficial pyramidal neurons contributing to the generation of synchronous oscillations in the visual cortex. Science 274, 109–113. doi:10.1126/science.274.5284.109

Grimm, S., Schmidt, C.F., Bermpohl, F., Heinzel, A., Dahlem, Y., Wyss, M., Hell, D., Boesiger, P., Boeker, H., Northoff, G., 2006. Segregated neural representation of distinct emotion dimensions in the prefrontal cortex—an fMRI study. NeuroImage 30, 325–340. doi:10.1016/j.neuroimage.2005.09.006

Haig, A.R., Gordon, E., De Pascalis, V., Meares, R.A., Bahramali, H., Harris, A., 2000. Gamma activity in schizophrenia: evidence of impaired network binding? Clin. Neurophysiol. 111, 1461–1468. doi:10.1016/S1388-2457(00)00347-3

Hamilton, M., 1960. A Rating Scale for Depression. J. Neurol. Neurosurg. Psychiatry 23, 56–62. doi:10.1136/jnnp.23.1.56

Hangya, B., Tihanyi, B.T., Entz, L., Fabó, D., Eross, L., Wittner, L., Jakus, R., Varga, V., Freund, T.F., Ulbert, I., 2011. Complex propagation patterns characterize human cortical activity during slow-wave sleep. J. Neurosci. 31, 8770–8779. doi:10.1523/JNEUROSCI.1498-11.2011

Hanlon, E.C., Vyazovskiy, V.V., Faraguna, U., Tononi, G., Cirelli, C., 2011. Synaptic potentiation and sleep need: clues from molecular and electrophysiological studies. Curr. Top. Med. Chem. 11, 2472–2482.

Harvey, A.G., 2008. Sleep and circadian rhythms in bipolar disorder: seeking synchrony, harmony, and regulation. Am. J. Psychiatry 165, 820–829. doi:10.1176/appi.ajp.2008.08010098

Hasey, G., 2001. Transcranial magnetic stimulation in the treatment of mood disorder: a review and comparison with electroconvulsive therapy. Can. J. Psychiatry Rev. Can. Psychiatr. 46, 720–727.

Hasler, G., Van Der Veen, J.W., Tumonis, T., Meyers, N., Shen, J., Drevets, W.C., 2007. Reduced prefrontal glutamate/glutamine and γ-aminobutyric acid levels in major depression determined using proton magnetic resonance spectroscopy. Arch. Gen. Psychiatry 64, 193–200. doi:10.1001/archpsyc.64.2.193

Hecht, D., 2010. Depression and the hyperactive right-hemisphere. Neurosci. Res. 68, 77–87. doi:10.1016/j.neures.2010.06.013

Hedeker, D., Gibbons, R.D., 1996. MIXREG: a computer program for mixed-effects regression analysis with autocorrelated errors. Comput. Methods Programs Biomed. 49, 229–252.

Hefti, K., Holst, S.C., Sovago, J., Bachmann, V., Buck, A., Ametamey, S.M., Scheidegger, M., Berthold, T., Gomez-Mancilla, B., Seifritz, E., Landolt, H.-P., 2013. Increased metabotropic glutamate receptor subtype 5 availability in human brain after one night without sleep. Biol. Psychiatry 73, 161–168. doi:10.1016/j.biopsych.2012.07.030

Herrmann, C.S., Demiralp, T., 2005. Human EEG gamma oscillations in neuropsychiatric disorders. Clin. Neurophysiol. 116, 2719–2733. doi:10.1016/j.clinph.2005.07.007

Hill, S., Tononi, G., 2005. Modeling Sleep and Wakefulness in the Thalamocortical System. J. Neurophysiol. 93, 1671–1698. doi:10.1152/jn.00915.2004

Hill, T., Lewicki, P., 2006. Statistics: Methods and applications. Compr. Ref. Sci. Ind. Data Min.

Hobson, J.A., McCarley, R.W., 1971. Cortical unit activity in sleep and waking. Electroencephalogr. Clin. Neurophysiol. 30, 97–112. doi:10.1016/0013-4694(71)90271-9

Hoel, E.P., Albantakis, L., Tononi, G., 2013. Quantifying causal emergence shows that macro can beat micro. Proc. Natl. Acad. Sci. U. S. A. 110, 19790–19795. doi:10.1073/pnas.1314922110

Horne, J.A., 1993. Human sleep, sleep loss and behaviour. Implications for the prefrontal cortex and psychiatric disorder. Br. J. Psychiatry J. Ment. Sci. 162, 413–419.

Huber, R., Mäki, H., Rosanova, M., Casarotto, S., Canali, P., Casali, A.G., Tononi, G., Massimini, M., 2013. Human Cortical Excitability Increases with Time Awake. Cereb. Cortex 23, 1–7. doi:10.1093/cercor/bhs014

Ilmoniemi, R.J., Virtanen, J., Ruohonen, J., Karhu, J., Aronen, H.J., Näätänen, R., Katila, T., 1997. Neuronal responses to magnetic stimulation reveal cortical reactivity and connectivity. Neuroreport 8, 3537–3540.

Inostroza, M., Born, J., 2013. Sleep for preserving and transforming episodic memory, Annual Review of Neuroscience.

Iriki, A., Pavlides, C., Keller, A., Asanuma, H., 1991. Long-term potentiation of thalamic input to the motor cortex induced by coactivation of thalamocortical and corticocortical afferents. J. Neurophysiol. 65, 1435–1441.

Kähkönen, S., Kesäniemi, M., Nikouline, V.V., Karhu, J., Ollikainen, M., Holi, M., Ilmoniemi, R.J., 2001. Ethanol modulates cortical activity: direct evidence with combined TMS and EEG. NeuroImage 14, 322–328. doi:10.1006/nimg.2001.0849

Keller, C.J., Bickel, S., Entz, L., Ulbert, I., Milham, M.P., Kelly, C., Mehta, A.D., 2011. Intrinsic functional architecture predicts electrically evoked responses in the human brain. Proc. Natl. Acad. Sci. U. S. A. 108, 10308–10313. doi:10.1073/pnas.1019750108

King, J.-R., Gramfort, A., Schurger, A., Naccache, L., Dehaene, S., 2014. Two Distinct Dynamic Modes Subtend the Detection of Unexpected Sounds. PLoS ONE 9, e85791. doi:10.1371/journal.pone.0085791

Kirkwood, A., Dudek, S.M., Gold, J.T., Aizenman, C.D., Bear, M.F., 1993. Common forms of synaptic plasticity in the hippocampus and neocortex in vitro. Science 260, 1518–1521. doi:10.1126/science.8502997

Knapp, M., Romeo, R., Mogg, A., Eranti, S., Pluck, G., Purvis, R., Brown, R.G., Howard, R., Philpot, M., Rothwell, J., Edwards, D., McLoughlin, D.M., 2008. Cost-effectiveness of transcranial magnetic stimulation vs. electroconvulsive therapy for severe depression: a multi-centre randomised controlled trial. J. Affect. Disord. 109, 273–285. doi:10.1016/j.jad.2008.01.001

Komssi, S., Kähkönen, S., 2006. The novelty value of the combined use of electroencephalography and transcranial magnetic stimulation for neuroscience research. Brain Res. Rev. 52, 183–192. doi:10.1016/j.brainresrev.2006.01.008

Komssi, S., Savolainen, P., Heiskala, J., Kähkönen, S., 2007. Excitation threshold of the motor cortex estimated with transcranial magnetic stimulation electroencephalography. Neuroreport 18, 13–16. doi:10.1097/WNR.0b013e328011b89a

Kouider, S., Andrillon, T., Barbosa, L.S., Goupil, L., Bekinschtein, T.A., 2014. Inducing Task-Relevant Responses to Speech in the Sleeping Brain. Curr. Biol. 24, 2208–2214. doi:10.1016/j.cub.2014.08.016

Krueger, J.M., Obál, F., Fang, J., Kubota, T., Taishi, P., 2001. The Role of Cytokines in Physiological Sleep Regulation. Ann. N. Y. Acad. Sci. 933, 211–221. doi:10.1111/j.1749-6632.2001.tb05826.x

Kunugi, H., Ida, I., Owashi, T., Kimura, M., Inoue, Y., Nakagawa, S., Yabana, T., Urushibara, T., Kanai, R., Aihara, M., Yuuki, N., Otsubo, T., Oshima, A., Kudo, K., Inoue, T., Kitaichi, Y., Shirakawa, O., Isogawa, K., Nagayama, H., Kamijima, K., Nanko, S., Kanba, S., Higuchi, T., Mikuni, M., 2006. Assessment of the dexamethasone/CRH test as a state-dependent marker for hypothalamic-pituitary-adrenal (HPA) axis abnormalities in major depressive episode: a Multicenter Study. Neuropsychopharmacol. Off. Publ. Am. Coll. Neuropsychopharmacol. 31, 212–220. doi:10.1038/sj.npp.1300868

Kupka, R.W., Altshuler, L.L., Nolen, W.A., Suppes, T., Luckenbaugh, D.A., Leverich, G.S., Frye, M.A., Keck, P.E., McElroy, S.L., Grunze, H., Post, R.M., 2007. Three times more days depressed than manic or hypomanic in both bipolar I and bipolar II disorder1. Bipolar Disord. 9, 531–535. doi:10.1111/j.1399-5618.2007.00467.x

Kwon, J.S., O'Donnell, B.F., Wallenstein, G.V., Greene, R.W., Hirayasu, Y., Nestor, P.G., Hasselmo, M.E., Potts, G.F., Shenton, M.E., McCarley, R.W., 1999. Gamma frequency-range abnormalities to auditory stimulation in schizophrenia. Arch. Gen. Psychiatry 56, 1001–1005. doi:10.1001/archpsyc.56.11.1001

Laarne, P., Hyttinen, J., Dodel, S., Malmivuo, J., Eskola, H., 2000. Accuracy of two dipolar inverse algorithms applying reciprocity for forward calculation. Comput. Biomed. Res. Int. J. 33, 172–185. doi:10.1006/cbmr.1999.1538

Lamme, V.A.F., Zipser, K., Spekreijse, H., 1998. Figure-ground activity in primary visual cortex is suppressed by anesthesia. Proc. Natl. Acad. Sci. U. S. A. 95, 3263–3268. doi:10.1073/pnas.95.6.3263

Lam, R.W., Chan, P., Wilkins-Ho, M., Yatham, L.N., 2008. Repetitive transcranial magnetic stimulation for treatment-resistant depression: a systematic review and metaanalysis. Can. J. Psychiatry Rev. Can. Psychiatr. 53, 621–631.

Laureys, S., Owen, A.M., Schiff, N.D., 2004. Brain function in coma, vegetative state, and related disorders. Lancet Neurol. 3, 537–546. doi:10.1016/S1474-4422(04)00852-X

Lee, P.-S., Chen, Y.-S., Hsieh, J.-C., Su, T.-P., Chen, L.-F., 2010. Distinct neuronal oscillatory responses between patients with bipolar and unipolar disorders: A magnetoencephalographic study. J. Affect. Disord. 123, 270–275. doi:10.1016/j.jad.2009.08.020

Lee, W.H., Deng, Z.-D., Kim, T.-S., Laine, A.F., Lisanby, S.H., Peterchev, A.V., 2012. Regional electric field induced by electroconvulsive therapy in a realistic finite element head model: Influence of white matter anisotropic conductivity. NeuroImage 59, 2110–2123. doi:10.1016/j.neuroimage.2011.10.029

Lefaucheur, J.P., Lucas, B., Andraud, F., Hogrel, J.Y., Bellivier, F., Del Cul, A., Rousseva, A., Leboyer, M., Paillère-Martinot, M.L., 2008. Inter-hemispheric asymmetry of motor corticospinal excitability in major depression studied by transcranial magnetic stimulation. J. Psychiatr. Res. 42, 389–398. doi:10.1016/j.jpsychires.2007.03.001

Lehmann, D., Skrandies, W., 1980. Reference-free identification of components of checkerboard-evoked multichannel potential fields. Electroencephalogr. Clin. Neurophysiol. 48, 609–621. doi:10.1016/0013-4694(80)90419-8

Leibenluft, E., Moul, D.E., Schwartz, P.J., Madden, P.A., Wehr, T.A., 1993. A clinical trial of sleep deprivation in combination with antidepressant medication. Psychiatry Res. 46, 213–227.

Lempel, A., Ziv, J., 2006. On the Complexity of Finite Sequences. IEEE Trans Inf Theor 22, 75–81. doi:10.1109/TIT.1976.1055501

Levinson, A.J., Fitzgerald, P.B., Favalli, G., Blumberger, D.M., Daigle, M., Daskalakis, Z.J., 2010. Evidence of Cortical Inhibitory Deficits in Major Depressive Disorder. Biol. Psychiatry, Cortical Inhibitory Deficits in Depression 67, 458–464. doi:10.1016/j.biopsych.2009.09.025

Levinson, A.J., Young, L.T., Fitzgerald, P.B., Daskalakis, Z.J., 2007. Cortical inhibitory dysfunction in bipolar disorder: A study using transcranial magnetic stimulation. J. Clin. Psychopharmacol. 27, 493–497. doi:10.1097/jcp.0b013e31814ce524

Lewis, D.A., Hashimoto, T., Volk, D.W., 2005. Cortical inhibitory neurons and schizophrenia. Nat. Rev. Neurosci. 6, 312–324. doi:10.1038/nrn1648

Lewis, L.D., Weiner, V.S., Mukamel, E.A., Donoghue, J.A., Eskandar, E.N., Madsen, J.R., Anderson, W.S., Hochberg, L.R., Cash, S.S., Brown, E.N., Purdon, P.L., 2012. Rapid fragmentation of neuronal networks at the onset of propofol-induced unconsciousness. Proc. Natl. Acad. Sci. U. S. A. 109, E3377–E3386. doi:10.1073/pnas.1210907109

Libet, B., 1982. Brain stimulation in the study of neuronal functions for conscious sensory experiences. Hum. Neurobiol. 1, 235–242.

Light, G.A., Hsu, J.L., Hsieh, M.H., Meyer-Gomes, K., Sprock, J., Swerdlow, N.R., Braff, D.L., 2006. Gamma Band Oscillations Reveal Neural Network Cortical Coherence Dysfunction in Schizophrenia Patients. Biol. Psychiatry 60, 1231–1240. doi:10.1016/j.biopsych.2006.03.055

Lioumis, P., Kičić, D., Savolainen, P., Mäkelä, J.P., Kähkönen, S., 2009. Reproducibility of TMS—Evoked EEG responses. Hum. Brain Mapp. 30, 1387–1396. doi:10.1002/hbm.20608

Liu, S.-K., Fitzgerald, P.B., Daigle, M., Chen, R., Daskalakis, Z.J., 2009. The Relationship Between Cortical Inhibition, Antipsychotic Treatment, and the Symptoms of Schizophrenia. Biol. Psychiatry, Impaired Neuroplasticity in Schizophrenia 65, 503–509. doi:10.1016/j.biopsych.2008.09.012

Liu, T.-Y., Hsieh, J.-C., Chen, Y.-S., Tu, P.-C., Su, T.-P., Chen, L.-F., 2012. Different patterns of abnormal gamma oscillatory activity in unipolar and bipolar disorder patients during an implicit emotion task. Neuropsychologia 50, 1514–1520. doi:10.1016/j.neuropsychologia.2012.03.004

Liu, Z.-W., Faraguna, U., Cirelli, C., Tononi, G., Gao, X.-B., 2010. Direct evidence for wake-related increases and sleep-related decreases in synaptic strength in rodent cortex. J. Neurosci. Off. J. Soc. Neurosci. 30, 8671–8675. doi:10.1523/JNEUROSCI.1409-10.2010

Li, X., Nahas, Z., Kozel, F.A., Anderson, B., Bohning, D.E., George, M.S., 2004. Acute left prefrontal transcranial magnetic stimulation in depressed patients is associated with immediately increased activity in prefrontal cortical as well as subcortical regions. Biol. Psychiatry 55, 882–890. doi:10.1016/j.biopsych.2004.01.017

Luczak, A., Barthó, P., Marguet, S.L., Buzsáki, G., Harris, K.D., 2007. Sequential structure of neocortical spontaneous activity in vivo. Proc. Natl. Acad. Sci. 104, 347–352. doi:10.1073/pnas.0605643104

Lumer, E.D., Edelman, G.M., Tononi, G., 1997. Neural dynamics in a model of the thalamocortical system. II. The role of neural synchrony tested through perturbations of spike timing. Cereb. Cortex 7, 228–236.

Madsen, T.M., Treschow, A., Bengzon, J., Bolwig, T.G., Lindvall, O., Tingström, A., 2000. Increased neurogenesis in a model of electroconvulsive therapy. Biol. Psychiatry 47, 1043–1049. doi:10.1016/S0006-3223(00)00228-6

Madsen, T.M., Yeh, D.D., Valentine, G.W., Duman, R.S., 2004. Electroconvulsive Seizure Treatment Increases Cell Proliferation in Rat Frontal Cortex. Neuropsychopharmacology 30, 27–34. doi:10.1038/sj.npp.1300565

Maeda, F., Keenan, J.P., Pascual-Leone, A., 2000. Interhemispheric asymmetry of motor cortical excitability in major depression as measured by transcranial magnetic stimulation. Br. J. Psychiatry 177, 169–173. doi:10.1192/bjp.177.2.169

Maharajh, K., Abrams, D., Rojas, D.C., Teale, P., Reite, M.L., 2007. Auditory steady state and transient gamma band activity in bipolar disorder. Int. Congr. Ser., New Frontiers in Biomagnetism. Proceedings of the 15th International Conference on Biomagnetism, Vancouver, BC, Canada, August 21-25, 2006 1300, 707–710. doi:10.1016/j.ics.2006.12.073

Malberg, J.E., Eisch, A.J., Nestler, E.J., Duman, R.S., 2000. Chronic antidepressant treatment increases neurogenesis in adult rat hippocampus. J. Neurosci. Off. J. Soc. Neurosci. 20, 9104–9110.

Malhi, G.S., Tanious, M., Das, P., Coulston, C.M., Berk, M., 2013. Potential mechanisms of action of lithium in bipolar disorder: Current understanding. CNS Drugs 27, 135–153. doi:10.1007/s40263-013-0039-0

Mamounas, L.A., Blue, M.E., Siuciak, J.A., Altar, C.A., 1995. Brain-derived neurotrophic factor promotes the survival and sprouting of serotonergic axons in rat brain. J. Neurosci. Off. J. Soc. Neurosci. 15, 7929–7939.

Manji, H.K., Drevets, W.C., Charney, D.S., 2001. The cellular neurobiology of depression. Nat. Med. 7, 541–547. doi:10.1038/87865

Mann, E.O., Kohl, M.M., Paulsen, O., 2009. Distinct Roles of GABAA and GABAB Receptors in Balancing and Terminating Persistent Cortical Activity. J. Neurosci. 29, 7513–7518. doi:10.1523/JNEUROSCI.6162-08.2009

Massimini, M., Boly, M., Casali, A., Rosanova, M., Tononi, G., 2009. A perturbational approach for evaluating the brain's capacity for consciousness. Prog. Brain Res. 177, 201–214. doi:10.1016/S0079-6123(09)17714-2

Massimini, M., Ferrarelli, F., Esser, S.K., Riedner, B.A., Huber, R., Murphy, M., Peterson, M.J., Tononi, G., 2007. Triggering sleep slow waves by transcranial magnetic stimulation. Proc. Natl. Acad. Sci. U. S. A. 104, 8496–8501. doi:10.1073/pnas.0702495104

Massimini, M., Ferrarelli, F., Huber, R., Esser, S.K., Singh, H., Tononi, G., 2005b. Breakdown of cortical effective connectivity during sleep. Science 309, 2228–2232. doi:10.1126/science.1117256

Massimini, M., Ferrarelli, F., Murphy, M., Huber, R., Riedner, B., Casarotto, S., Tononi, G., 2010. Cortical reactivity and effective connectivity during REM sleep in humans. Cogn. Neurosci. 1, 176–183. doi:10.1080/17588921003731578

Massimini, M., Ferrarelli, F., Sarasso, S., Tononi, G., 2012. Cortical mechanisms of loss of consciousness: insight from TMS/EEG studies. Arch. Ital. Biol. 150, 44–55.

Matsumoto, R., Nair, D.R., LaPresto, E., Najm, I., Bingaman, W., Shibasaki, H., Lüders, H.O., 2004. Functional connectivity in the human language system: A cortico-cortical evoked potential study. Brain 127, 2316–2330. doi:10.1093/brain/awh246

Mattson, M.P., 2008. Glutamate and Neurotrophic Factors in Neuronal Plasticity and Disease. Ann. N. Y. Acad. Sci. 1144, 97–112. doi:10.1196/annals.1418.005

Mayberg, H.S., 2003. Modulating dysfunctional limbic-cortical circuits in depression: towards development of brain-based algorithms for diagnosis and optimised treatment. Br. Med. Bull. 65, 193–207. doi:10.1093/bmb/65.1.193

McCormick, D.A., Wang, Z., Huguenard, J., 1993. Neurotransmitter control of neocortical neuronal activity and excitability. Cereb. Cortex N. Y. N 1991 3, 387–398.

McNamara, P., Johnson, P., McLaren, D., Harris, E., Beauharnais, C., Auerbach, S., 2010. Rem And Nrem Sleep Mentation, in: McNamara, A.C. and P. (Ed.), International Review of Neurobiology. Academic Press, pp. 69–86.

Merali, Z., Du, L., Hrdina, P., Palkovits, M., Faludi, G., Poulter, M.O., Anisman, H., 2004. Dysregulation in the Suicide Brain: mRNA Expression of Corticotropin-Releasing Hormone Receptors and GABAA Receptor Subunits in Frontal Cortical Brain Region. J. Neurosci. 24, 1478–1485. doi:10.1523/JNEUROSCI.4734-03.2004

Michael, N., Erfurth, A., Ohrmann, P., Arolt, V., Heindel, W., Pfleiderer, B., 2003. Metabolic changes within the left dorsolateral prefrontal cortex occurring with electroconvulsive therapy in patients with treatment resistant unipolar depression. Psychol. Med. null, 1277–1284. doi:10.1017/S0033291703007931

Millan, M.J., 2006. Multi-target strategies for the improved treatment of depressive states: Conceptual foundations and neuronal substrates, drug discovery and therapeutic application. Pharmacol. Ther. 110, 135–370. doi:10.1016/j.pharmthera.2005.11.006

Minichiello, L., 2009. TrkB signalling pathways in LTP and learning. Nat. Rev. Neurosci. 10, 850–860. doi:10.1038/nrn2738

Minzenberg, M.J., Firl, A.J., Yoon, J.H., Gomes, G.C., Reinking, C., Carter, C.S., 2010. Gamma oscillatory power is impaired during cognitive control independent of medication status in first-episode schizophrenia. Neuropsychopharmacology 35, 2590–2599. doi:10.1038/npp.2010.150

Mölle, M., Marshall, L., Gais, S., Born, J., 2002. Grouping of spindle activity during slow oscillations in human non-rapid eye movement sleep. J. Neurosci. Off. J. Soc. Neurosci. 22, 10941–10947.

Moreau, A.W., Amar, M., Callebert, J., Fossier, P., 2013. Serotonergic modulation of LTP at excitatory and inhibitory synapses in the developing rat visual cortex. Neuroscience 238, 148–158. doi:10.1016/j.neuroscience.2013.02.013

Mukovski, M., Chauvette, S., Timofeev, I., Volgushev, M., 2007. Detection of active and silent states in neocortical neurons from the field potential signal during slow-wave sleep. Cereb. Cortex 17, 400–414. doi:10.1093/cercor/bhj157

Murase, N., Duque, J., Mazzocchio, R., Cohen, L.G., 2004. Influence of Interhemispheric Interactions on Motor Function in Chronic Stroke. Ann. Neurol. 55, 400–409. doi:10.1002/ana.10848

Myles, P.S., Leslie, K., McNeil, J., Forbes, A., Chan, M.T.V., 2004. Bispectral index monitoring to prevent awareness during anaesthesia: the B-Aware randomised controlled trial. Lancet 363, 1757–1763. doi:10.1016/S0140-6736(04)16300-9

Nibuya, M., Morinobu, S., Duman, R.S., 1995. Regulation of BDNF and trkB mRNA in rat brain by chronic electroconvulsive seizure and antidepressant drug treatments. J. Neurosci. Off. J. Soc. Neurosci. 15, 7539–7547.

Nikolić, D., Fries, P., Singer, W., 2013. Gamma oscillations: precise temporal coordination without a metronome. Trends Cogn. Sci. 17, 54–55. doi:10.1016/j.tics.2012.12.003

Nir, Y., Staba, R.J., Andrillon, T., Vyazovskiy, V.V., Cirelli, C., Fried, I., Tononi, G., 2011. Regional Slow Waves and Spindles in Human Sleep. Neuron 70, 153–169. doi:10.1016/j.neuron.2011.02.043

Nita, D.A., Cissé, Y., Timofeev, I., Steriade, M., 2007. Waking–Sleep Modulation of Paroxysmal Activities Induced by Partial Cortical Deafferentation. Cereb. Cortex 17, 272–283. doi:10.1093/cercor/bhj145

Nobili, L., Ferrara, M., Moroni, F., De Gennaro, L., Russo, G.L., Campus, C., Cardinale, F., De Carli, F., 2011. Dissociated wake-like and sleep-like electro-cortical activity during sleep. NeuroImage 58, 612–619. doi:10.1016/j.neuroimage.2011.06.032

Nobler, M.S., Teneback, C.C., Nahas, Z., Bohning, D.E., Shastri, A., Kozel, F.A., George, M.S., 2000. Structural and functional neuroimaging of electroconvulsive therapy and transcranial magnetic stimulation. Depress. Anxiety 12, 144–156. doi:10.1002/1520-6394(2000)12:3<144::AID-DA6>3.0.CO;2-#

Novati, A., Hulshof, H.J., Granic, I., Meerlo, P., 2012. Chronic partial sleep deprivation reduces brain sensitivity to glutamate N-methyl-d-aspartate receptor-mediated neurotoxicity. J. Sleep Res. 21, 3–9. doi:10.1111/j.1365-2869.2011.00932.x

O'Donnell, B.F., Hetrick, W.P., Vohs, J.L., Krishnan, G.P., Carroll, C.A., Shekhar, A., 2004. Neural synchronization deficits to auditory stimulation in bipolar disorder. NeuroReport 15, 1369–1372.

O'Donnell, B.F., Vohs, J.L., Hetrick, W.P., Carroll, C.A., Shekhar, A., 2004. Auditory event-related potential abnormalities in bipolar disorder and schizophrenia. Int. J. Psychophysiol. 53, 45–55. doi:10.1016/j.ijpsycho.2004.02.001

O'Reardon, J.P., Solvason, H.B., Janicak, P.G., Sampson, S., Isenberg, K.E., Nahas, Z., McDonald, W.M., Avery, D., Fitzgerald, P.B., Loo, C., Demitrack, M.A., George, M.S., Sackeim, H.A., 2007. Efficacy and Safety of Transcranial Magnetic Stimulation in the Acute Treatment of Major Depression: A Multisite Randomized Controlled Trial. Biol. Psychiatry, Depression: New Perspectives on Treatment and Etiology 62, 1208–1216. doi:10.1016/j.biopsych.2007.01.018

Owen, A.M., Coleman, M.R., Boly, M., Davis, M.H., Laureys, S., Pickard, J.D., 2006. Detecting awareness in the vegetative state. Science 313, 1402. doi:10.1126/science.1130197

Özerdem, A., Güntekin, B., Atagün, İ., Turp, B., Başar, E., 2011. Reduced long distance gamma (28–48 Hz) coherence in euthymic patients with bipolar disorder. J. Affect. Disord. 132, 325–332. doi:10.1016/j.jad.2011.02.028

Padberg, F., George, M.S., 2009. Repetitive transcranial magnetic stimulation of the prefrontal cortex in depression. Exp. Neurol., Brain Stimulation in Psychiatry 219, 2–13. doi:10.1016/j.expneurol.2009.04.020

Palazidou, E., 2012. The neurobiology of depression. Br. Med. Bull. 101, 127–145. doi:10.1093/bmb/lds004

Palva, J.M., Palva, S., Kaila, K., 2005. Phase Synchrony among Neuronal Oscillations in the Human Cortex. J. Neurosci. 25, 3962–3972. doi:10.1523/JNEUROSCI.4250-04.2005

Park, H.-J., Friston, K., 2013. Structural and Functional Brain Networks: From Connections to Cognition. Science 342, 1238411. doi:10.1126/science.1238411

Paus, T., 2005. Inferring causality in brain images: a perturbation approach. Philos. Trans. R. Soc. Lond. B. Biol. Sci. 360, 1109–1114. doi:10.1098/rstb.2005.1652

Perera, T.D., Coplan, J.D., Lisanby, S.H., Lipira, C.M., Arif, M., Carpio, C., Spitzer, G., Santarelli, L., Scharf, B., Hen, R., Rosoklija, G., Sackeim, H.A., Dwork, A.J., 2007. Antidepressant-Induced Neurogenesis in the Hippocampus of Adult Nonhuman Primates. J. Neurosci. 27, 4894–4901. doi:10.1523/JNEUROSCI.0237-07.2007

Pigorini, A., Sarasso, S., Proserpio, P., Szymanski, C., Arnulfo, G., Casarotto, S., Fecchio, M., Rosanova, M., Mariotti, M., Lo Russo, G., Palva, J.M., Nobili, L., Massimini, M., 2015. Bistability breaks-off deterministic responses to

intracortical stimulation during non-REM sleep. NeuroImage 112, 105–113. doi:10.1016/j.neuroimage.2015.02.056

Pincus, S.M., Gladstone, I.M., Ehrenkranz, R.A., 1991. A regularity statistic for medical data analysis. J. Clin. Monit. 7, 335–345.

Post, R.M., Altshuler, L.L., Frye, M.A., Suppes, T., Keck, P.E., McElroy, S.L., Leverich, G.S., Luckenbaugh, D.A., Rowe, M., Pizzarello, S., Kupka, R.W., Grunze, H., Nolen, W.A., 2010. Complexity of pharmacologic treatment required for sustained improvement in outpatients with bipolar disorder. J. Clin. Psychiatry 71, 1176–1186; quiz 1252–1253. doi:10.4088/JCP.08m04811yel

Poulter, M.O., Du, L., Zhurov, V., Palkovits, M., Faludi, G., Merali, Z., Anisman, H., 2010. Altered Organization of GABA(A) Receptor mRNA Expression in the Depressed Suicide Brain. Front. Mol. Neurosci. 3, 3. doi:10.3389/neuro.02.003.2010

Price, R.B., Shungu, D.C., Mao, X., Nestadt, P., Kelly, C., Collins, K.A., Murrough, J.W., Charney, D.S., Mathew, S.J., 2009. Amino Acid Neurotransmitters Assessed by Proton Magnetic Resonance Spectroscopy: Relationship to Treatment Resistance in Major Depressive Disorder. Biol. Psychiatry, Social Stresses and Depression 65, 792–800. doi:10.1016/j.biopsych.2008.10.025

Purdon, P.L., Pierce, E.T., Mukamel, E.A., Prerau, M.J., Walsh, J.L., Wong, K.F.K., Salazar-Gomez, A.F., Harrell, P.G., Sampson, A.L., Cimenser, A., Ching, S., Kopell, N.J., Tavares-Stoeckel, C., Habeeb, K., Merhar, R., Brown, E.N., 2013. Electroencephalogram signatures of loss and recovery of consciousness from propofol. Proc. Natl. Acad. Sci. U. S. A. 110, E1142–E1151. doi:10.1073/pnas.1221180110

Ragazzoni, A., Pirulli, C., Veniero, D., Feurra, M., Cincotta, M., Giovannelli, F., Chiaramonti, R., Lino, M., Rossi, S., Miniussi, C., 2013. Vegetative versus Minimally Conscious States: A Study Using TMS-EEG, Sensory and Event-Related Potentials. PLoS ONE 8, e57069. doi:10.1371/journal.pone.0057069

Rajkowska, G., O'Dwyer, G., Teleki, Z., Stockmeier, C.A., Miguel-Hidalgo, J.J., 2007. GABAergic neurons immunoreactive for calcium binding proteins are reduced in the prefrontal cortex in major depression. Neuropsychopharmacology 32, 471–482. doi:10.1038/sj.npp.1301234

Rao, Y., Liu, Z.-W., Borok, E., Rabenstein, R.L., Shanabrough, M., Lu, M., Picciotto, M.R., Horvath, T.L., Gao, X.-B., 2007. Prolonged wakefulness induces experience-dependent synaptic plasticity in mouse hypocretin/orexin neurons. J. Clin. Invest. 117, 4022–4033. doi:10.1172/JCI32829

Richardson, A.G., Fetz, E.E., 2012. Brain state-dependence of electrically evoked potentials monitored with head-mounted electronics. IEEE Trans. Neural Syst. Rehabil. Eng. 20, 756–761. doi:10.1109/TNSRE.2012.2204902

Rodriguez, E., George, N., Lachaux, J.-P., Martinerie, J., Renault, B., Varela, F.J., 1999. Perception's shadow: Long-distance synchronization of human brain activity. Nature 397, 430–433. doi:10.1038/17120

Rosanova, M., Casali, A., Bellina, V., Resta, F., Mariotti, M., Massimini, M., 2009. Natural frequencies of human corticothalamic circuits. J. Neurosci. Off. J. Soc. Neurosci. 29, 7679–7685. doi:10.1523/JNEUROSCI.0445-09.2009

Rosanova, M., Casarotto, S., Pigorini, A., Canali, P., Casali, A.G., Massimini, M., 2012. Combining transcranial magnetic stimulation with electroencephalography to study human cortical excitability and effective connectivity, Neuromethods.

Rosanova, M., Gosseries, O., Casarotto, S., Boly, M., Casali, A.G., Bruno, M.-A., Mariotti, M., Boveroux, P., Tononi, G., Laureys, S., Massimini, M., 2012. Recovery of cortical effective connectivity and recovery of consciousness in vegetative patients. Brain J. Neurol. 135, 1308–1320. doi:10.1093/brain/awr340

Rossi, S., Hallett, M., Rossini, P.M., Pascual-Leone, A., 2009. Safety, ethical considerations, and application guidelines for the use of transcranial magnetic stimulation in clinical practice and research. Clin. Neurophysiol. 120, 2008–2039. doi:10.1016/j.clinph.2009.08.016

Ruohonen, J., Ilmoniemi, R.J., 1999. Modeling of the stimulating field generation in TMS. Electroencephalogr. Clin. Neurophysiol. Suppl. 51, 30–40.

Ruohonen, J., Karhu, J., 2010. Navigated transcranial magnetic stimulation. Neurophysiol. Clin. Neurophysiol. 40, 7–17. doi:10.1016/j.neucli.2010.01.006

Sackeim, H.A., 2004. Convulsant and anticonvulsant properties of electroconvulsive therapy: towards a focal form of brain stimulation. Clin. Neurosci. Res., Epilepsy and Anticonvulsant Treatment 4, 39–57. doi:10.1016/j.cnr.2004.06.013

Salvadore, G., Nugent, A.C., Lemaitre, H., Luckenbaugh, D.A., Tinsley, R., Cannon, D.M., Neumeister, A., Zarate Jr., C.A., Drevets, W.C., 2011. Prefrontal cortical abnormalities in currently depressed versus currently remitted patients with major depressive disorder. NeuroImage 54, 2643–2651. doi:10.1016/j.neuroimage.2010.11.011

Sanacora, G., Zarate, C.A., Krystal, J.H., Manji, H.K., 2008. Targeting the glutamatergic system to develop novel, improved therapeutics for mood disorders. Nat. Rev. Drug Discov. 7, 426–437. doi:10.1038/nrd2462

Sanchez-Vives, M.V., McCormick, D.A., 2000. Cellular and network mechanisms of rhythmic recurrent activity in neocortex. Nat. Neurosci. 3, 1027–1034. doi:10.1038/79848

Sandwell, D.T., 1987. Biharmonic spline interpolation of GEOS-3 and SEASAT altimeter data. Geophys. Res. Lett. 14, 139–142. doi:10.1029/GL014i002p00139

Sarasso, S., Rosanova, M., Casali, A.G., Casarotto, S., Fecchio, M., Boly, M., Gosseries, O., Tononi, G., Laureys, S., Massimini, M., 2014. Quantifying cortical EEG responses to TMS in (un)consciousness. Clin. EEG Neurosci. 45, 40–49. doi:10.1177/1550059413513723

Savelyev, S.A., Rantamäki, T., Rytkönen, K.-M., Castren, E., Porkka-Heiskanen, T., 2012. Sleep homeostasis and depression: studies with the rat clomipramine model of depression. Neuroscience 212, 149–158. doi:10.1016/j.neuroscience.2012.03.029

Schiff, N.D., 2010. Recovery of consciousness after brain injury: a mesocircuit hypothesis. Trends Neurosci. 33, 1–9. doi:10.1016/j.tins.2009.11.002

Schloesser, R.J., Martinowich, K., Manji, H.K., 2012. Mood-stabilizing drugs: mechanisms of action. Trends Neurosci. 35, 36–46. doi:10.1016/j.tins.2011.11.009

Seth, A.K., 2005. Causal connectivity of evolved neural networks during behavior. Netw. Bristol Engl. 16, 35–54.

Seth, A.K., Barrett, A.B., Barnett, L., 2011. Causal density and integrated information as measures of conscious level. Philos. Transact. A Math. Phys. Eng. Sci. 369, 3748–3767. doi:10.1098/rsta.2011.0079

Seth, A.K., Dienes, Z., Cleeremans, A., Overgaard, M., Pessoa, L., 2008. Measuring consciousness: relating behavioural and neurophysiological approaches. Trends Cogn. Sci. 12, 314–321. doi:10.1016/j.tics.2008.04.008

Shaw, A., Brealy, J., Richardson, H., Muthukumaraswamy, S.D., Edden, R.A., John Evans, C., Puts, N.A.J., Singh, K.D., Keedwell, P.A., 2013. Marked Reductions in Visual Evoked Responses But Not γ-Aminobutyric Acid Concentrations or γ-Band Measures in Remitted Depression. Biol. Psychiatry, New Insights into the Treatment of Mood Disorders 73, 691–698. doi:10.1016/j.biopsych.2012.09.032

Silber, M.H., Ancoli-Israel, S., Bonnet, M.H., Chokroverty, S., Grigg-Damberger, M.M., Hirshkowitz, M., Kapen, S., Keenan, S.A., Kryger, M.H., Penzel, T., Pressman, M.R., Iber, C., 2007. The visual scoring of sleep in adults. J. Clin. Sleep Med. 3, 121–131.

Sinkkonen, J., Tiitinen, H., Näätänen, R., 1995. Gabor filters: an informative way for analysing event-related brain activity. J. Neurosci. Methods 56, 99–104. doi:10.1016/0165-0270(94)00111-S

Slotema, C.W., Blom, J.D., Hoek, H.W., Sommer, I.E.C., 2010. Should we expand the toolbox of psychiatric treatment methods to include Repetitive Transcranial Magnetic Stimulation (rTMS)? A meta-analysis of the efficacy of rTMS in psychiatric disorders. J. Clin. Psychiatry 71, 873–884. doi:10.4088/JCP.08m04872gre

Sohal, V.S., Zhang, F., Yizhar, O., Deisseroth, K., 2009. Parvalbumin neurons and gamma rhythms enhance cortical circuit performance. Nature 459, 698–702. doi:10.1038/nature07991

Sommer, M., Dieterich, A., Rüther, E., Paulus, W., Wiltfang, J., 2002. Increased transcranial magnetic motor threshold after ECT. Eur. Arch. Psychiatry Clin. Neurosci. 252, 250–252. doi:10.1007/s00406-002-0387-0

Spencer, K.M., 2009. The Functional Consequences of Cortical Circuit Abnormalities on Gamma Oscillations in Schizophrenia: Insights from Computational Modeling. Front. Hum. Neurosci. 3. doi:10.3389/neuro.09.033.2009

Spencer, K.M., Salisbury, D.F., Shenton, M.E., McCarley, R.W., 2008. γ-Band Auditory Steady-State Responses Are Impaired in First Episode Psychosis. Biol. Psychiatry, Glutamatergic Mechanisms of Schizophrenia Vulnerability and Treatment 64, 369–375. doi:10.1016/j.biopsych.2008.02.021

Spoormaker, V.I., Czisch, M., Maquet, P., Jäncke, L., 2011. Large-scale functional brain networks in human non-rapid eye movement sleep: Insights from combined electroencephalographic/functional magnetic resonance imaging studies. Philos. Trans. R. Soc. Math. Phys. Eng. Sci. 369, 3708–3729. doi:10.1098/rsta.2011.0078

Sporns, O., 2013. Network attributes for segregation and integration in the human brain. Curr. Opin. Neurobiol., Macrocircuits 23, 162–171. doi:10.1016/j.conb.2012.11.015

Steriade, M., 2006. Grouping of brain rhythms in corticothalamic systems. Neuroscience 137, 1087–1106. doi:10.1016/j.neuroscience.2005.10.029

Steriade, M., Amzica, F., 1996. Intracortical and corticothalamic coherency of fast spontaneous oscillations. Proc. Natl. Acad. Sci. U. S. A. 93, 2533–2538. doi:10.1073/pnas.93.6.2533

Steriade, M., Nuñez, A., Amzica, F., 1993. A novel slow (<1 Hz) oscillation of neocortical neurons in vivo: Depolarizing and hyperpolarizing components. J. Neurosci. 13, 3252–3265.

Steriade, M., Timofeev, I., Grenier, F., 2001. Natural waking and sleep states: a view from inside neocortical neurons. J. Neurophysiol. 85, 1969–1985.

Stewart, C., Jeffery, K., Reid, I., 1994. LTP-like synaptic efficacy changes following electroconvulsive stimulation. Neuroreport 5, 1041–1044.

Stewart, L.M., Walsh, V., Rothwell, J.C., 2001. Motor and phosphene thresholds: a transcranial magnetic stimulation correlation study. Neuropsychologia 39, 415–419. doi:10.1016/S0028-3932(00)00130-5

Stickgold, R., Hobson, J.A., Fosse, R., Fosse, M., 2001. Sleep, learning, and dreams: Off-line memory reprocessing. Science 294, 1052–1057. doi:10.1126/science.1063530

Suwa, T., Namiki, C., Takaya, S., Oshita, A., Ishizu, K., Fukuyama, H., Suga, H., Murai, T., 2012. Corticolimbic balance shift of regional glucose metabolism in depressed patients treated with ECT. J. Affect. Disord. 136, 1039–1046. doi:10.1016/j.jad.2011.11.040

Symond, M.B., Harris, A.W.F., Gordon, E., Williams, L.M., 2005. "Gamma synchrony" in first-episode schizophrenia: A disorder of temporal connectivity? Am. J. Psychiatry 162, 459–465. doi:10.1176/appi.ajp.162.3.459

Tagliazucchi, E., von Wegner, F., Morzelewski, A., Brodbeck, V., Borisov, S., Jahnke, K., Laufs, H., 2013. Large-scale brain functional modularity is reflected in slow electroencephalographic rhythms across the human non-rapid eye movement sleep cycle. NeuroImage 70, 327–339. doi:10.1016/j.neuroimage.2012.12.073

Thielscher, A., Opitz, A., Windhoff, M., 2011. Impact of the gyral geometry on the electric field induced by transcranial magnetic stimulation. NeuroImage 54, 234–243. doi:10.1016/j.neuroimage.2010.07.061

Timofeev, I., Grenier, F., Steriade, M., 2001. Disfacilitation and active inhibition in the neocortex during the natural sleep-wake cycle: An intracellular study. Proc. Natl. Acad. Sci. U. S. A. 98, 1924–1929. doi:10.1073/pnas.041430398

Timofeev, I., Grenier, F., Steriade, M., 2000. Impact of intrinsic properties and synaptic factors on the activity of neocortical networks in vivo. J. Physiol.-Paris 94, 343–355. doi:10.1016/S0928-4257(00)01097-4

Tononi, G., 2008. Consciousness as integrated information: a provisional manifesto. Biol. Bull. 215, 216–242.

Tononi, G., 2004. An information integration theory of consciousness. BMC Neurosci. 5, 42. doi:10.1186/1471-2202-5-42

Tononi, G., Cirelli, C., 2014. Sleep and the Price of Plasticity: From Synaptic and Cellular Homeostasis to Memory Consolidation and Integration. Neuron 81, 12–34. doi:10.1016/j.neuron.2013.12.025

Tononi, G., Cirelli, C., 2006. Sleep function and synaptic homeostasis. Sleep Med. Rev. 10, 49–62. doi:10.1016/j.smrv.2005.05.002

Tononi, G., Edelman, G.M., 1998. Consciousness and complexity. Science 282, 1846–1851.

Tononi, G., Sporns, O., Edelman, G.M., 1994. A measure for brain complexity: relating functional segregation and integration in the nervous system. Proc. Natl. Acad. Sci. U. S. A. 91, 5033–5037.

Traub, R.D., Bibbig, A., LeBeau, F.E.N., Cunningham, M.O., Whittington, M.A., 2005. Persistent gamma oscillations in superficial layers of rat auditory neocortex: Experiment and model. J. Physiol. 562, 3–8. doi:10.1113/jphysiol.2004.074641

Tritsch, N.X., Sabatini, B.L., 2012. Dopaminergic modulation of synaptic transmission in cortex and striatum. Neuron 76, 33–50. doi:10.1016/j.neuron.2012.09.023

Uhlhaas, P.J., Haenschel, C., Nikolić, D., Singer, W., 2008. The role of oscillations and synchrony in cortical networks and their putative relevance for the pathophysiology of schizophrenia. Schizophr. Bull. 34, 927–943. doi:10.1093/schbul/sbn062

Uhlhaas, P.J., Singer, W., 2010. Abnormal neural oscillations and synchrony in schizophrenia. Nat. Rev. Neurosci. 11, 100–113. doi:10.1038/nrn2774

UK ECT Review Group, T.U.E.R., 2003. Efficacy and safety of electroconvulsive therapy in depressive disorders: a systematic review and meta-analysis. The Lancet 361, 799–808. doi:10.1016/S0140-6736(03)12705-5

Valderrama, M., 2012. Cortical mapping of gamma oscillations during human slow wave sleep. PLoS One 7.

Valentín, A., Anderson, M., Alarcón, G., García Seoane, J.J., Selway, R., Binnie, C.D., Polkey, C.E., 2002. Responses to single pulse electrical stimulation identify epileptogenesis in the human brain in vivo. Brain 125, 1709–1718.

van de Velde, M., van Erp, G., Cluitmans, P.J., 1998. Detection of muscle artefact in the normal human awake EEG. Electroencephalogr. Clin. Neurophysiol. 107, 149–158.

Van Kerkoerle, T., Self, M.W., Dagnino, B., Gariel-Mathis, M.-A., Poort, J., Van Der Togt, C., Roelfsema, P.R., 2014. Alpha and gamma oscillations characterize feedback and feedforward processing in monkey visual cortex. Proc. Natl. Acad. Sci. U. S. A. 111, 14332–14341. doi:10.1073/pnas.1402773111/-/DCSupplemental

Veniero, D., Maioli, C., Miniussi, C., 2010. Potentiation of Short-Latency Cortical Responses by High-Frequency Repetitive Transcranial Magnetic Stimulation. J. Neurophysiol. 104, 1578–1588. doi:10.1152/jn.00172.2010

Virtanen, J., Ruohonen, J., Näätänen, R., Ilmoniemi, R.J., 1999. Instrumentation for the measurement of electric brain responses to transcranial magnetic stimulation. Med. Biol. Eng. Comput. 37, 322–326.

Voderholzer, U., Fiebich, B.L., Dersch, R., Feige, B., Piosczyk, H., Kopasz, M., Riemann, D., Lieb, K., 2012. Effects of sleep deprivation on nocturnal cytokine concentrations in depressed patients and healthy control subjects. J. Neuropsychiatry Clin. Neurosci. 24, 354–366. doi:10.1176/appi.neuropsych.11060142

Voderholzer, U., Hohagen, F., Klein, T., Jungnickel, J., Kirschbaum, C., Berger, M., Riemann, D., 2004. Impact of sleep deprivation and subsequent recovery sleep on cortisol in unmedicated depressed patients. Am. J. Psychiatry 161, 1404–1410. doi:10.1176/appi.ajp.161.8.1404

Volk, D.W., Lewis, D.A., 2002. Impaired prefrontal inhibition in schizophrenia: relevance for cognitive dysfunction. Physiol. Behav. 77, 501–505. doi:10.1016/S0031-9384(02)00936-8

Vyazovskiy, V.V., Cirelli, C., Pfister-Genskow, M., Faraguna, U., Tononi, G., 2008. Molecular and electrophysiological evidence for net synaptic potentiation in wake and depression in sleep. Nat. Neurosci. 11, 200–208. doi:10.1038/nn2035

Vyazovskiy, V.V., Olcese, U., Lazimy, Y.M., Faraguna, U., Esser, S.K., Williams, J.C., Cirelli, C., Tononi, G., 2009. Cortical firing and sleep homeostasis. Neuron 63, 865–878. doi:10.1016/j.neuron.2009.08.024

West, E.D., 1981. Electric convulsion therapy in depression: a double-blind controlled trial. Br Med J Clin Res Ed 282, 355–357. doi:10.1136/bmj.282.6261.355

Whittington, M.A., Cunningham, M.O., LeBeau, F.E., Racca, C., Traub, R.D., 2011. Multiple origins of the cortical gamma rhythm. Dev. Neurobiol. 71, 92–106. doi:10.1002/dneu.20814

Whittington, M.A., Faulkner, H.J., Doheny, H.C., Traub, R.D., 2000. Neuronal fast oscillations as a target site for psychoactive drugs. Pharmacol. Ther. 86, 171–190. doi:10.1016/S0163-7258(00)00038-3

Whittington, M.A., Traub, R.D., Jefferys, J.G.R., 1995. Synchronized oscillation in interneuron networks driven by metabotropic glutamate receptor activation. Nature 373, 612–615.

Whittington, M.A., Traub, R.D., Kopell, N., Ermentrout, B., Buhl, E.H., 2000. Inhibition-based rhythms: experimental and mathematical observations on network dynamics. Int. J. Psychophysiol. 38, 315–336. doi:10.1016/S0167-8760(00)00173-2

Whyte, J., Myers, R., 2009. Incidence of clinically significant responses to zolpidem among patients with disorders of consciousness: a preliminary placebo controlled trial. Am. J. Phys. Med. Rehabil. Assoc. Acad. Physiatr. 88, 410–418. doi:10.1097/PHM.0b013e3181a0e3a0

Wirz-Justice, A., Benedetti, F., Berger, M., Lam, R.W., Martiny, K., Terman, M., Wu, J.C., 2005. Chronotherapeutics (light and wake therapy) in affective disorders. Psychol. Med. 35, 939–944.

Wirz-Justice, A., Benedetti, F., Terman, M., 2013. Chronotherapeutics for Affective Disorders: A Clinician's Manual for Light and Wake Therapy. S. Karger AG.

Wirz-Justice, A., Terman, M., Oren, D.A., Goodwin, F.K., Kripke, D.F., Whybrow, P.C., Wisner, K.L., Wu, J.C., Lam, R.W., Berger, M., Danilenko, K.V., Kasper, S., Smeraldi, E., Takahashi, K., Thompson, C., van den Hoofdakker, R.H., 2004. Brightening depression. Science 303, 467–469. doi:10.1126/science.303.5657.467c

Wirz-Justice, A., Van den Hoofdakker, R.H., 1999. Sleep deprivation in depression: what do we know, where do we go? Biol. Psychiatry 46, 445–453.

Wisor, J.P., Clegern, W.C., Schmidt, M.A., 2011. Toll-like receptor 4 is a regulator of monocyte and electroencephalographic responses to sleep loss. Sleep 34, 1335–1345. doi:10.5665/SLEEP.1274

Yan, J., Li, J.-C., Xie, M.-L., Zhang, D., Qi, A.-P., Hu, B., Huang, W., Xia, J.-X., Hu, Z.-A., 2011. Short-term sleep deprivation increases intrinsic excitability of prefrontal cortical neurons. Brain Res. 1401, 52–58. doi:10.1016/j.brainres.2011.05.032

Yatham, L.N., Liddle, P.F., Lam, R.W., Zis, A.P., Stoessl, A.J., Sossi, V., Adam, M.J., Ruth, T.J., 2010. Effect of electroconvulsive therapy on brain 5-HT2 receptors in major depression. Br. J. Psychiatry 196, 474–479. doi:10.1192/bjp.bp.109.069567

Zarate, C.A., Du, J., Quiroz, J., Gray, N.A., Denicoff, K.D., Singh, J., Charney, D.S., Manji, H.K., 2003. Regulation of Cellular Plasticity Cascades in the Pathophysiology and Treatment of Mood Disorders. Ann. N. Y. Acad. Sci. 1003, 273–291. doi:10.1196/annals.1300.017

Zarate, C.A., Mathews, D.C., Furey, M.L., 2013. Human biomarkers of rapid antidepressant effects. Biol. Psychiatry 73, 1142–1155. doi:10.1016/j.biopsych.2012.11.031

Ziemann, U., 2011. Transcranial Magnetic Stimulation at the Interface with Other Techniques A Powerful Tool for Studying the Human Cortex. The Neuroscientist 17, 368–381. doi:10.1177/1073858410390225

Ziemann, U., Reis, J., Schwenkreis, P., Rosanova, M., Strafella, A., Badawy, R., Müller-Dahlhaus, F., 2015. TMS and drugs revisited 2014. Clin. Neurophysiol. 126, 1847–1868. doi:10.1016/j.clinph.2014.08.028